

UNCLASSIFIED

AD NUMBER

ADB002185

LIMITATION CHANGES

TO:

Approved for public release; distribution is unlimited. Document partially illegible.

FROM:

Distribution authorized to U.S. Gov't. agencies only; Test and Evaluation; AUG 1974. Other requests shall be referred to Air Force Flight Dynamics Laboratory, FEC, Wright-Patterson AFB, OH 45433. Document partially illegible.

AUTHORITY

AFWAL LTR 16 FEB 1982

THIS PAGE IS UNCLASSIFIED

**THIS REPORT HAS BEEN DELIMITED
AND CLEARED FOR PUBLIC RELEASE
UNDER DOD DIRECTIVE 5200.20 AND
NO RESTRICTIONS ARE IMPOSED UPON
ITS USE AND DISCLOSURE.**

DISTRIBUTION STATEMENT A

**APPROVED FOR PUBLIC RELEASE,
DISTRIBUTION UNLIMITED.**

7
AFFDL-TR-74-127

AD B 002185

**DESIGN STUDY OF A
ROTARY RECIPROCATING THERMAL COMPRESSOR**

**R. W. BRECKENRIDGE, JR.
R. W. MOORE, JR.
P. M. O'FARRELL**

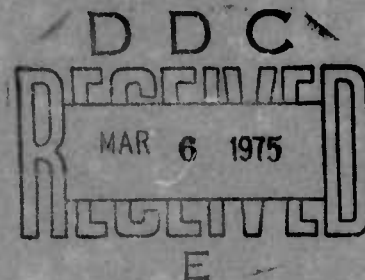
**ARTHUR D. LITTLE, INC.
CAMBRIDGE, MASSACHUSETTS 02140**

TECHNICAL REPORT AFFDL-TR-74-127

OCTOBER 1974

Distribution limited to U.S. Government agencies only;
test and evaluation; statement applied Aug. 1974. Other
requests for this document must be referred to A. F. Flight
Dynamics Laboratory (FEC) Wright-Patterson AFB, Ohio 45433.

**AIR FORCE FLIGHT DYNAMICS LABORATORY
AIR FORCE SYSTEMS COMMAND
WRIGHT-PATTERSON AIR FORCE BASE, OHIO 45433**



NOTICE

When Government drawings, specifications, or other data are used for any purpose other than in connection with a definitely related Government procurement operation, the United States Government thereby incurs no responsibility nor any obligation whatsoever; and the fact that the Government may have formulated, furnished, or in any way supplied the said drawings, specifications, or other data, is not to be regarded by implication or otherwise as in any manner licensing the holder or any other person or corporation, or conveying any rights or permission to manufacture, use, or sell any patented invention that may in any way be related thereto.

Copies of this report should not be returned unless return is required by security considerations, contractual obligations, or notice on a specific document.

DESIGN STUDY OF A
ROTARY RECIPROCATING THERMAL COMPRESSOR

R. W. BRECKENRIDGE, JR.

R. W. MOORE, JR.

P. M. O'FARRELL


Distribution limited to U.S. Government agencies only; test and evaluation; statement applied August 1974. Other requests for this document must be referred to A.F. Flight Dynamics Laboratory (FEE), Wright-Patterson AFB, Ohio 45433.

FOREWORD

This report, prepared by staff members of Arthur D. Little, Inc., Acorn Park, Cambridge, Massachusetts, is the final technical report on a design study to determine the feasibility of a rotary-reciprocating thermal compressor for use in spaceborne, cryogenic refrigeration systems. The work was carried out under U.S.A.F. Contract F33615-74-C-3082 (Arthur D. Little, Inc., Case No. 77056). The contract was in support of Project No. 6146, Task 6146 03 19, and was made possible by the use of Laboratory Director's Funds. The work was administered under the direction of the Air Force Flight Dynamics Laboratory, Vehicle Equipment Division, with Lt. David C. Brubaker, AFFDL/FEE, as Project Engineer.

This report covers work from April to August 1974 and was released by the author in October 1974 for publication as a technical report.

This technical report has been reviewed and is approved.


William C. Savage
Chief, Environmental Control Branch
Vehicle Equipment Division
Air Force Flight Dynamics Laboratory

ABSTRACT

This report presents the results of a design study program on a rotary reciprocating compressor which uses heat as the source of driving energy. The objective of the study program was to determine the feasibility of using a thermal compressor in a spaceborne, cryogenic refrigeration system. The report explains the principles of operation of a thermal compressor, and presents the equations which describe its behavior. It also describes a computer program constructed to manipulate these equations. The results of a number of runs made with this program are discussed, and the design of a thermal compressor to meet a specific set of performance requirements is described. Finally, a comparison is made between two types of spaceborne, closed-cycle, cryogenic refrigeration systems--one incorporating a thermal compressor and the other incorporating an electrically driven compressor.

It is concluded that a thermal compressor is a viable alternative to an electrically driven compressor in refrigeration systems where heat is preferred over electricity as the energy source. For the specific case studied, the refrigeration system incorporating a thermal compressor required 92 watts of electrical power and 1,064 watts of heat at 1,250°F; while the system incorporating an electric compressor required 587 watts of electrical power. The weights and sizes of the two refrigeration systems were comparable. No serious technical problems are foreseen in building a thermal compressor.

TABLE OF CONTENTS

I. Introduction and Summary	1
II. Principles of Operation of a Thermal Compressor	7
III. Thermodynamic Cycle Analysis	11
IV. Parametric Analysis of Thermodynamic Processes	17
A. General	17
B. Analytical Model	17
C. Computer Program	30
D. Results	30
V. Design of Baseline Thermal Compressor	43
A. General	43
B. First Stage Cylinder Assembly	43
C. Second Stage Cylinder Assembly	53
D. Drive Assemblies	53
E. Summary of the Design	56
VI. System Comparisons	59
VII. Conclusions	63
References	65
Appendix I Derivation of Equations Describing the Performance of a Thermal Compressor	67
Appendix II Description of a Thermal Compressor Computer Program	79

LIST OF FIGURES

<u>Figure No.</u>		<u>Page No.</u>
1	Outline Drawing of Thermal Compressor	5
2	Thermal Compression Process	8
3	Shaft Power Versus Pressure Ratio	13
4	Refrigerator Weight Versus Pressure Ratio	14
5	Thermodynamic Cycle for Refrigerator Incorporating a Thermal Compressor	16
6	Displacer Positions	18
7	Combined Hot & Cold PX Diagrams	19
8	Volume Definitions	21
9	Flow/Pressure Ratio Characteristic for One Stage of Compression	24
10	Cold End PV Diagrams for a Range of Designs	25
11	Heat Exchanger Configurations	27
12	Energy Flow in Thermal Compressor	29
13	Thermal Compressor Configurations	32
14	Power and Size as a Function of Speed	35
15	Losses as a Function of Speed	37
16	Power as a Function of Matrix Size	39
17	Hot End Power Versus Displacer Drive Power	40
18	First Stage of Thermal Compressor	45
19	Second Stage of Thermal Compressor	47
20	Cold Working Volume Pressure as a Function of Displacer Position	51

Figure No.

Page No.

21	Flowsheet of Thermal Compressor Computer Program	80
22	Listing of Computer Program	88
23	Sample Problem - First Stage Design	99
24	Sample Problem - Second Stage Design	103

LIST OF TABLES

<u>Table No.</u>		<u>Page No.</u>
I	Refrigeration Specifications	2
II	Specifications for the Thermal Compressor	3
III	Summary of Thermal Compressor Design	4
IV	Comparison of Refrigerator Types	6
V	Void Volume Summary	22
VI	Comparison of Compressor Configurations	33
VII	Summary of Baseline Design Thermal Compressor	44
VIII	Breakdown of Input Power for Baseline Design	
	Thermal Compressor	52
IX	Actuator Drive Power	55
X	Breakdown of Electric Input Power for Baseline	
	Thermal Compressor	57
XI	Weight Breakdown of Thermal Compressor	58
XII	System Comparisons	60
XIII	Input Data to Program	82

LIST OF ABBREVIATIONS AND SYMBOLS

A	Regenerator heat transfer surface area (cm ²)
AC	Regenerator minimum free flow area (cm ²)
ADIF	Difference between hot and cold displacer areas (cm ²)
AFP	Cross-sectional area of fluid passage to heat exchanger (cm ²)
AFR	Frontal area of regenerator (cm ²)
AINS	Insulation area (cm ²)
AR	A ₂ /A ₃ + RVF (dimensionless)
AT	A ₂ /A ₃ - TC/TH (dimensionless)
A ₂	Ambient displacer area (cm ²)
A ₂ A ₃	Ratio of ambient to hot displacer areas (dimensionless)
A ₃	Hot displacer area (cm ²)
BAN	Perimeter of annular heat exchanger (cm)
BP	Passage width in multipassage design (cm)
C	Radial clearance between displacer and cylinder (cm)
CP	Specific heat of helium (5.193 J/g-K)
D	Cylinder diameter (cm)
DH	Hydraulic diameter of regenerator matrix (cm)
DPCFP	Pressure drop in ambient fluid passage (atm)
DPCHX	Pressure drop in ambient heat exchanger (atm)
DPFP	Pressure drop in fluid passage (atm)
DPHFP	Pressure drop in hot fluid passage (atm)
DPHHX	Pressure drop in hot heat exchanger (atm)
DPHX	Pressure drop through the heat exchanger (atm)
DPREG	Pressure drop through regenerator (atm)
DRS	Diameter of regenerator shell (cm)
DYNH	Dynamic head in fluid passage (atm)
DYNHC	Dynamic head in fluid passage to ambient heat exchanger (atm)
DYNHH	Dynamic head in fluid passage to hot heat exchanger (atm)
E	Effectiveness
ECHX	Effectiveness of ambient heat exchanger (dimensionless)
EHX	Effectiveness of hot heat exchanger (dimensionless)
F	Friction factor
G	Instantaneous flow stream mass velocity (g/cm ² -sec)
GBAR	Mean flow stream mass velocity (g/cm ² -sec)
HBAR	Mean heat transfer coefficient of matrix (watt/cm ² -K)
ICHX	Flags indicating type of heat exchanger selected: 1 = annular 2 = multipassage
IHHX	
IHX	
IMTX	Flag indicating matrix material: 1 = spheres, 2 = screens, 3 = tubes
IREG	Flag indicating type of regenerator selected: 1 = annular (integral with cylinder), 2 = separate from cylinder
JBAR	Mean Colburn modulus of matrix, StPr ^{2/3} (dimensionless)
KCW	Thermal conductivity of cylinder wall (watt/cm-K)
KDIS	Thermal conductivity of displacer wall (watt/cm-K)
KG	Thermal conductivity of helium (watt/cm-K)
KINS	Thermal conductivity of insulation (watt/cm-K)

KRM	Bulk thermal conductivity of regenerator matrix (watt/cm-K)
KRMM	Thermal conductivity of regenerator matrix material (watt/cm-K)
KRS	Thermal conductivity of regenerator shell (watt/cm-K)
K4	Thermal conductivity of helium at temperature T4 (watt/cm-K)
L	Heat exchanger length (cm)
LCFP	Length of fluid passage from ambient heat exchanger (cm)
LFP	Length of fluid passage (cm)
LHC	Length of cylinder between hot and cold ends (cm)
LHFP	Length of fluid passage to hot heat exchanger (cm)
LP	Length of a single passage in multipassage design (cm)
LPC	Multipassage length in ambient heat exchanger (cm)
LPH	Multipassage length in hot heat exchanger (cm)
LR	Regenerator length (cm)
MA	Mass in system at point a (g)
MC	Mass in system at point c (g)
MCY	Mass throughput per cycle, one cylinder (g)
MPDOT	Leakage flow in pumping loss (g/sec)
M2	Mass of gas in volume 2 (g)
M3A	Regenerator mass throughput in one cycle (g)
N	Speed (Hz)
NC	Number of cylinders (dimensionless)
NNU	Nusselt number
NP	Number of passages in multipassage design (dimensionless)
NPR	Prandtl number of helium (0.667)
NR	Reynolds number, instantaneous flow condition
NRBAR	Reynolds number, mean flow conditions
NST	Stanton number
NTU	Number of heat transfer units
NTUBAR	Number of heat transfer units based on mean flow conditions
NV	Volumetric efficiency (dimensionless)
P	Instantaneous pressure at ambient end (atm)
PD	Discharge pressure (atm)
PDA	Displacer power output due to ambient-hot area difference (watts)
PDISP	Net displacer power required (watts)
PDP	Displacer power input required to overcome pressure drops in regenerator, heat exchangers, and fluid passages (watts)
PI, π	3.1415926536
PS	Suction pressure (atm)
P2P3	Pressure difference between ambient and hot ends; equals total pressure drop through regenerator, heat exchangers, and fluid passages (atm)
P3	Hot end pressure (atm)
QCW	Conduction loss through cylinder wall (watts)
QDIS	Conduction loss through displacer wall (watts)
QINBAR	Total hot end heat input (watts)
QINS	Conduction loss through insulation (watts)
QPL	Pumping loss (watts)
QREG	Regenerator heat loss (watts)
QRM	Regenerator matrix conduction loss (watts)

QSH	Shuttle heat transfer loss (watts)
Q3	Ideal hot end heat input (watts)
Q32	Heat loss from hot end to ambient end (watts)
R	Gas constant for helium (2.079 J/g-K)
RHO	Density of helium (g/cm ³)
RVF	Reduced void fraction (dimensionless)
S	Stroke (cm)
SDR	Stroke-to-diameter ratio (dimensionless)
T	Reservoir temperature for one side of heat exchanger (K)
TC	Ambient end temperature (K)
TCR	TC/TH + RVF
TD	Displacer wall thickness (cm)
TH	Hot end temperature (K)
TINS	Insulation thickness (cm)
TRS	Thickness of regenerator shell (cm)
TWGO	Heat exchanger exit ΔT (K)
TYP	Array used to facilitate printing of output
T4	Log mean average ΔT in regenerator (K)
U	Absolute viscosity of helium (g/cm-sec)
U4	Absolute viscosity of helium at temperature T4 (g/cm-sec)
V	Specific volume of helium (cm ³ /g)
VCHX	Volume of ambient heat exchanger (cm ³)
VCL	Clearance volume (cm ³)
VCL2	Ambient end clearance volume (cm ³)
VCL3	Hot end clearance volume (cm ³)
VFC	Ambient end void fraction (dimensionless)
VFH	Hot end void fraction (dimensionless)
VFI	Intermediate void fraction (dimensionless)
VFP	Volume of heat exchanger fluid passage (cm ³)
VFPORT	Porting void fraction (dimensionless)
VFR	Regenerator void fraction (dimensionless)
VHHX	Volume of hot heat exchanger (cm ³)
VHX	Heat exchanger volume (cm ³)
VPDC	Clearance volume around displacer periphery (cm ³)
VV	Heat exchanger void volume (cm ³)
VVREG	Regenerator void volume (cm ³)
V2	Instantaneous value of ambient volumes (void volume plus working volume (cm ³))
V2D	Ambient end displacement volume
V2V	Ambient end void volume (cm ³)
V3D	Hot end displacement volume (cm ³)
V3V	Hot end void volume (cm ³)
V4V	Intermediate void volume (cm ³)
W	Total mass flow rate through compressor, all cylinders (g/sec)
WCHX	Array used to format output
WD	Discharge flow rate (g/sec)
WDA	Displacer work produced from displacer area difference (J)
WDP	Displacer work required to overcome regenerator and heat exchanger pressure drops (J)
WR	Instantaneous flow through the regenerator (g/sec)
WRBAR	Mean mass flow rate through regenerator (g/sec)
WS	Suction flow rate (g/sec)

W32	P-V work associated with displacer movement (J)
X	Displacer position measured positive away from ambient end TDC (cm)
XB	Displacer position at which suction port opens (cm)
XCL2	Ambient end axial clearance (cm)
XCL3	Hot end axial clearance (cm)
XD	Displacer position at which discharge port opens (cm)
XDOT	Displacer velocity (cm/sec)
X1	Array containing 100 displacer positions in cycle (cm)
Z }	
Z1 }	Dummy variables used to facilitate FORTRAN coding

I. INTRODUCTION AND SUMMARY

For a number of years, the Air Force has supported the development of rotary-reciprocating refrigeration systems. These systems have been designed to produce refrigeration at cryogenic temperatures in spaceborne applications where long, maintenance-free life and low input power are primary system requirements. A complete 77 K refrigeration system has been developed (see Reference 1) and components of a 3.6 K refrigerator have been built and tested (see Reference 2). A system which produces refrigeration simultaneously at 12 K and 60 K is presently under development (see Reference 3). All of these systems utilize the reversed Brayton thermodynamic cycle and employ reciprocating compressors and expansion engines. In all these systems, all of the input power to the refrigerator has been in the form of electrical energy--with approximately 80% of this energy being used to compress the gas in the compressor working volumes, and the balance being used to rotate pistons, to overcome losses, and to actuate the expander pistons.

In recent years, the Air Force has become interested in reducing the electrical power requirements of spaceborne, closed-cycle refrigeration systems by using heat rather than electrical energy as the major energy source for the refrigerator. In a refrigerator which uses the reversed Brayton cycle, a major reduction in the electrical power requirement can be accomplished by employing a compressor which uses heat rather than electricity to supply the work of compression. A heat-driven compressor of this sort, generally referred to as a thermal compressor, may be used in place of the electrically driven compressor with relatively minor changes to other portions of the refrigeration system.

A thermal compressor is a reciprocating machine which consists of two basic elements: a cylinder assembly and a drive mechanism. The cylinder assembly consists of a cylinder and a displacer. The displacer separates the cylinder into two working volumes. These two working volumes are connected by flow passages which contain heat exchangers and a thermal regenerator. One end of the cylinder is maintained at an elevated temperature by the addition of heat, and the other end is maintained at ambient temperature by rejecting heat to a heat sink. As the displacer is moved back and forth in the cylinder by the drive mechanism, the pressure in the cylinder fluctuates. Valving in the ambient temperature working volume communicates this working volume with inlet and discharge manifolds when the pressure in the cylinder matches the pressure in the manifolds. All of these actions result in gas being compressed from inlet pressure to discharge pressure by the heat that is added to the hot end of the cylinder. The principles of operation of a thermal compressor are described in more detail in Section II of this report.

In a rotary-reciprocating thermal compressor, the displacer is actuated by an electrically-powered drive assembly which is similar to that used in an electric rotary-reciprocating compressor. The drive assembly comprises a rotary motor to rotate the displacer, a linear actuator to reciprocate the

displacer, and a gas spring to provide a restoring force to the displacer. The rotation activates self-acting gas bearings which completely support the displacer. Gas flows in and out of the compressor are regulated by ports in the cylinder assembly which are opened and closed by the rotating, reciprocating action of the displacer. The electrical power required by the drive assembly is determined principally by the power required to move the displacer. Since the pressures at both ends of the displacer are approximately the same, relatively little electrical energy is required to move the displacer. Thus, the electric input to the compressor is minimal, the major source of input energy being the heat supplied to the hot end of the cylinder.

In recognition of the potential advantages of a thermal compressor in reducing electrical input power to spaceborne refrigeration systems, the Air Force has supported the design study program which is summarized in this report. The objective of the study program has been to determine the feasibility of a thermal compressor for a rotary-reciprocating cryogenic refrigeration system. The study has consisted of analyzing and designing a thermal compressor to the point where technical feasibility and characteristics could be determined, and then comparing a rotary-reciprocating refrigerator incorporating a thermal compressor with a rotary-reciprocating refrigerator incorporating an electrical compressor--with both systems being designed to meet a specified set of refrigeration requirements. The refrigeration requirements, which were specified by the Air Force at the outset of the study, are listed in Table I.

TABLE I

REFRIGERATION REQUIREMENTS

Refrigeration Capacity	
0.3 Watts at 12 K	
3.0 Watts at 28 K	
6.0 Watts at 75 K	
Heat Rejection Temperature	300 K

The first step in the study program was to determine an appropriate thermodynamic cycle for a refrigeration system employing a thermal compressor. This was done to determine the required performance specifications for the thermal compressor and to identify ranges of cycle parameters that would lead to practical designs of the compressor. This task was included in recognition of the fact that the most suitable thermodynamic cycle utilizing a thermal compressor might have a different pressure ratio and pressure level than if the cycle incorporated an electrically driven compressor. The cycle selection process is discussed in Section III of this report, and the compressor specifications resulting from the cycle selected are listed in Table II.

TABLE II

SPECIFICATIONS FOR THE THERMAL COMPRESSOR

Process Fluid	Helium Gas
Mass Flow Rate	3.66 LB/HR
Inlet Pressure	29.4 LB/IN ²
Discharge Pressure	58.8 LB/IN ²
Inlet Temperature	300 K

A parametric analysis was conducted in order to design the working volumes of the thermal compressor and to determine, in a general way, the characteristics of a thermal compressor. The analysis consisted of deriving the equations which describe the various elements of the compressor (working volumes, heat exchangers, regenerators, etc.). These equations were then programmed for a digital computer and a number of cases were run with the program. The basis for the parametric analysis and the results of the analysis are presented in Section IV of this report. A listing of the equations which describe a thermal compressor is contained in Appendix I and the computer program based on these equations is described in Appendix II.

Based on the results of the parametric analysis, we developed the preliminary design of a thermal compressor to meet the performance specifications which were listed in Table II. This design is summarized in Table III, and an outline drawing of the machine is shown in Figure 1. The design of the thermal compressor is discussed in more detail in Section V.

An overall comparison between a rotary-reciprocating refrigerator employing a thermal compressor and one employing an electric compressor is shown in Table IV. From this table it can be seen that a refrigerator utilizing a thermal compressor is somewhat heavier than a refrigerator incorporating an electric compressor. The refrigerator incorporating a thermal compressor requires 495 watts less electrical power than an electric-driven refrigerator, but will require 1,064 watts of thermal power at 1,250°F. The two refrigerators are virtually the same size. A more detailed comparison between the two refrigeration systems is contained in Section VI.

We conclude that the thermal compressor is a viable alternative to an electrically driven compressor in spaceborne, rotary reciprocating, cryogenic systems, and recommend that thermal compressor refrigerators be considered along with electric compressor refrigerators in spacecraft system studies. Further conclusions drawn from the study are contained in Section VII.

TABLE III

SUMMARY OF THERMAL COMPRESSOR DESIGN

Mass Flow	3.66 LB/HR
Inlet Pressure	29.4 LB/IN ² (2 Atmospheres)
Discharge Pressure	58.8 LB/IN ² (4 Atmospheres)
Inlet Temperature	300 K
Number of Stages	2
Number of Cylinders Per Stage	1
Compressor Size	See Figure 1
Compressor Weight	155 LB
Input Power	
Thermal (At 1,250°F)	1,064 Watts
Electrical (100 V DC) ⁽¹⁾	72 Watts

(1) The system may also be designed for 28 V DC

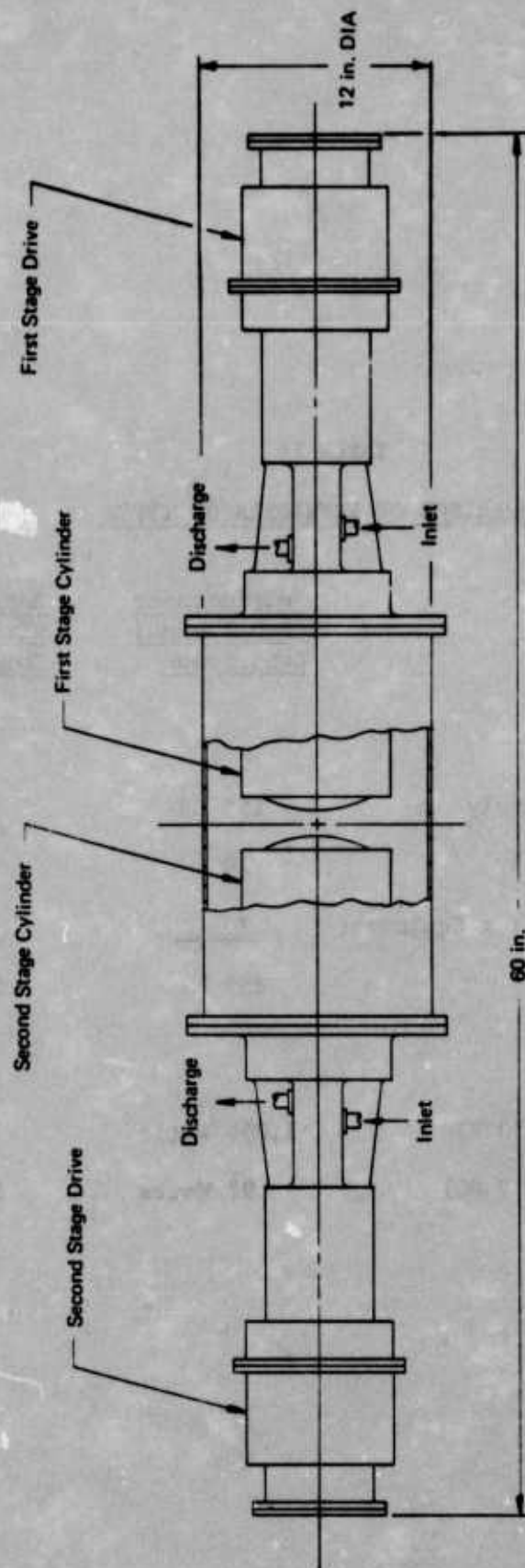


FIGURE 1 OVERALL VIEW OF THERMAL COMPRESSOR

TABLE IV
COMPARISON OF REFRIGERATOR TYPES

	<u>Refrigerator with Thermal Compressor</u>	<u>Refrigerator with Electric Compressor</u>
WEIGHT		
Compressor Assembly	155 LB	70 LB
Expander Assembly	70	70
Power Conditioning Equipment	<u>30</u>	<u>35</u>
TOTAL	255 LB	175 LB
INPUT POWER		
Thermal (At 1,250°F)	1,064 Watts	---
Electrical (100 V DC)	92 Watts	587 Watts

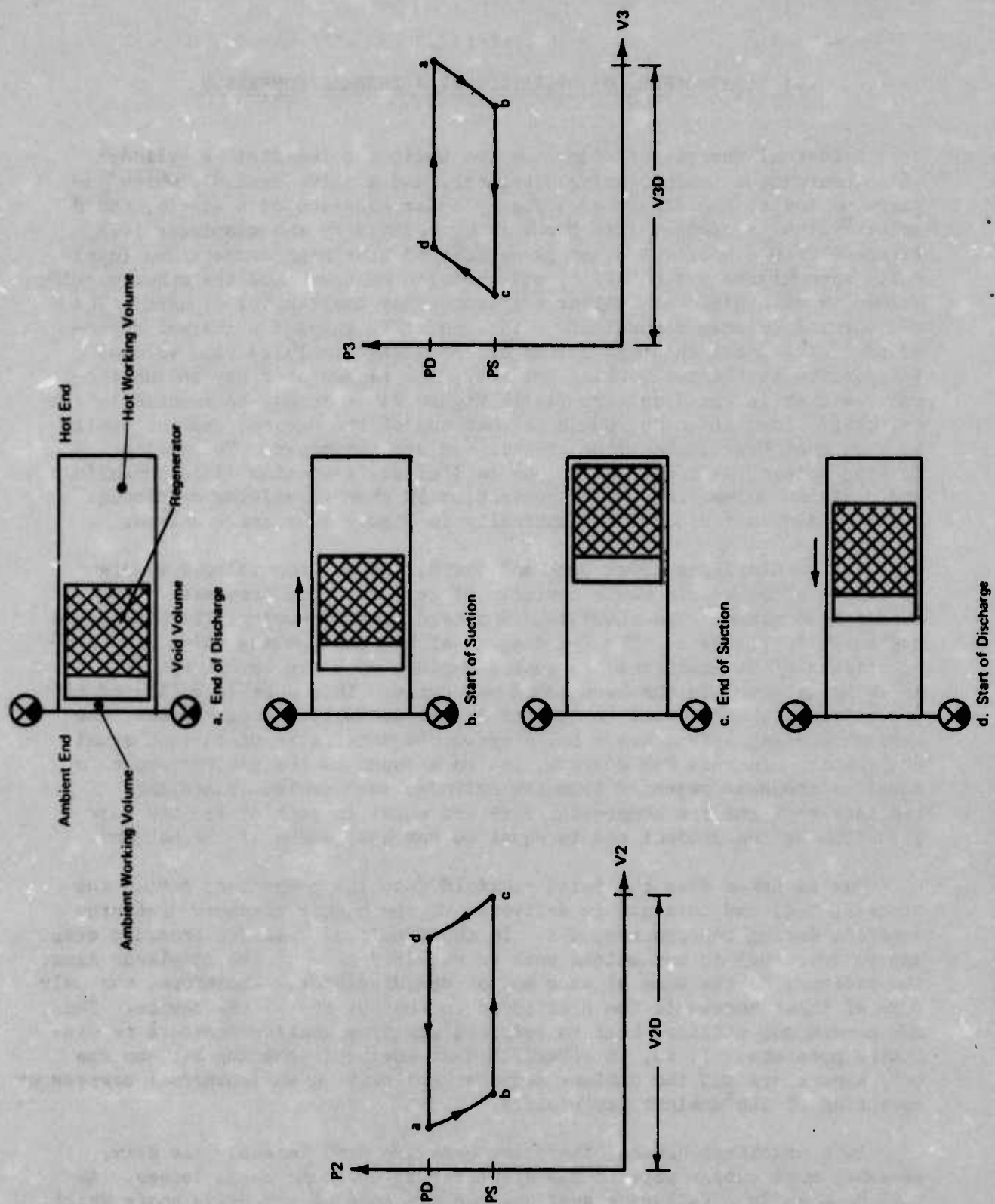
II. PRINCIPLES OF OPERATION OF A THERMAL COMPRESSOR

A thermal compressor comprises two basic subelements: a cylinder which contains a reciprocating displacer, and a drive assembly which imparts motion to the displacer. The cylinder consists of a single, fixed volume which is divided into two working volumes by the displacer (see Figure 2). One working volume is maintained at a high temperature (typically approximately 1,000°F) by the addition of heat, and the other working volume is maintained at ambient temperature by the removal of heat. The two working volumes communicate with each other through a thermal regenerator. The total internal volume of the device includes void volumes in addition to the two working volumes. The regenerator may be incorporated either in the displacer (as in Figure 2) or it may be mounted in the cylinder. Insulation surrounds the hot end of the device, and the design is such that heat losses from the hot end are minimized. The ambient working volume, is connected to two manifolds: a suction (inlet) manifold and a discharge manifold. The connection is through valving or through porting, and is indicated schematically in Figure 2 by check valves.

As the displacer moves back and forth, the working volumes undergo pressure-volume events characteristic of reciprocating compressors and expansion engines. The resulting idealized pressure-volume (P-V) diagrams are shown in Figure 2. The P-V diagram of the hot working volume is characteristic of an isothermal expansion engine, with the work output per cycle being equal to the heat added per cycle. This work is delivered to the displacer, and thence to the gas in the ambient working volume. The ambient working volume has a P-V diagram characteristic of an isothermal compressor. In this P-V diagram, the work input to the gas per cycle is equal to the heat rejected from the cylinder each cycle. Since the expander work and the compressor work are equal to each other, the heat rejection at the ambient end is equal to the heat added at the hot end.

Gas is taken from the inlet manifold into the compressor during the process, b-c, and this gas is delivered to the higher pressure discharge manifold during the process, d-a. In the idealized case (no pressure drop and no friction) no mechanical work is required to move the displacer since the pressure is the same at each end of the displacer. Therefore, the only form of input energy is the heat added to the hot end of the device. Thus, the compressor utilizes heat to compress gas from suction pressure to discharge pressure. It is, in effect, a heat engine (operating between the hot temperature and the ambient temperature) driving an isothermal compressor operating at the ambient temperature.

In a practical device, there are pressure drop losses. The drive assembly must supply work to the displacer to overcome these losses. As will be seen in a following section, the presence of the drive shaft which connects the ambient end of the displacer to the drive assembly slightly reduces the amount of work delivered to the compressor working volume from the expander working volume, since the areas of the two working volumes



are different. This results in the expander working volume delivering some work to the displacer assembly, and thus reduces the amount of work which must be provided by the drive assembly.

In a rotary-reciprocating thermal compressor, the drive assembly rotates the displacer as well as reciprocating it. The rotation activates self-acting gas bearings which support the displacer. Further, ports in the drive shaft are opened and closed by the displacer motion, to control gas flows into and out of the ambient working volume.

The thermal compressor is not a new idea, nor does it require development of new technology. A thermal compressor was patented by Bush in 1939 (Reference 4). In recent years, the National Institutes of Health have sponsored several developments of miniature thermal compressors for use as a component in a completely implantable artificial heart system (Reference 5, 6, and 7). Technology directly applicable to thermal compressors have been sponsored by the U.S. Air Force and NASA in the form of development of Vuilleumier (VM) cycle refrigerators (the hot end of the VM refrigerator is, in effect, a thermal compressor which supplies compressed gas to the cold end of the refrigerator). Additionally, the technology associated with Stirling cycle engines is also applicable to the thermal compressor. Thus, there is a technology base on which to draw for the development of a rotary reciprocating thermal compressor.

III. THERMODYNAMIC CYCLE ANALYSIS

The thermodynamic cycle analysis has been performed by using an existing rotary reciprocating computer program to analyze a number of reversed Brayton cycles (see Reference 8). The object of the analysis has been to select a thermodynamic cycle for a refrigerator incorporating a thermal compressor, and to set the performance of specifications for the compressor.

Our approach to the cycle selection has been to use the system analysis computer program to determine the characteristics of an electrically driven refrigerator as a function of various cycle parameters. For purposes of sizing a thermal compressor, we have selected the cycle which has the "best" combination of:

1. Low input power to the electrically driven compressor
2. Low system weight for an electrically driven compressor
3. Reasonable pressure ratio for the thermal compressor
4. Reasonable expander assembly design

The basis for using the results of cycle analysis on the electrically driven compressor for selecting a cycle for the thermal compressor is that the trend of input power to the thermal compressor will follow the trend of input power to the electrically driven compressor. Thus, the cycle which results in minimum power for the electrically driven compressor will also result in minimum input power to the thermal compressor. Since refrigerator weight is a direct function of input power, this selection process will also result in a refrigerator of minimum weight.

In the cycle analysis, most cycle parameters can be considered to be constant, with only a few carried as variables. The fact that there are three heat loads dictates a three expander cycle incorporating five process heat exchangers. The following values have been used to describe the expanders and heat exchangers:

Efficiency of Expander No. 1	80%
Efficiency of Expander No. 2	75%
Efficiency of Expander No. 3	70%
Heat exchanger effectiveness	98% (all exchangers)
Heat exchanger pressure loss coefficient	.01 (all exchangers)

These values are representative of values obtainable in practice. There are only two variables in addition to those mentioned above required in order to completely specify the thermodynamic cycle. They are the two pressure levels in the cycle. A number of cases have been run, considering the two pressure levels as variables. The cases which have been run are within the following range:

Low side pressure	.5 to 4 atmospheres
Pressure ratio ⁽¹⁾	1.5 to 4

A refrigerator design could not be obtained for pressure ratios less than 2.0 because the work extraction capability of the expanders was not sufficient to offset the parasitic heat loads. As a result, the cycle selection is based on pressure ratios between 2 and 4.

The refrigerator characteristics of primary interest to the cycle selection process are the refrigerator input power and the refrigerator weight. These two characteristics are plotted in Figures 3 and 4 as a function of cycle pressure ratio and cycle low side pressure. It should be noted that the weights shown in Figure 4 are lower than may actually be achievable in practice, but the trends are correct.

Based on these curves, we draw the following conclusions:

1. The minimum input power is obtained at a cycle pressure ratio of 2.5.
2. The pressure ratio at which the minimum input power is obtained is relatively insensitive to the low side pressure (i.e., the cycle pressure level).
3. The refrigerator weight decreases with increasing cycle pressure level and with increasing cycle pressure ratio.

Note on Figure 3 that the vertical axis is compressor shaft power.

This is the shaft power that would have to be supplied to an electrically driven compressor which has an isentropic efficiency of 84%. This power figure takes into account inefficiencies in the compression processes, but not losses (e.g., in the gas springs, linear actuators, power supplies, etc.), or power to drive the rotary motors.

Based solely on these conclusions, we would select a thermodynamic cycle with a pressure ratio of 2.5 (to minimize input power) and a low

(1) Pressure Ratio = $\frac{\text{high side (discharge) pressure}}{\text{low side (suction) pressure}}$

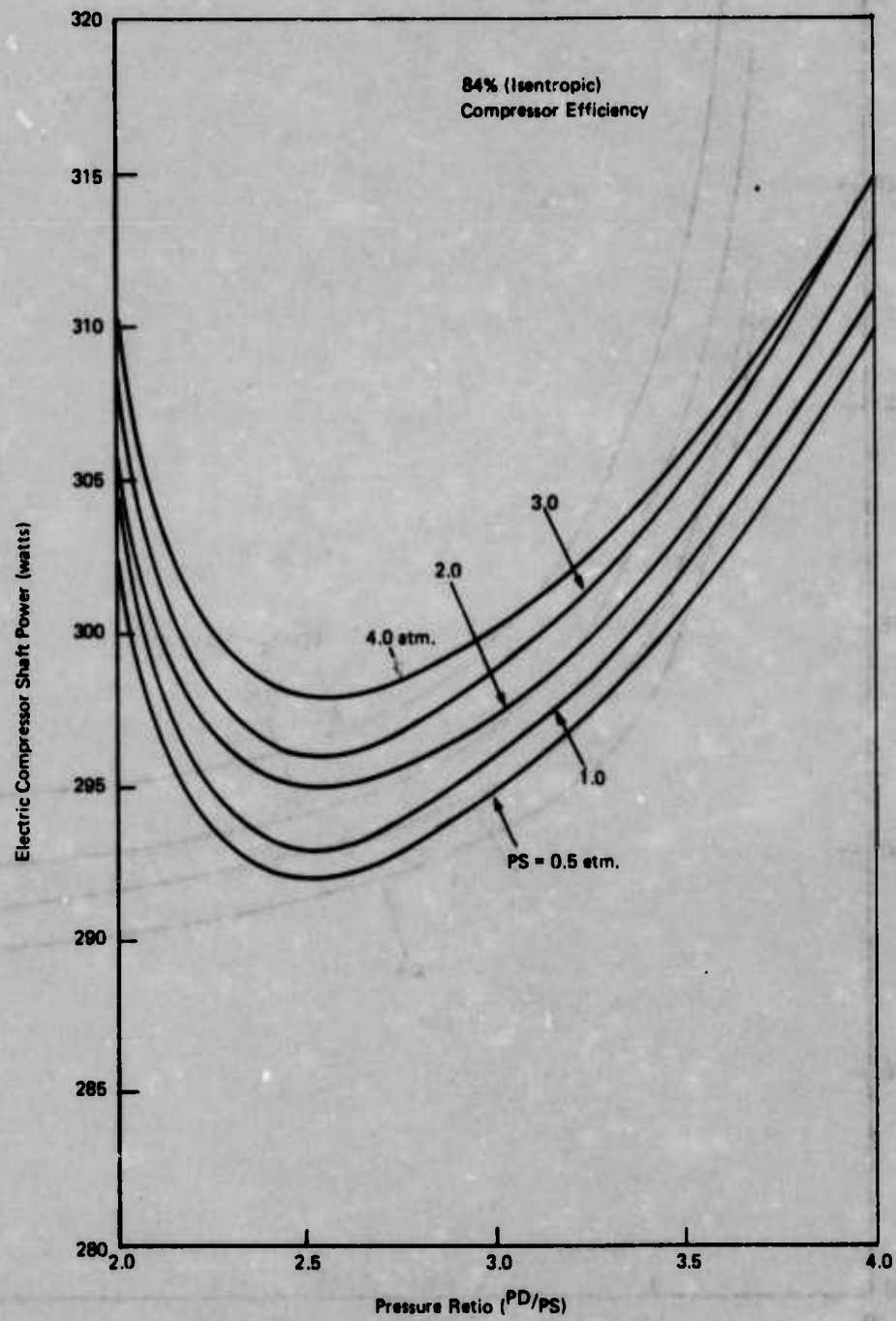


FIGURE 3 COMPRESSOR SHAFT POWER VERSUS PRESSURE RATIO

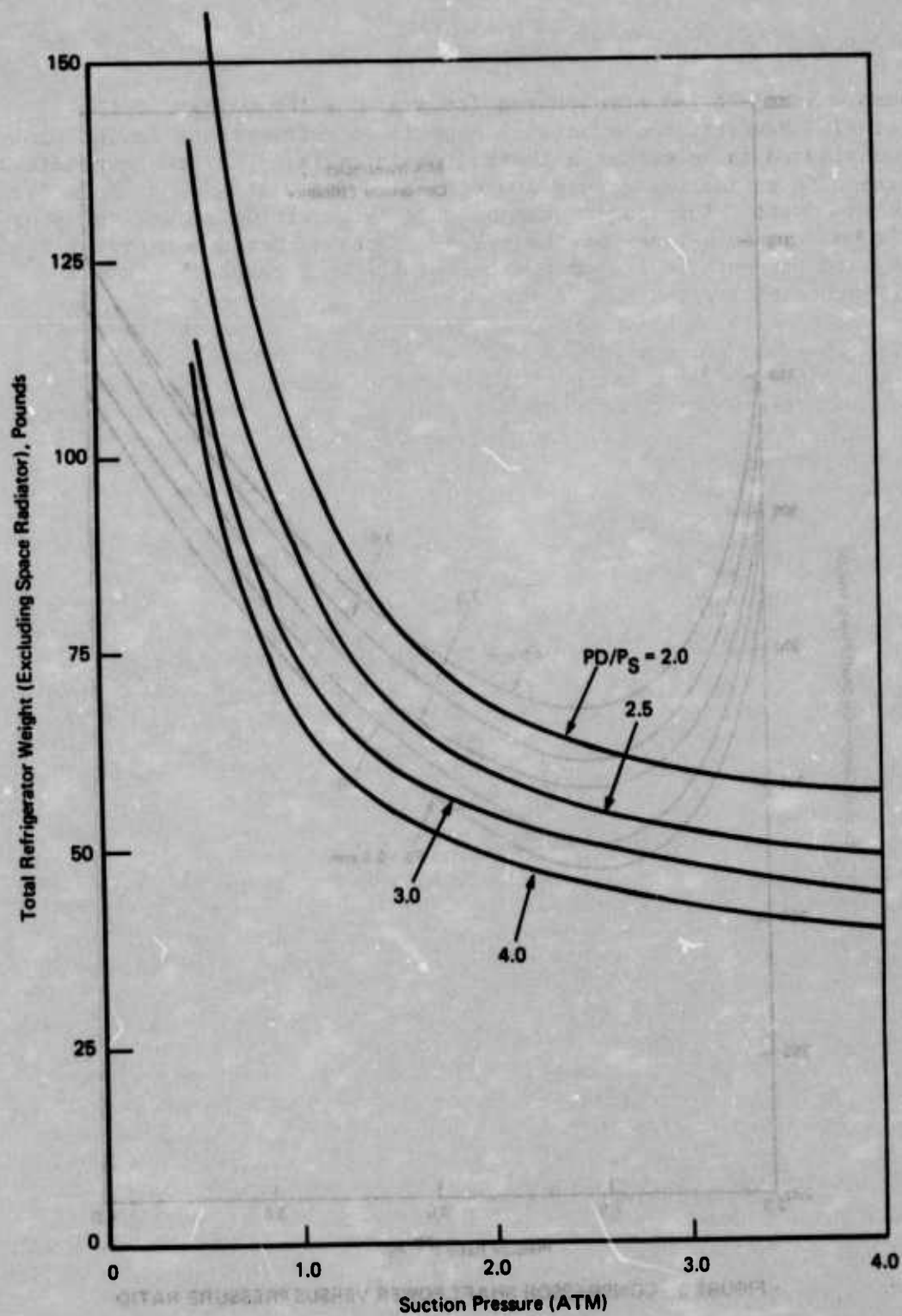


FIGURE 4 REFRIGERATOR WEIGHT VERSUS SUCTION PRESSURE (Electric Compressor)

side pressure level of 3-4 atmospheres (to minimize the weight of the refrigerator). However, the practical aspects of refrigerator design must also be considered in selecting a thermodynamic cycle. The low temperature (12 K) expansion engine has a very low capacity, and will have a small diameter piston in any event. This engine can be made larger if we reduce the pressure ratio and pressure level of the cycle. Since a pressure ratio of 2, and a low side pressure of 2 atmospheres results in a reasonably sized (i.e., .5 inch diameter piston) low temperature expansion engine, these parameters were selected for the thermodynamic cycle. The penalties of selecting this cycle are not severe. In reducing the pressure ratio to 2 from the optimum pressure ratio of 2.5, we increase the compressor shaft power only slightly (see Figure 3). Additionally, we do not change the size of the displacer in the thermal compressor, since the increase in gas flow rate required by the lower pressure ratio cycle is offset by the increase in volumetric efficiency of the compressor at the lower pressure ratio (see Section IV, B).

Selection of a three expander cycle is an obvious choice from a thermodynamic standpoint because work is extracted from the gas at temperatures very near those at which the heat loads are absorbed. An alternative to the three expander cycle is a two expander cycle in which the second stage engine absorbs both the lower temperature heat loads at 12 K. The rationale for considering a cycle of lower thermal efficiency is, first of all, that two expanders rather than three would be required, and secondly that the second stage engine would be larger (the bore would be about 0.75 inch) and therefore more easily designed.

We analyzed a two expander cycle with pressure ratios between 1.5 and 4.0 and with low side pressures between 0.5 atmospheres and 4.0 atmospheres. Qualitatively, the results were the same as in the three expander cycle, viz., the minimum input power is obtained at a pressure ratio of 2.5 and is relatively insensitive to low side pressure. However the compressor shaft power for the two cycle types were vastly different--the input power for a refrigerator utilizing the two expander cycle being over three times that for a refrigerator utilizing the three expander cycle. With a compressor efficiency of 84%, the two expander cycle compressor would require 929 watts of input power compared to 307 watts for a three expander cycle compressor. This increase in input power far outweighs any advantages which might be gained in the mechanical design of the two expander refrigerator. Consequently, the two expander cycle was not considered further.

The thermodynamic cycle selected for the thermal compressor refrigerator is shown in Figure 5. The thermal compressor discussed in following sections has been designed to meet the requirements of this cycle.

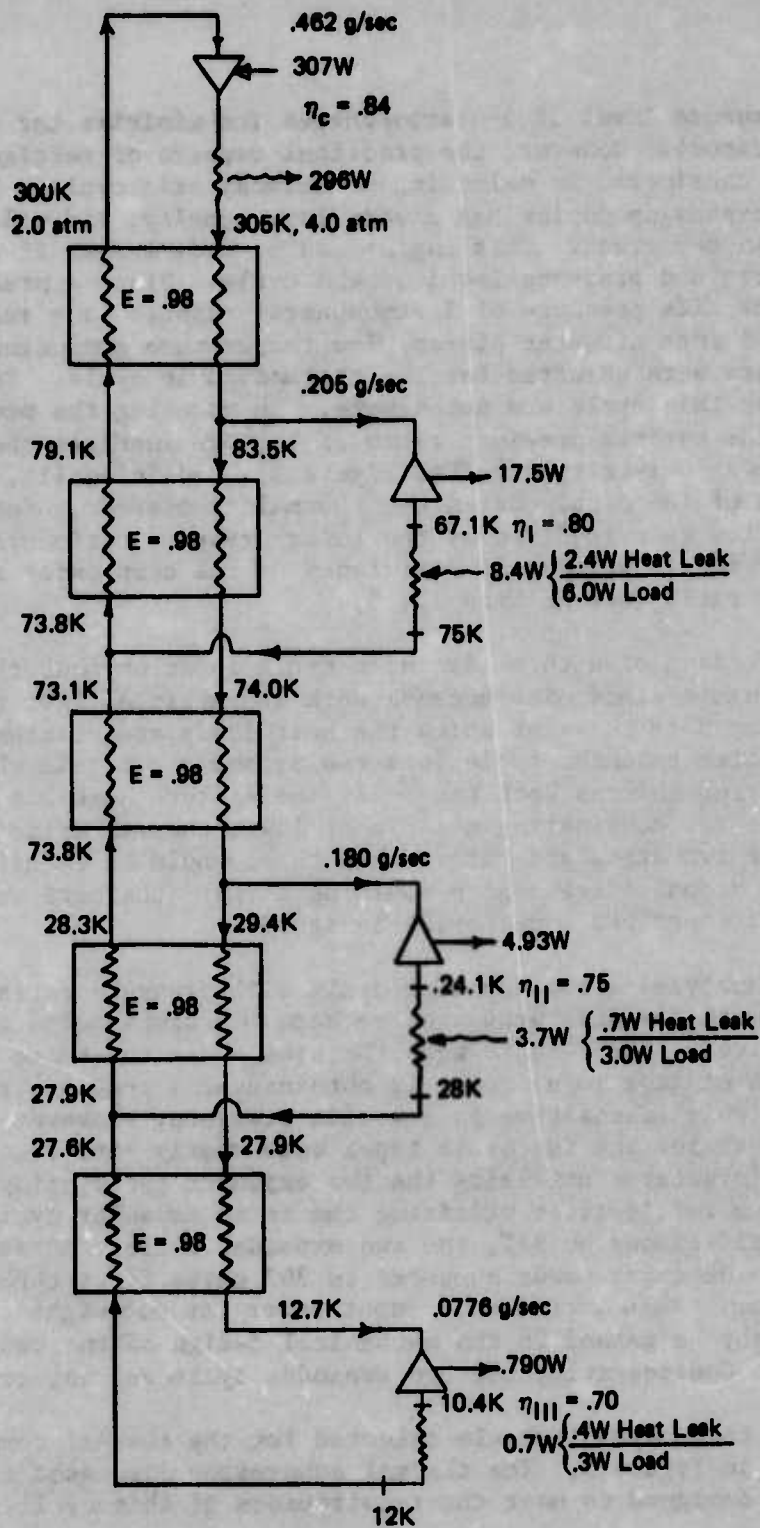


FIGURE 5 THERMODYNAMIC CYCLE FOR REFRIGERATOR INCORPORATING A THERMAL COMPRESSOR

IV. PARAMETRIC ANALYSIS OF THERMODYNAMIC PROCESSES

A. GENERAL

This section discusses the parametric analysis of the thermodynamic processes which occur in a thermal compressor, and also presents the results of the analysis and the conclusions drawn from it. We present a physical description of the analytical model used to define the thermal compressor, and the assumptions upon which the model is based. In the course of the analysis, we derived a number of equations which describe the thermodynamic processes occurring in the compressor and which are used in arriving at a design and determining its characteristics. These equations are listed and discussed in Appendix I. Since a large number of equations is required to define a thermal compressor, and since there are a number of independent variables to consider in the design optimization process, we constructed a digital computer program to manipulate the equations. This program is covered briefly in this section, and is described in detail in Appendix II. All terminology used in this section, as well as in Appendices I and II is defined in the list of abbreviations and symbols. The computer program was used extensively in the course of designing a thermal compressor to meet the performance specifications which resulted from the thermodynamic cycle analysis. The final part of this section presents the results of these computer runs, and the conclusions drawn from the results. The section concludes with a description of a baseline design point to which the thermal compressor was designed.

B. ANALYTICAL MODEL

1. Operating Characteristics

This analysis is concerned with the processes occurring in the hot and ambient ends of the cylinder, in the regenerator, in the hot and ambient heat exchangers and in void volumes. It is also concerned with how these processes interact to determine the pressure ratio/flow performance characteristics and the power input requirements to the cylinder and the displacer.

It is convenient to subdivide the cyclic operation of the compressor into four regimes: re-expansion, suction, compression, and discharge. The positions of the displacer at the four points corresponding to the transition from one regime to the next are shown in Figure 6. A diagram of the pressures in the hot and ambient ends versus stroke, on which the four positions are indicated as a, b, c and d, is shown in Figure 7. At Position a, most of the gas in the cylinder is at the hot end. During the re-expansion process from a to b, both the inlet and discharge ports in the ambient end are closed, isolating the cylinder from the suction and discharge reservoirs. The displacer moves toward the hot end, displacing gas from there to the ambient end and causing the pressure in the cylinder to decrease from the discharge pressure level to the suction pressure level. At Point b, when the suction

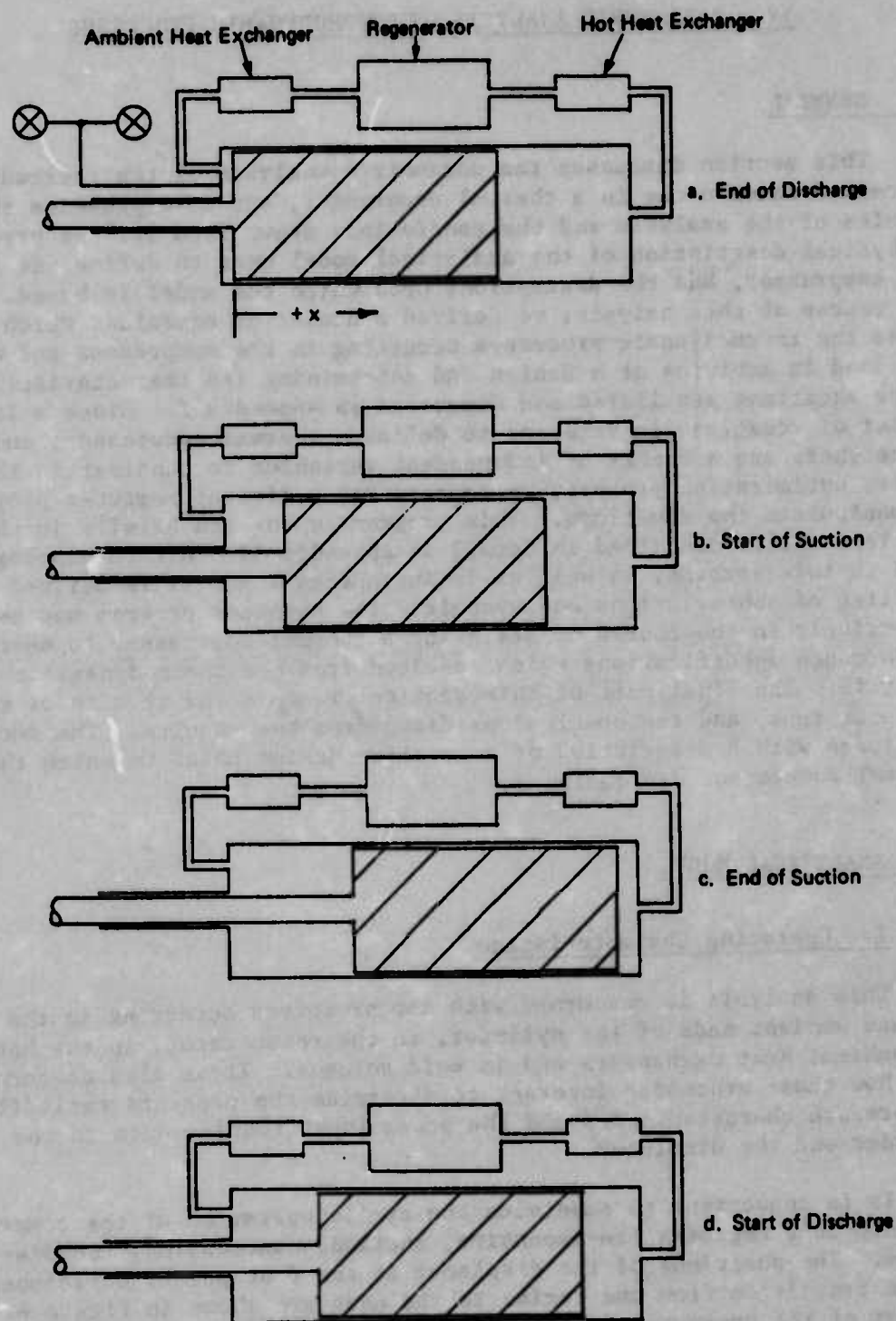


FIGURE 6 DISPLACER POSITIONS

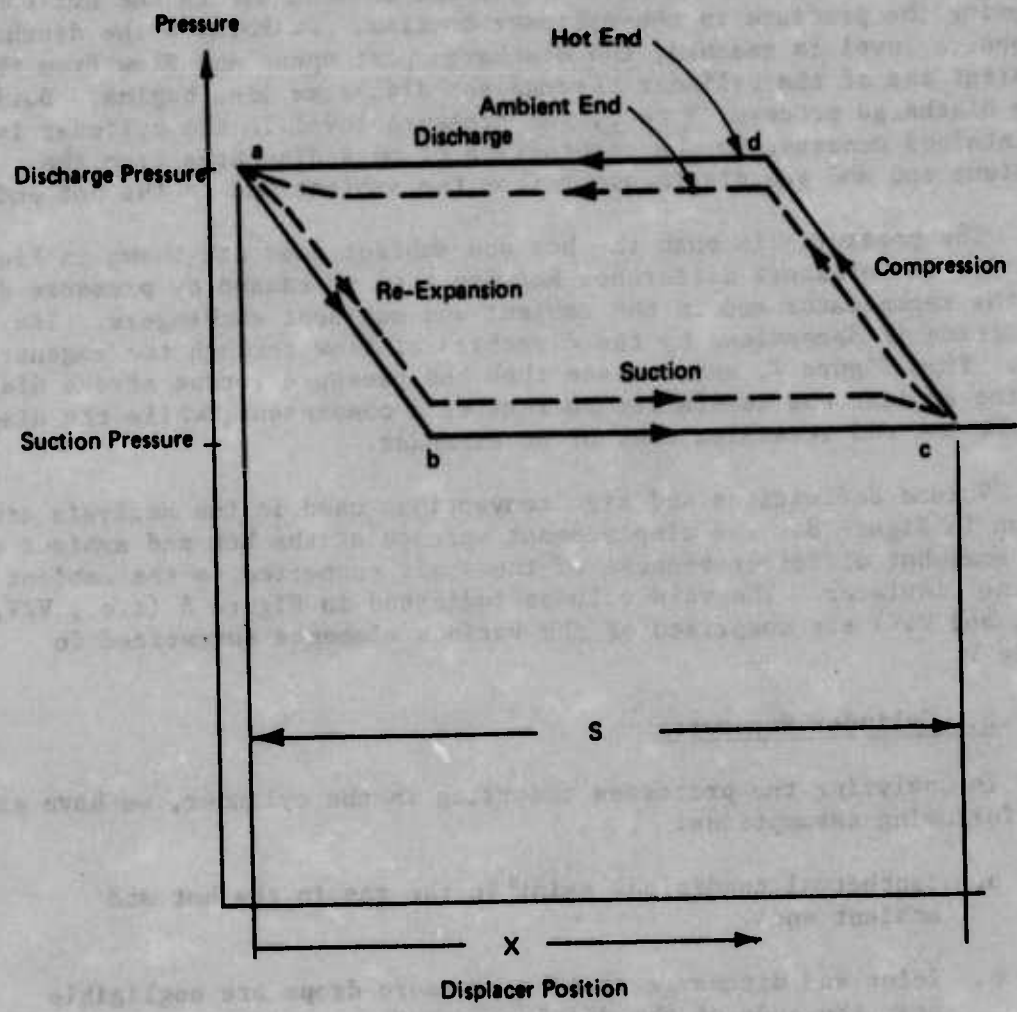


FIGURE 7 COMBINED HOT AND COLD END P-X DIAGRAMS

pressure is reached, the suction port opens, admitting gas to the cylinder from the suction line. Movement of the displacer continues from b to c until the displacer reaches its extreme position near the hot end, at which time the suction stroke is complete. In the compression process, from c to d, again both the suction and discharge ports are closed, and gas is displaced from the ambient end to the hot end, causing the pressure in the cylinder to rise. At Point d the discharge pressure level is reached, the discharge port opens and flow from the ambient end of the cylinder through the discharge line begins. During the discharge process, d to a, the pressure level in the cylinder is maintained constant by the combination of mass discharge from the ambient end and gas displacement from the ambient end to the hot end.

The pressures in both the hot and ambient ends are shown in Figure 7. The pressure difference between them is caused by pressure drop in the regenerator and in the ambient and hot heat exchangers. Its direction is determined by the direction of flow through the regenerator. From Figure 7, one can see that the pressure versus stroke diagram of the ambient end is similar to that of a compressor, while the diagram of the hot end resembles that of an expander.

Volume definitions and sign conventions used in the analysis are shown in Figure 8. The displacement volumes at the hot and ambient ends are somewhat different because of the shaft connected to the ambient end of the displacer. The void volumes indicated in Figure 8 (i.e., V2V, V3V, and V4V) are comprised of the various elements summarized in Table V.

2. Cylinder Processes

In analyzing the processes occurring in the cylinder, we have made the following assumptions:

- a. Isothermal conditions exist in the gas in the hot and ambient ends.
- b. Inlet and discharge porting pressure drops are negligible near the ends of the displacer stroke.
- c. Temperature of gas in void volumes will be either TH, TC or an intermediate temperature equal to the log mean temperature.
- d. The displacer motion is sinusoidal.
- e. The working fluid is a perfect gas.

Assumption 1 is usually made in analyses of this class of device, i.e., in Vuilleumier cycle and Stirling cycle analyses. During the constant pressure suction and discharge processes, the temperature of the gas in the hot and ambient ends should, in fact, be isothermal. During

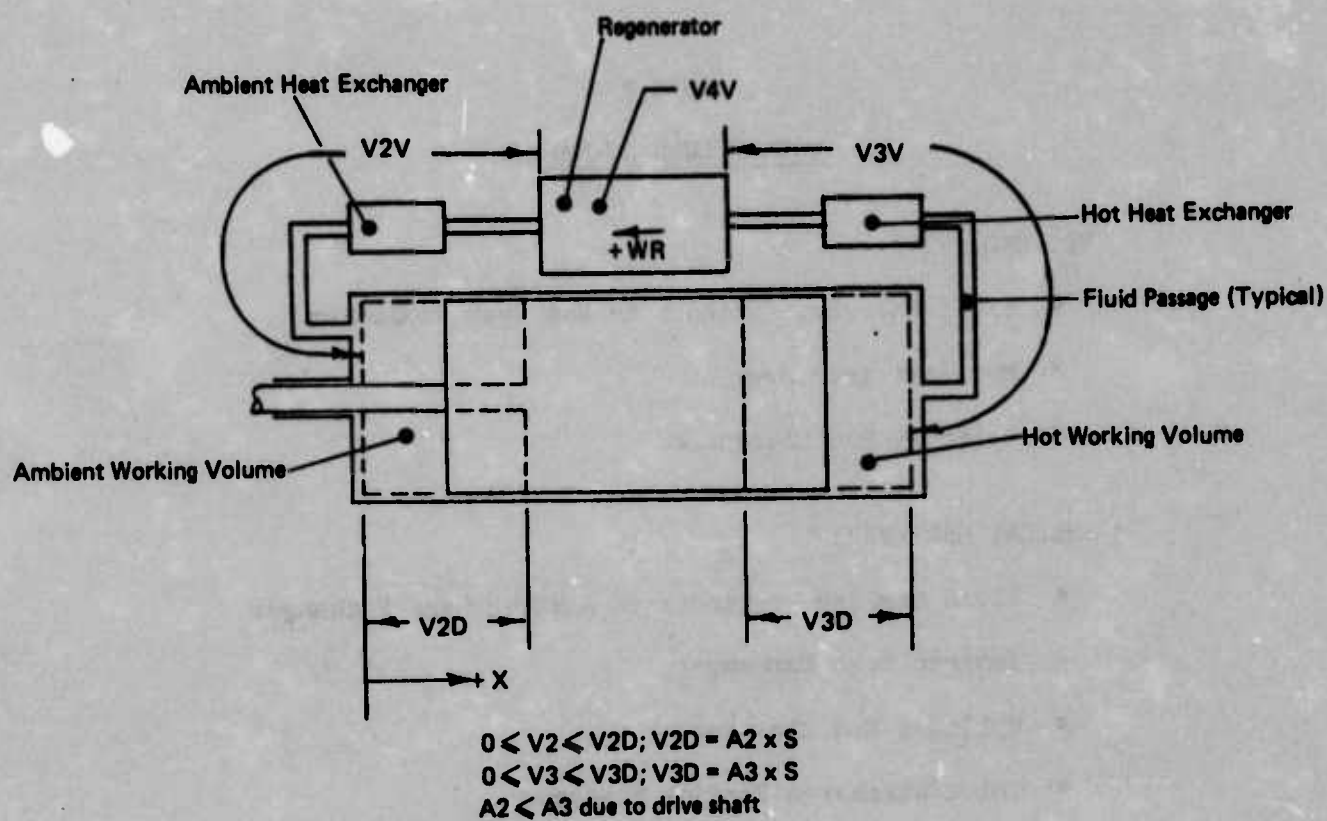


FIGURE 8 VOLUME DEFINITIONS

TABLE V
VOID VOLUME SUMMARY

HOT END (V3V)

- Fluid Passage, Cylinder to Hot Heat Exchanger
- Hot Heat Exchanger
- Cylinder End Clearance

AMBIENT END (V2V)

- Fluid Passage, Cylinder to Ambient Heat Exchanger
- Ambient Heat Exchanger
- Cylinder End Clearance
- Inlet/Discharge Porting Passages

INTERMEDIATE (V4V)

- Regenerator
- Displacer/Cylinder Radial Clearance

the re-expansion process, there is a tendency for the gas in the cylinder to cool; and during the compression process, there is a tendency for the gas to warm up. Maintaining isothermal conditions during the latter two processes will rely on adequate heat transfer to and from the cylinder walls. Such heat transfer will be augmented by circulations in the gas induced by rotation of the piston. For devices in the size range of our interest and at the low operating speeds that are appropriate for a thermal compressor, we believe that Assumption 1 is a reasonable approximation.

Assumption 2 is based on the fact that, with sinusoidal displacer motion, the flow rate into the cylinder as Point c is approached, and out of the cylinder as Point a is approached, goes to zero. Hence, porting pressure drop should be negligible at the ends of the stroke. Experience with the electric-driven rotary-reciprocating compressor, including measurements of pressure-volume diagrams, has indicated that this assumption is valid.

Assumptions 3 and 5 are good approximations and are self-explanatory. Assumption 4 is also an excellent approximation since the oscillating displacer mass experiences only a small damping force due to the pressure difference between the hot and ambient ends.

There is a pressure difference between hot and ambient ends which is caused by pressure drop through the regenerator and the heat exchangers. It determines the necessary electric power input to maintain motion of the displacer. Our approach has been to calculate the pressure difference between hot and ambient ends as a function of the displacer position and to integrate the resulting force times differential displacement throughout a cycle to obtain the displacer power input.

Using the assumptions above, it is possible to determine the relationships between cylinder pressure and the mass of gas in each of the volumes as a function of displacer position. These relationships lead to definition of cylinder size, power input and other important parameters required to achieve given flow rate and suction and discharge pressures. The equations used to describe these processes are presented in Appendix I, Section A.

A basic characteristic of thermal compressors that emerges from our analysis is the relationship between volumetric efficiency and pressure ratio. This relationship is shown in Figure 9. For a given pressure ratio and flow rate, the volumetric efficiency determines cylinder size. Hence, this relationship is important in sizing the device. Figure 9 shows that there is a direct trade-off between volumetric efficiency and pressure ratio. The ambient end pressure-volume diagrams for the two extreme cases (one in which the volumetric efficiency is a maximum and the pressure ratio is unity, and the other in which the pressure ratio is maximum and the volumetric efficiency is zero), are shown in Figure 10. Maximum volumetric efficiency is achieved when the gas is not compressed, i.e., when the ratio of discharge pressure to suction

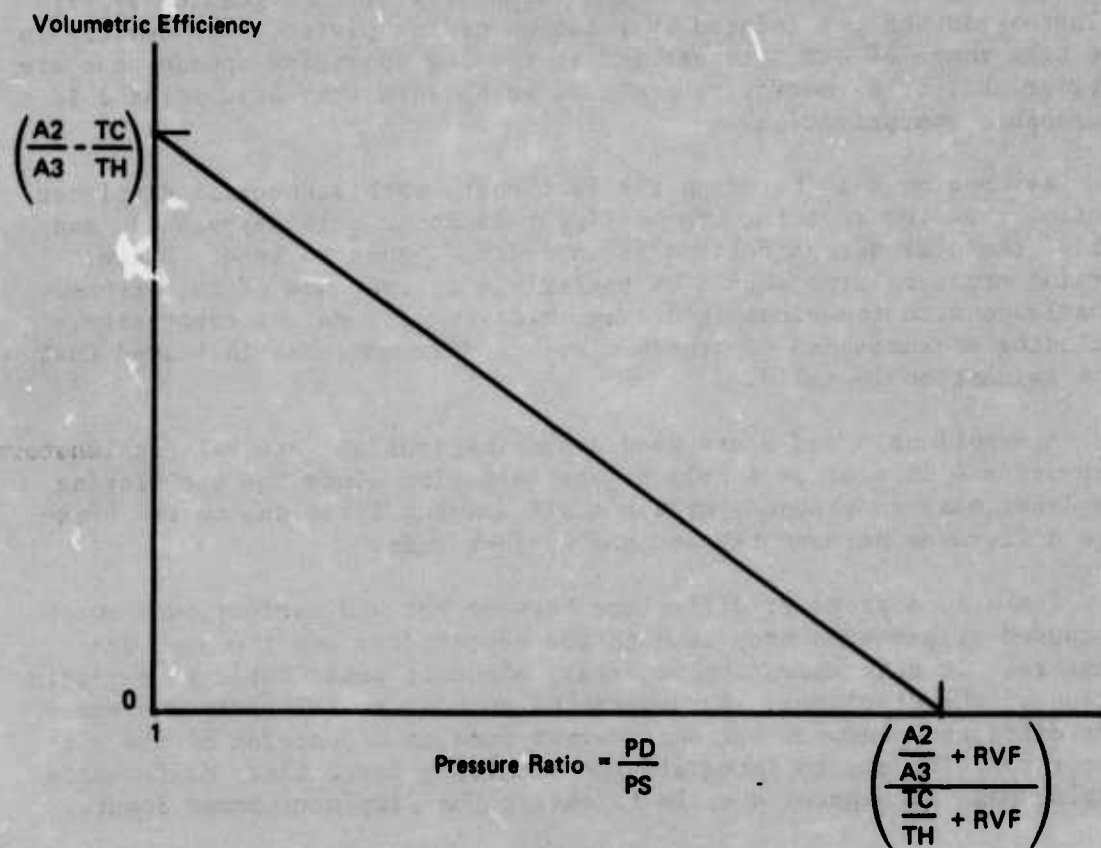


FIGURE 9 FLOW/PRESSURE RATIO CHARACTERISTIC FOR ONE STAGE OF COMPRESSION

Nominal Design: $a-b-c-d-a$

Maximum Pressure Ratio, $NV \rightarrow 0$: $a_1-b_1-c-d_1-a_1$

Maximum NV, Pressure Ratio $\rightarrow 0$: $a_2-b_2-c-d_2-a_2$

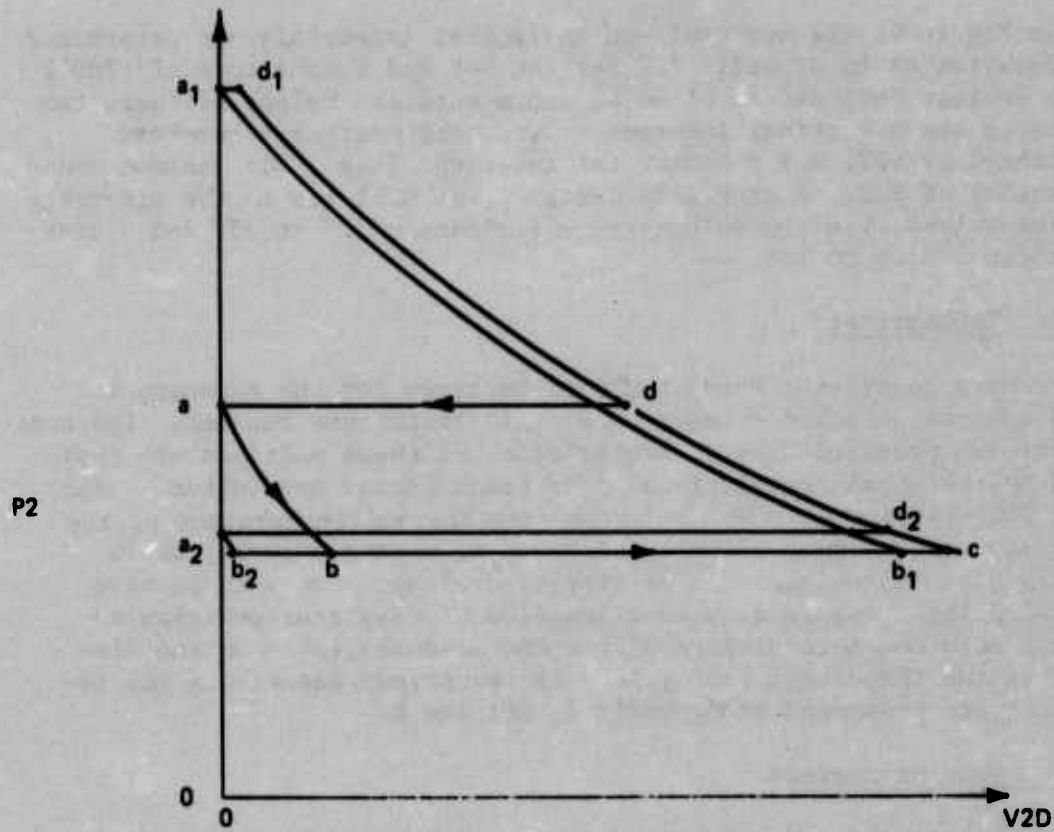


FIGURE 10 AMBIENT END PRESSURE-VOLUME DIAGRAMS FOR A RANGE OF DESIGNS

pressure is one. In this case a large portion of the gas entering the cylinder during the suction stroke is forced out of the cylinder during the discharge stroke at slightly above suction pressure. Maximum pressure ratio is achieved when there is no through-flow, i.e., when the volumetric efficiency is zero. In this case the gas in the cylinder simply shuttles back and forth between the hot and ambient ends. Neither of these extremes are useful in our application. Hence, one of the major design choices is to select a pressure ratio per cylinder that yields a reasonable volumetric efficiency and cylinder size.

In Figure 9, the vertical and horizontal intercepts are determined from Equation A5 in Appendix I. For the hot end temperature of 1200°F and an ambient temperature of 80°F, representative values of these two intercepts are a vertical intercept (i.e., the maximum volumetric efficiency) of 60%, and a horizontal intercept (i.e., the maximum pressure ratio) of 2.0. A practical design point will lie in the mid-range of these values, i.e., a volumetric efficiency of 25 to 35% and a pressure ratio of 1.4 to 1.6.

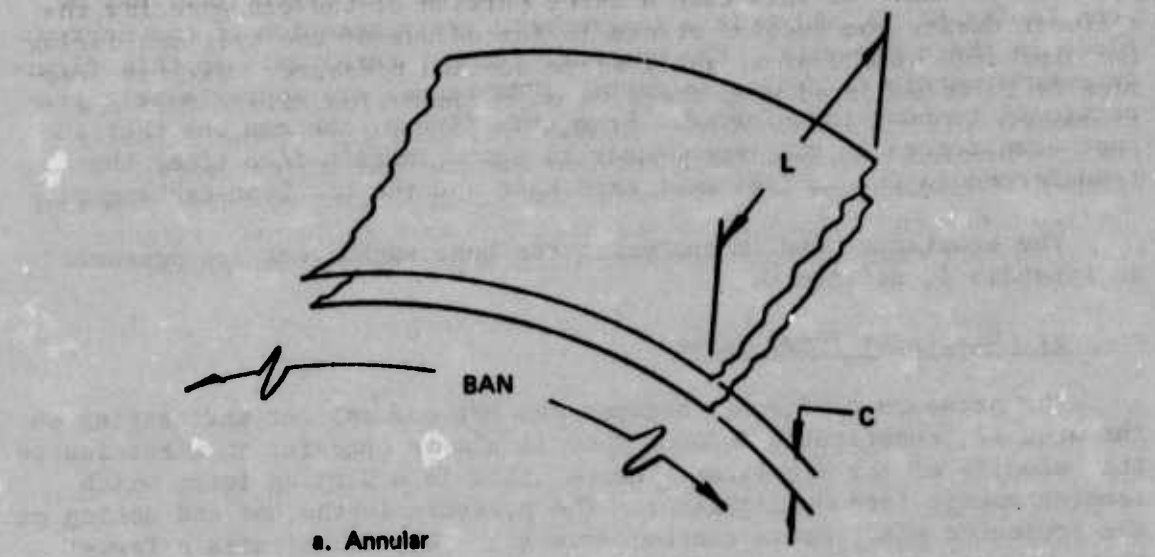
3. Regenerator

We have considered three types of matrices for the regenerator: packed spheres, stacked screens, and cylindrical tube bundles. The heat transfer and pressure drop characteristics of these matrices are represented by the usual correlations of friction factor and Colburn factor versus Reynolds number. We have based the thermal performance of the regenerator on the mean flow rate through it during a cycle, as is commonly done in the analysis of similar devices. However, we have calculated the pressure drop as a function of displacer position to obtain a more complete picture of how the pressure force on the displacer varies throughout the cycle. The equations describing the regenerator are presented in Appendix I, Section B.

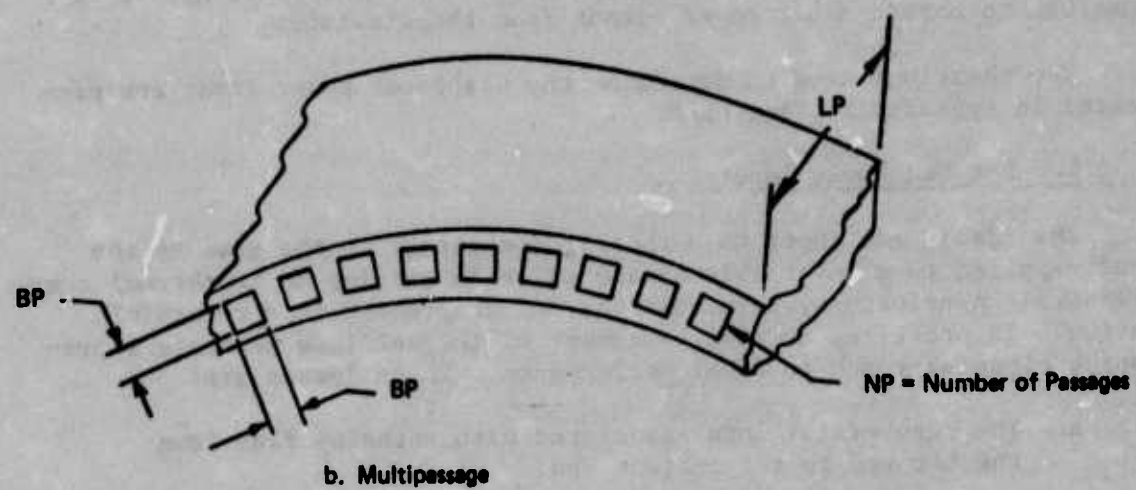
4. Heat Exchangers

We have considered two types of hot and ambient heat exchanger configurations--annular and multipassage, as shown in Figure 11. The annular configuration is simply a thin annular passage, while the multipassage configuration consists of a number of small tubes, with either square or circular cross section, in parallel. The thermal/fluid processes in the heat exchanger are analyzed in a manner similar to the regenerator, i.e., thermal performance is based on the mean flow rate, but pressure drop is calculated as a function of the position of the displacer. The Reynolds number and the length-to-hydraulic diameter ratio for these exchangers are such that we can assume that fully developed laminar flow will exist throughout most of the stroke.

It is worth noting that the heat transferred in the hot and ambient heat exchangers is much less than the heat transferred in the regenerator. Hence, the design of these exchangers, though important, is not nearly as critical as that of the regenerator. The relative amount of



a. Annular



b. Multipassage

FIGURE 11 HEAT EXCHANGER CONFIGURATIONS

heat transferred in the heat exchangers and in the regenerator may be seen in Figure 12, which is a diagrammatic representation of the energy flows in the compressor. The vertical (temperature) axis on this figure is approximately to scale, so vertical distances are approximately proportional to heat transferred. From this figure, one can see that the heat transferred in the regenerator is approximately five times that transferred in the ambient heat exchanger and the hot heat exchanger.

The equations used in analyzing the heat exchangers are presented in Appendix I, Section C.

5. Displacer Power Input

The pressure difference between the hot and ambient ends acting on the area A_2 , constitutes a force that is always opposite in direction to the velocity of the displacer. Hence, this is a damping force which removes energy from the displacer. The pressure in the hot end acting on the projected shaft cross section area ($A_3 - A_2$) constitutes a force that, when integrated around the cycle, provides an energy input to the displacer. The difference between these two energy values determines the net power input which is required to sustain motion of the displacer. A net power input to the displacer is required for most practical designs. However, in extreme cases, in which either the pressure drop through the regenerator is unusually small, or the area ($A_3 - A_2$) is large, it is possible to obtain a net power output from the displacer.

The equations used to determine the displacer power input are presented in Appendix I, Section F.

6. Hot End Power Input

The ideal heat input to a thermal compressor is the same as the heat supplied to a reversible engine which is driving an isothermal compressor. In principle, then, the thermal compressor is a reversible device. In practice, however, a number of thermal loss mechanisms prevent a close approach to ideal performance. These losses are:

- a. The regenerator loss associated with enthalpy flux from the hot end to the ambient end.
- b. Shuttle heat transfer
- c. Displacer/cylinder clearance pumping loss
- d. Conduction through the displacer
- e. Conduction through cylinder walls
- f. Conduction through the regenerator shell(s)
- g. Conduction through the regenerator matrix

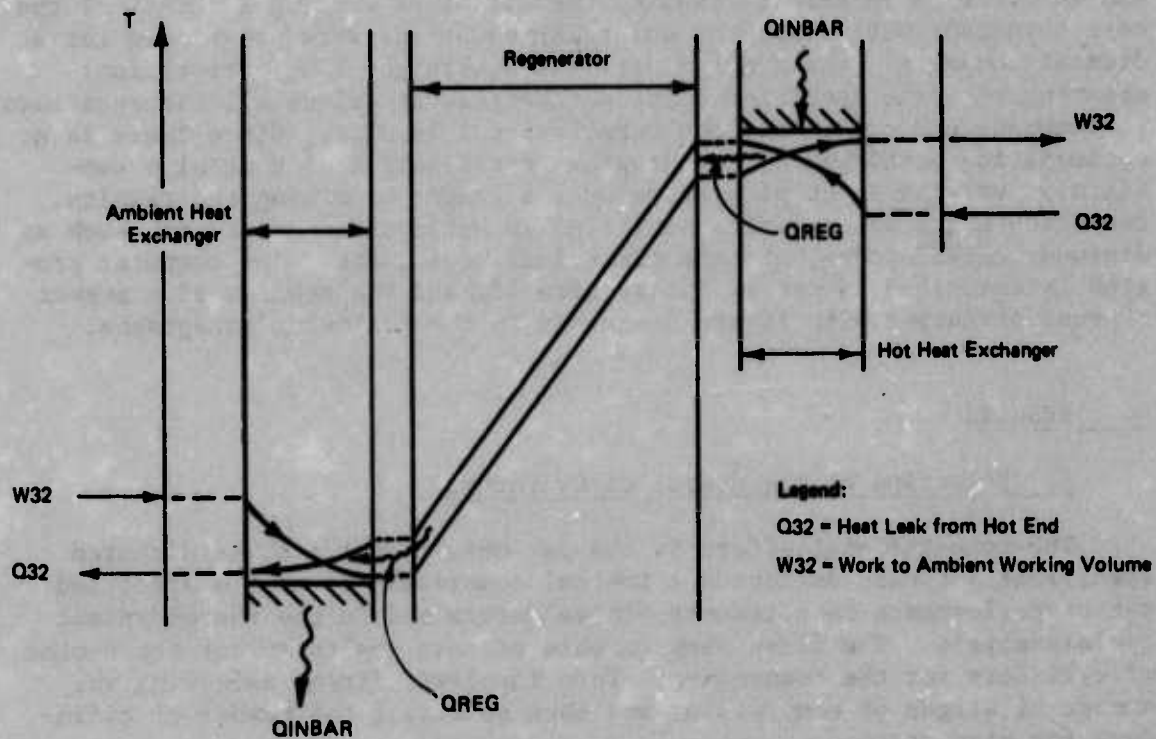
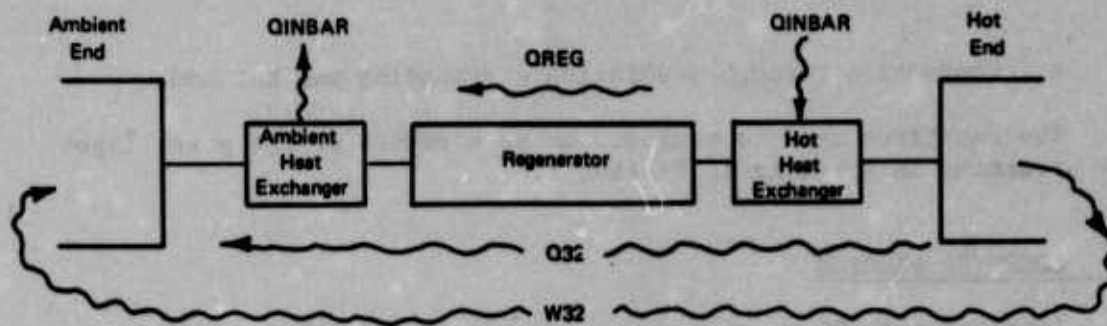


FIGURE 12 ENERGY FLOWS IN THERMAL COMPRESSOR

h. Conduction through insulation surrounding the hot end.

The equations used to evaluate these elements of the power input are presented in Appendix I, Section E.

C. COMPUTER PROGRAM

Approximately 90 equations are required to define the thermodynamic processes which occur in a thermal compressor, and to design the cylinder assembly. Further, 41 input variables must be specified in order to perform the calculations. In order to expedite calculations and in order to be able to examine the effect of varying a number of the more important variables, the governing equations were programmed for a digital computer. The program performs a straight line computation; starting with the specified input parameters, it solves all the equations in sequence and prints out the computational results. Since there is no optimization performed by the program, optimization of a machine consists of varying input parameters over a range, examining the results, and selecting a design which satisfies an optimization criterion such as minimum thermal power, minimum electrical power, etc. The computer program is described in detail in Appendix II, and the results of a number of runs performed with it are described in the following paragraphs.

D. RESULTS

1. Selection of the Number of Cylinders

The computational effort in the parametric analysis was directed specifically toward designing a thermal compressor to meet a specified set of performance requirements--those determined in the thermodynamic cycle analysis. The first step in this process was to select the number of cylinders for the compressor. This involved, first, selecting the number of stages of compression and then selecting the number of cylinders for each stage.

In determining the number of stages of compression, one must consider the flow/pressure ratio characteristic for a single stage of a thermal compressor. Figure 9 showed a plot of volumetric efficiency versus pressure ratio. On this plot, a representative value for the vertical intercept (i.e., the maximum volumetric efficiency) is 60%, and a representative value of the horizontal intercept (i.e., the maximum pressure ratio) is 2.0. A practical design point must, of course, lie between these extremes. Since the overall compression ratio for the compressor is 2.0, it is impractical to use a single stage machine. If two stages were used, each stage would have a compression ratio of 1.41 (the square root of 2); and if three stages were used, each stage would have a compression ratio of 1.26 (the cube root of 2). The corresponding volumetric efficiencies are 36% and 44%. Two stages of compression were selected because this results in less machinery than a machine with

more stages and because the displacer dimensions are reasonable, even though the volumetric efficiency is lower than for a three stage machine.

The next question which must be resolved is the number of cylinders to use for each stage and the overall arrangement of these cylinders and their drive assemblies. In this decision, the following items must be taken into consideration:

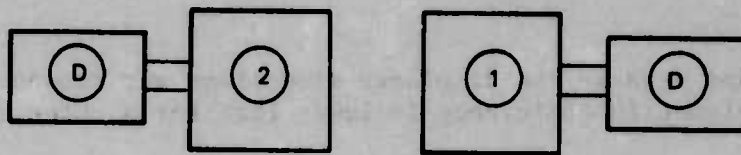
- a. The desire to minimize thermal losses.
- b. The requirement to mount displacers in pairs on a common center line to achieve dynamic balance of the machine.
- c. The desire to minimize the length of the compressor assembly for ease of integration of the refrigerator into the spacecraft.
- d. The desire to minimize the number of components in order to maximize the reliability of the refrigerator and minimize its size, complexity, and cost.
- e. The desire to have a small displacer diameter in order to minimize its fabrication problems.

Three compressor configurations were considered. They are:

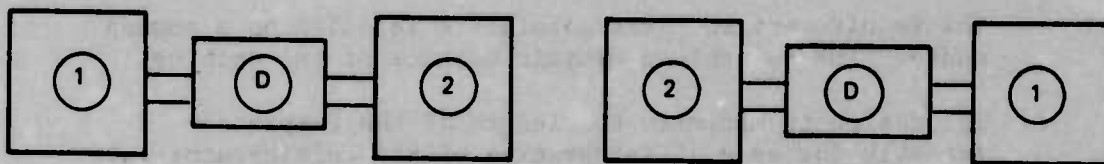
- a. Configuration I, which utilizes one cylinder per stage (for a total of two cylinders) with a drive assembly for each displacer. This results in two compressor modules, each incorporating one cylinder and one drive.
- b. Configuration II, which utilizes two cylinders per stage (for a total of four cylinders) with a double-ended drive assembly for each pair of displacers. This results in two compressor modules, each incorporating two cylinders and one drive.
- c. Configuration III, which utilizes two cylinders per stage (for a total of four cylinders) with a drive assembly for each displacer. This results in four compressor modules, each incorporating one cylinder and one drive.

These three configurations are shown schematically in Figure 13.

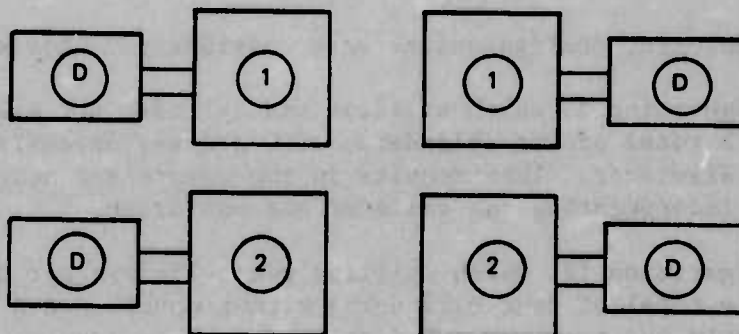
The three configurations are compared in Table VI. Configuration I contains the minimum number of components, and results in the shortest package length. It also permits one heat source, which will simplify the hot end design if heat is transferred to the hot cylinders by, for instance, a heat pipe. Additionally, since Configuration I utilizes the minimum number of cylinders, the heat losses from the hot end will



Configuration I



Configuration II



Configuration III

Legend :

- ⓓ = Displacer Drive Assembly
- ① = First Stage Cylinder
- ② = Second Stage Cylinder

FIGURE 13 THERMAL COMPRESSOR CONFIGURATIONS

TABLE VI

Number of Components							
CONFIGURATION	CYLINDERS	GAS SPRINGS	LINEAR ACTUATORS	ROTARY MOTORS	LVDT's	BEARINGS	TOTAL
I	2	2	2	2	2	4	14
II	4	2	4	2	2	12	26
III	4	4	4	4	4	8	28

be minimized because the parasitic heat losses from a single cylinder compressing the full flow of gas are less than the parasitic heat losses from two cylinders each of which compresses half of the full flow. The displacers in Configuration I are larger than the displacers in Configurations II and III, but they are not excessively large considering previous experience (see Reference 9). Therefore, since Configuration I is reasonable in size, and since it results in the simplest, lowest loss design, this configuration was selected for the compressor. As a result of this selection, the parametric analysis reduced to determining the best configuration for compressor cylinders to meet the following specifications:

	<u>First Stage</u> <u>Cylinder</u>	<u>Second Stage</u> <u>Cylinder</u>
Mass Flow Rate, lb/hr	3.66	3.66
Inlet Pressure, psia	29.4	41.6
Discharge Pressure, psia	41.6	58.8

In accordance with previous experience with Vuilleumier cycle refrigerators, we have used a hot end gas temperature of 1,200°F. For purposes of design, an 80°F ambient end gas temperature was used.

2. Preliminary Screening Runs

Initially, a number of screening runs on the first stage were performed with the thermal compressor computer program, with the object of determining which variables are most critical, which variables could be set early on, and which variables would have to be examined further. A further object was to generate enough information so that some of the input variables could be fixed. In these runs the following items were varied: running speed, the ratio of stroke to piston diameter, regenerator length, and hot cylinder length. The regenerator length was the same as the hot cylinder length in these runs. Initial estimates (based on hand calculations and experience) were used for the other input variables, and remained fixed during these runs. The insulation heat leak (normally calculated from the cylinder geometry) was fixed at 30 watts, a value which can reasonably be achieved in practice.

The initial runs showed that there are two major sources of heat loss from the hot end, shuttle heat transfer and regenerator ineffectiveness. The way in which these losses vary is shown in Figure 14. The trends which are apparent from this figure are:

- a. The shuttle loss decreases rapidly with increasing speed and less rapidly with decreasing stroke-to-diameter ratio.
- b. The shuttle loss decreases with increasing hot cylinder length, and is unacceptably high for a 2 inch hot cylinder length at the lower end of the speed range considered (300 CPM).

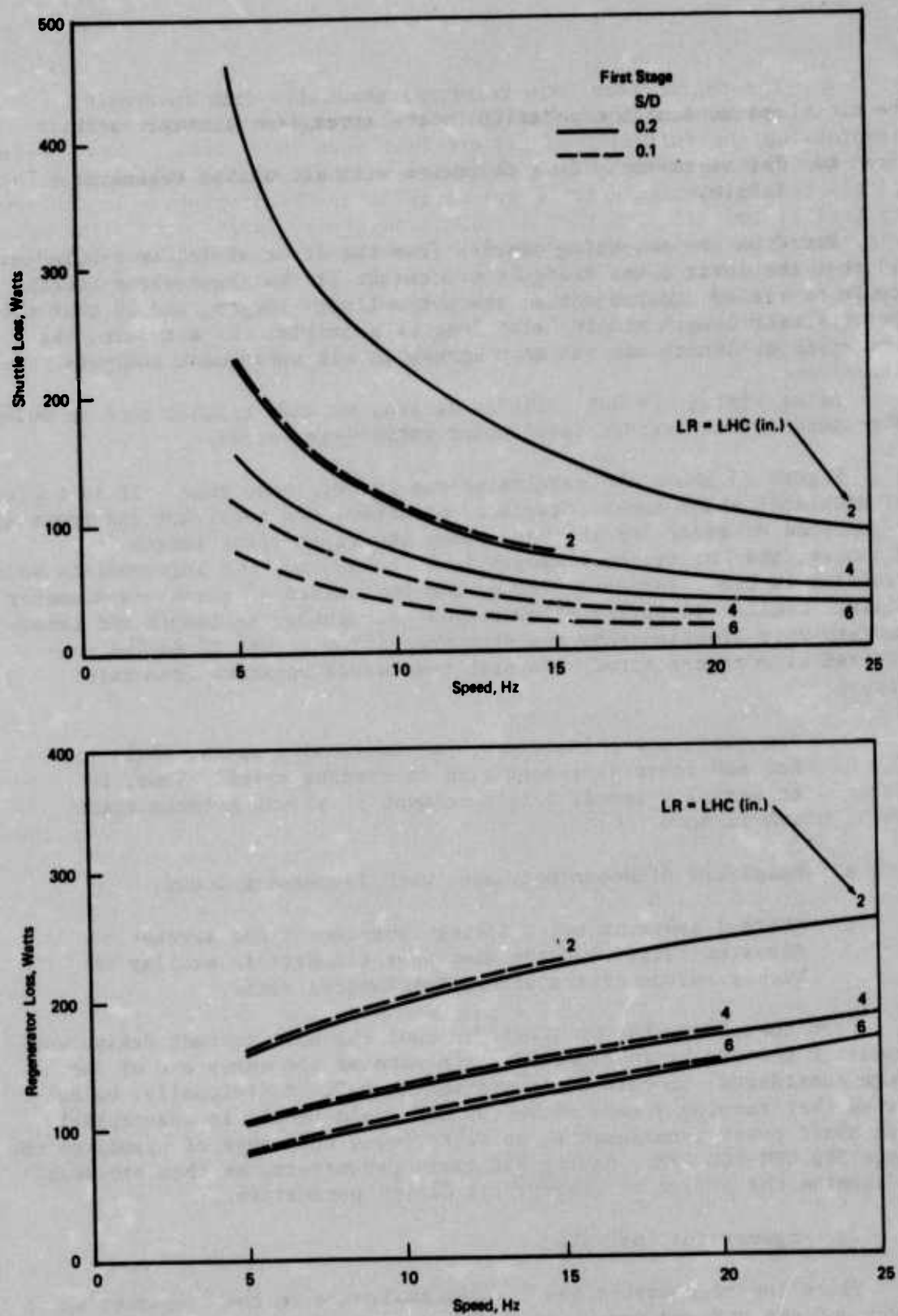


FIGURE 14 LOSSES AS A FUNCTION OF SPEED

- c. The regenerator loss increases gradually with increasing speed, and is unaffected by the stroke-to-diameter ratio.
- d. The regenerator loss decreases with increasing regenerator length.

Based on the foregoing results from the first stage, we concluded: 1) that the least power design would result if the regenerator length could be varied independent of the hot cylinder length, and 2) that the hot cylinder length should be as long as possible. As a result, the hot cylinder length was set at 6 inches in all subsequent analysis.

After fixing the hot cylinder length, we made further runs in which the speed and the stroke-to-diameter ratio were varied.

Figure 15 shows the results of one set of these runs. It is a plot of displacer shaft power, displacer diameter, and total hot end power as a function of speed for the case where the regenerator length is 2 inches, the hot cylinder length is 6 inches, and the intermediate void fraction is 0.5. Data are plotted for two values of stroke-to-diameter ratio. Similar plots for other values of regenerator length and intermediate void fraction show the same trends, so Figure 15 may be considered as representative. Several trends are apparent from this figure.

- a. The shaft power increases with increasing speed, while the hot end power decreases with increasing speed. Thus, in selecting a speed, a balance must be struck between these two factors.
- b. Displacer diameter decreases with increasing speed.
- c. Thermal power is not a strong function of the stroke-to-diameter ratio, but the displacer diameter is smaller at higher values of the stroke-to-diameter ratio.

From these results, we concluded that the most compact design would result if the stroke-to-diameter ratio were at the upper end of the range considered, so this ratio was set at 0.2. Additionally, we concluded that running speeds above 900 CPM would result in unacceptably high shaft power requirements, so we narrowed the range of speeds to the range 300 CPM-900 CPM. Having set these parameters, we then proceeded to examine the effect of regenerator design parameters.

3. Regenerator Analysis

Since the regenerator has a major influence on the displacer shaft power and the hot end power, we made a number of computer runs in order that we might select a regenerator design which would result in a reasonable balance between these two input powers. In these runs, the

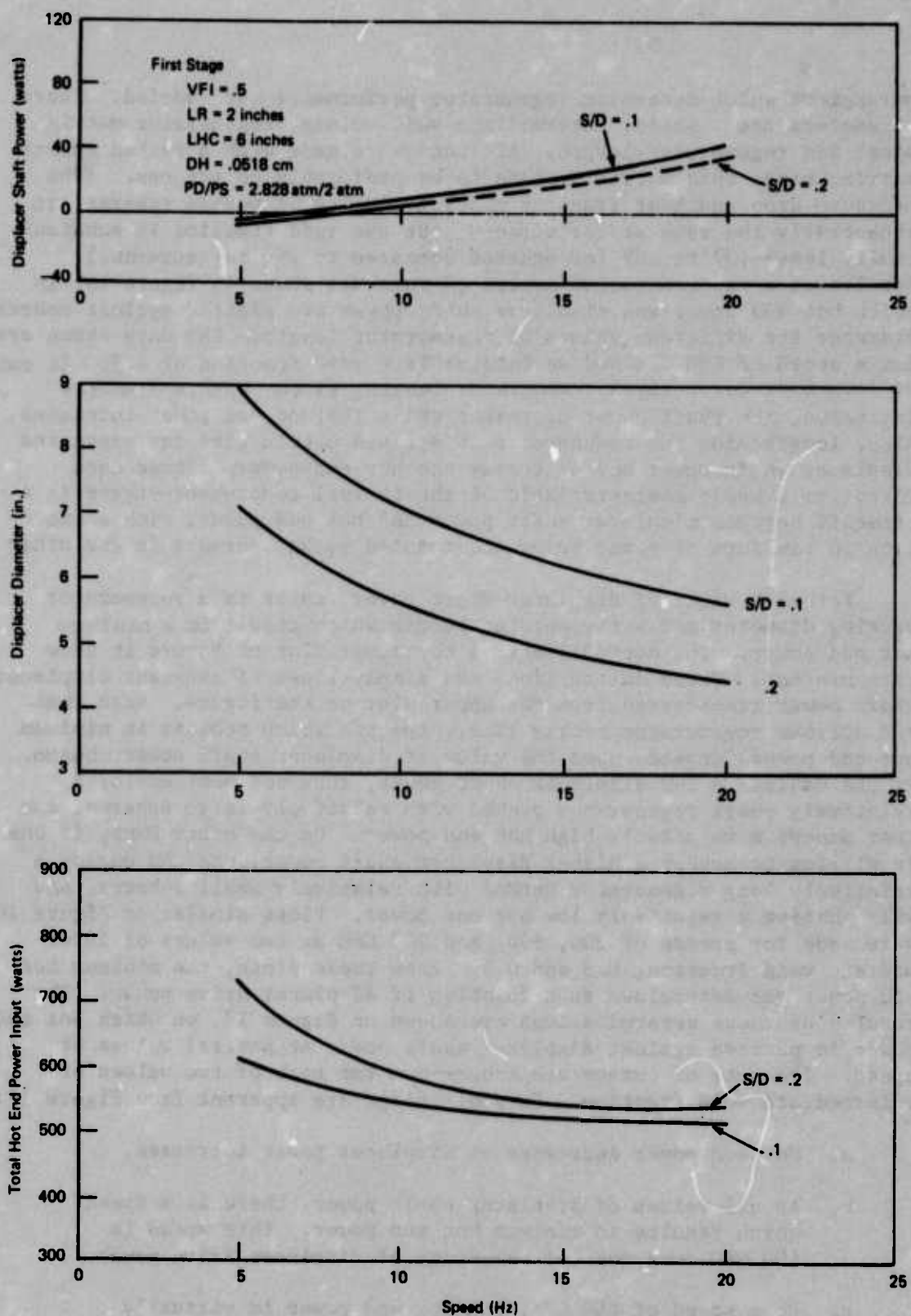


FIGURE 15 POWER AND SIZE AS A FUNCTION OF SPEED

parameters which determine regenerator performance were varied. These parameters are: speed, intermediate void volume, regenerator matrix size, and regenerator length. All runs were made with a packed sphere matrix, since this matrix appears to be preferable to screens. (The pressure drop and heat transfer characteristics of packed spheres are essentially the same as for screens, but the void fraction is substantially less--.37 to .39 for spheres compared to .60 for screens.) Results of a representative series of runs are shown in Figure 16, in which hot end power and displacer shaft power are plotted against sphere diameter for different values of regenerator length. The data shown are for a speed of 600 CPM and an intermediate void fraction of 0.5. It can be seen that for a given regenerator length, as the sphere diameter increases, the shaft power decreases while the hot end power increases. Also, lengthening the regenerator at a fixed matrix size increases the displacer shaft power and decreases the hot end power. These data reconfirm a basic characteristic of the thermal compressor--there is a tradeoff between displacer shaft power and hot end power, with a reduction in one form of power being accompanied by an increase in the other.

For each value of displacer shaft power, there is a regenerator packing diameter and a regenerator length which result in a minimum hot end power. The dotted lines on the lower plot of Figure 16 show this minimum. These dotted lines are simply lines of constant displacer shaft power transferred from the upper plot on the figure. Note that the optimum regenerator matrix (i.e., the one which results in minimum hot end power) depends upon the value of displacer shaft power chosen. If one desires a low displacer shaft power, then one must employ a relatively short regenerator packed with relatively large spheres, and must accept a relatively high hot end power. On the other hand, if one is willing to accept a higher displacer shaft power, one can employ a relatively long regenerator packed with relatively small spheres, and will achieve a relatively low hot end power. Plots similar to Figure 16 were made for speeds of 300, 600, and 900 CPM at two values of intermediate void fraction, 0.3 and 0.5. From these plots, the minimum hot end power was determined as a function of displacer drive power. The results of these determinations are shown on Figure 17, on which hot end power is plotted against displacer shaft power at several values of speed. Two sets of curves are shown--one for each of two values of intermediate void fraction. Several things are apparent from Figure 17:

- a. Hot end power decreases as displacer power increases.
- b. At all values of displacer shaft power, there is a speed which results in minimum hot end power. This speed is 600 CPM over most of the range of displacer drive power.
- c. At a speed of 600 CPM, the hot end power is virtually independent of intermediate void fraction.

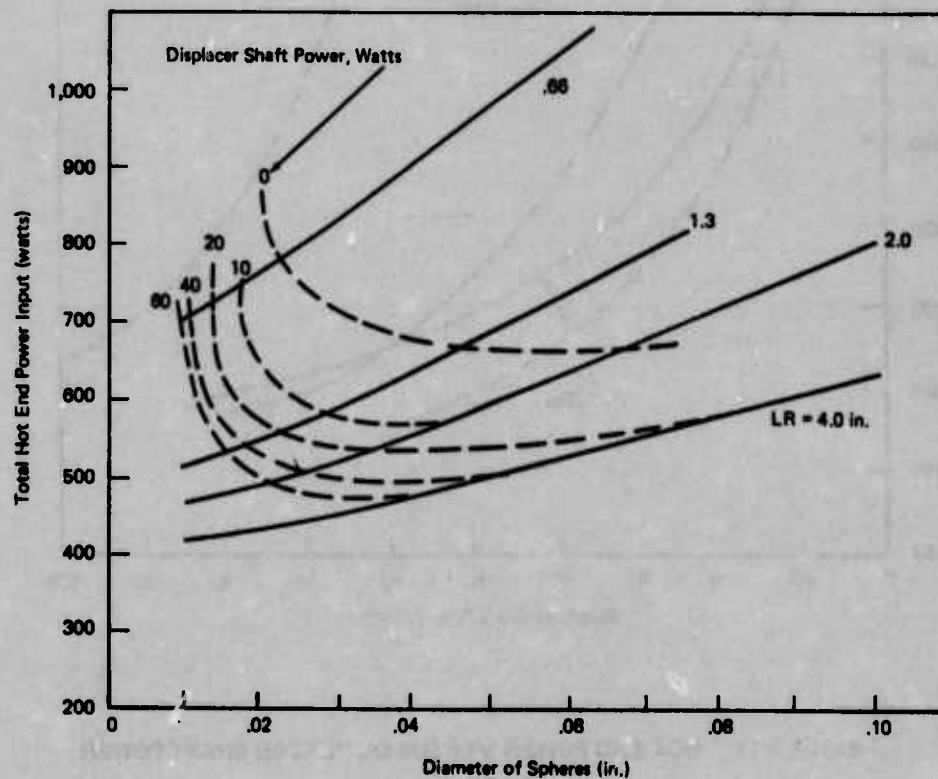
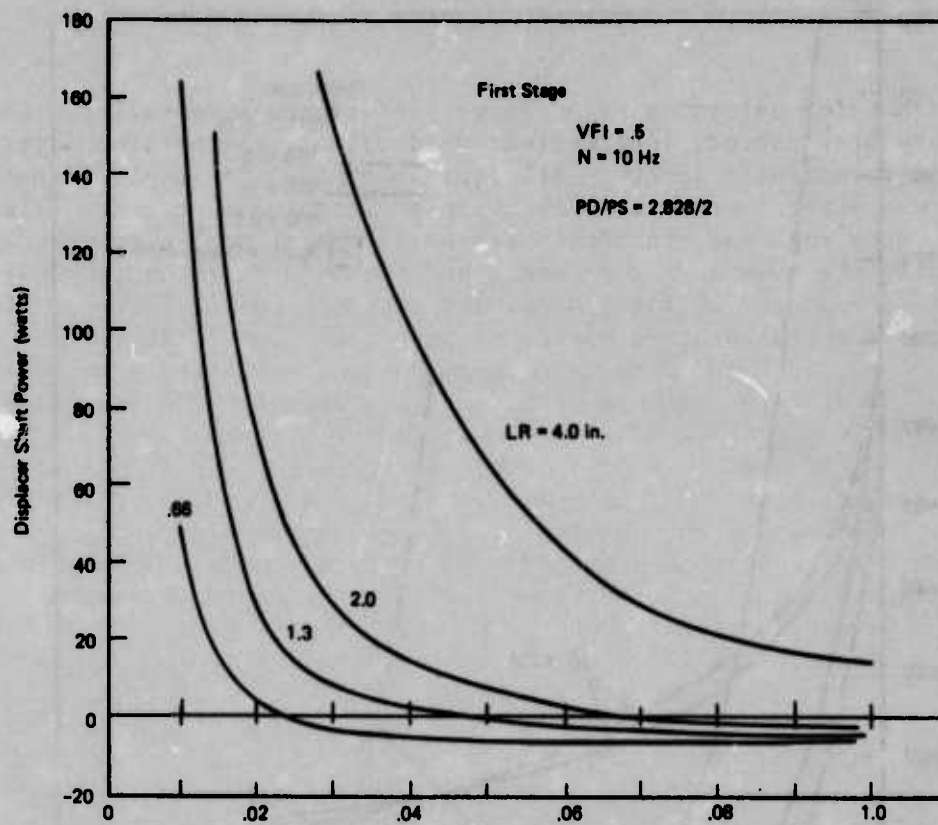


FIGURE 16 POWER AS A FUNCTION OF REGENERATOR MATRIX SIZE

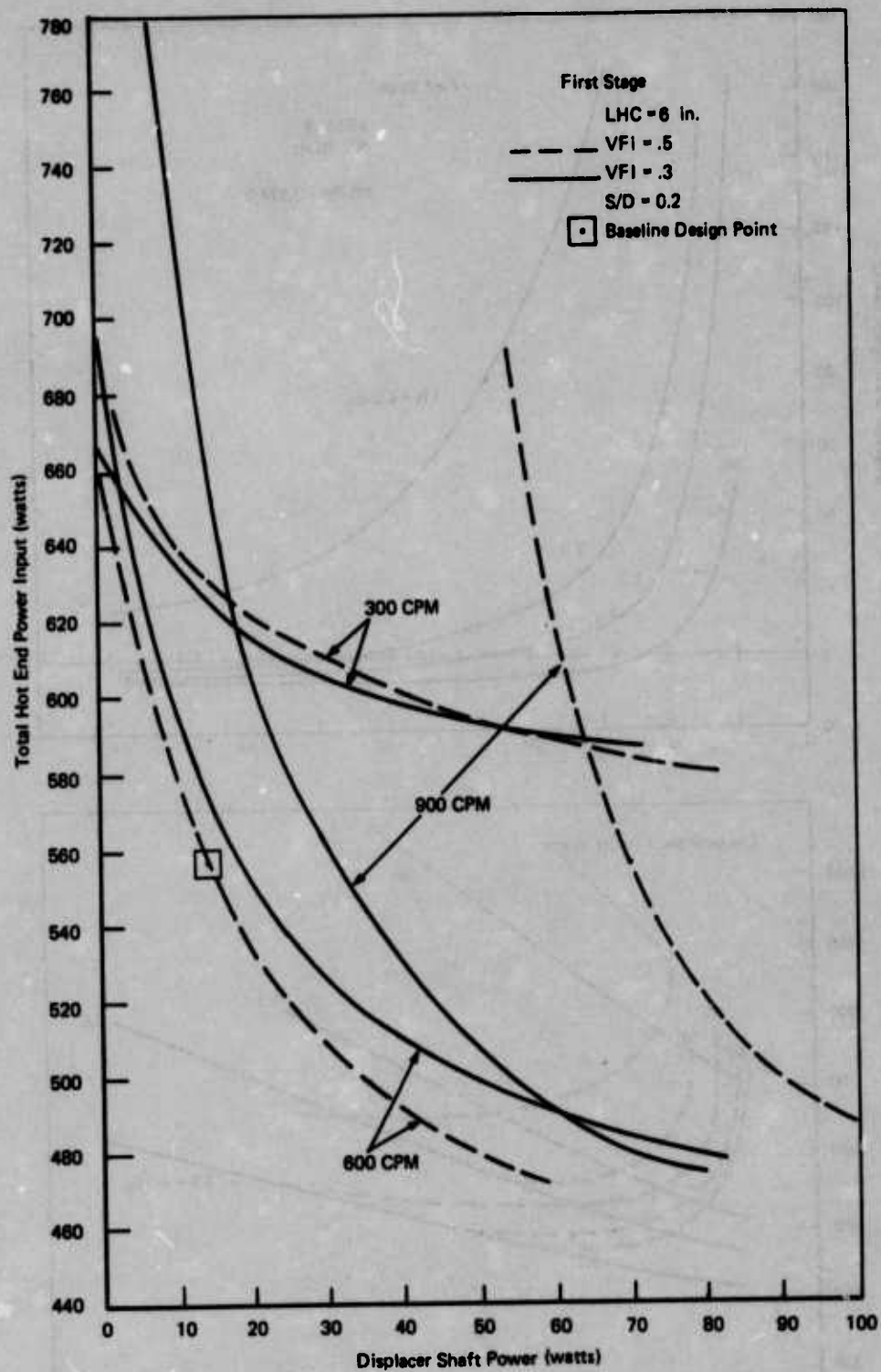


FIGURE 17 HOT END POWER VERSUS DISPLACER SHAFT POWER

4. Selection of Baseline Design Point

The Baseline Design Point was selected primarily by considering the information contained in Figure 17, and the conclusions resulting from it. A speed of 600 CPM was selected, since this results in minimum hot end power. At a speed of 600 CPM, an intermediate void fraction of 0.5 results in somewhat lower hot end power, so an intermediate void fraction of 0.5 was selected.

The selection of regenerator matrix size and regenerator length is not so straightforward, since these parameters determine the displacer shaft power and the hot end power which will be required to run the compressor. Thus, implicit in the selection of the regenerator length and matrix size is a value judgment regarding the relative importance of hot end power (thermal power) and displacer shaft power (electrical power). A prime feature of the thermal compressor is that it reduces the electric drive power required for the refrigerator by substituting thermal power for some of the electric power required by an electric compressor. As noted previously low values of displacer drive power are accompanied by high values of hot end power and vice versa. Thus, in selecting a baseline design point, we must strike a balance between the electric power and the thermal power. In seeking this balance, we ask the following two questions: 1) is there a displacer drive power below which thermal power increases rapidly and above which thermal power decreases rather slowly?; and 2) considering the refrigeration system as a whole, is the electric input power required to overcome pressure differences across the two displacers in proportion to the electric power required for other portions of the refrigerator system? A nominal value of 15 watts of drive power per displacer (or 30 watts for the two displacers) seems to satisfy both these criteria reasonably well. As to the first question, on Figure 17 one can see that, for a speed of 600 CPM and an intermediate void fraction of 0.5, the hot end power increases rapidly at displacer drive powers of less than approximately 15 watts, but that it increases rather slowly at displacer drive powers greater than approximately 15 watts. As regards overall electric power, the entire thermal compressor refrigerator is estimated to require 92 watts of electric power (see Section VI), 20 of which are required by the expander assembly, and thus are completely independent of the compressor design. It does not seem out of proportion to allot 30 watts (approximately one third of the total power) to overcome pressure drop losses in the compressor assembly. Based on the foregoing, we adopted a target of 15 watts for a displacer drive power for each compressor stage. During the compressor design, we selected a regenerator length and matrix size which corresponded to this design point. For the first stage, this results in a regenerator length of two inches and a matrix comprised of .040 inch diameter spheres (from Figure 16).

Summarizing, then, a number of variables were selected and fixed during the course of the parametric analysis. The fixing of these variables specifies a compressor we have termed the baseline design. The primary variables for this design (that is, the ones which have been discussed in this section) are repeated below.

Number of Stages	2
Number of Cylinders Per Stage	1
Stroke-to-Diameter Ratio	.2
Hot Cylinder Length	6 in
Hot End Gas Temperature	1200°F
Ambient Gas Temperature	80°F
Speed	600 CPM
Intermediate Void Fraction	0.5
Displacer Shaft Power	15 watts

Other variables which were fixed during the course of the detailed compressor design are discussed in the next section and/or are displayed in the sample problems in Appendix II.

The baseline design compressor was examined in somewhat more detail in the course of actually laying out the design of the compressor. The examination took the form of making final adjustments to hot and ambient void fractions, and in taking into account in more detail the pressure drop in gas passages which interconnect the working volumes, the regenerators, and the two heat exchangers. As a result of these further refinements of the design, the actual compressor design performance is somewhat different than shown in the parametric curves in this section. The final baseline design is described in the following section.

V. DESIGN OF BASELINE THERMAL COMPRESSOR

A. GENERAL

We have generated the preliminary design of a rotary-reciprocating thermal compressor to meet performance specifications listed in Table II; that is, a compressor to compress 3.66 lb/hr of helium gas at 300 K from 29.4 lb/in² inlet pressure to 58.8 lb/in² discharge pressure. The design of the compression cylinders has utilized the results of the parametric analysis described in the preceding section. The major emphasis in the design of the cylinder assemblies has been on the displacers, heat exchangers, regenerators, and valving. Relatively little emphasis has been directed toward the type of heat source used or its integration with the cylinders. The design of the drive assemblies has drawn upon our previous experience with rotary-reciprocating compressors and expanders. The drive assemblies have been designed along the lines of previous devices--that is, they utilize a rotary motor and linear actuator to drive the displacer, and contain gas springs to provide a restoring force to the displacer.

The first stage of the baseline design thermal compressor is shown in Figure 18, and the second stage is shown in Figure 19. The compressor is a two-cylinder machine, with the two cylinders arranged in line on a common axis. The hot ends of both cylinders are in the center of the assembly, and are surrounded by a vacuum shell containing high temperature insulation. Electrical cables connect the drive assemblies to a power conditioning equipment (PCE) assembly. The PCE assembly controls the power to the linear actuators and rotary motors in the drive assembly. The characteristics of the baseline design are summarized in Table VII. The following paragraphs describe the various elements in the compressor.

B. FIRST STAGE CYLINDER ASSEMBLY

The first stage cylinder assembly consists of the cylinder, the displacer, the regenerator, the hot and ambient heat exchangers, and a porting system. The pressure-containing shell of the cylinder bolts onto a large flange on the end of the vacuum shell. There is a .010 inch thick cylindrical section in this piece immediately adjacent to the attachment flange. This section is the outer shell of the regenerator. The wall is thin in this zone to minimize axial conduction down the wall of the regenerator, since the entire temperature gradient in the machine appears across this section. The wall thickness of the cylinder is increased in the zone between the regenerator and the head of the cylinder. This zone contains two gas flow passages and the hot heat exchanger. The head of the cylinder is also thick--both to reduce stresses and to provide a good conductive heat transfer path across the entire cylinder head. A hollow tubular insert in the shell of the cylinder contains the cylinder itself and the inner boundaries

TABLE VII
SUMMARY OF BASELINE DESIGN THERMAL COMPRESSOR

Process Fluid	Helium Gas	
Flow Rate	3.66 LB/HR	
Hot End Gas Temperature	1,200°F	
Ambient End Gas Temperature	80°F	
	<u>First Stage</u>	<u>Second Stage</u>
Inlet Temperature °F	80	80
Inlet Pressure, LB/IN ²	29.4	41.6
Discharge Pressure, LB/IN	41.6	58.8
Displacer Diameter, IN	5.6	4.7
Stroke, IN	1.12	1.12
Reciprocating Speed, Cycles/Min	600	600
Rotational Speed, Rev/Min	300	300
Input Power (Total for Both Stages)		
Thermal, Watts	1,064	
Electrical, Watts	72	
Overall Diameter ⁽¹⁾ , IN	12	
Overall Length ⁽¹⁾ , IN	60	
Weight ⁽¹⁾ , Pounds	155	

⁽¹⁾Not including power conditioning equipment.

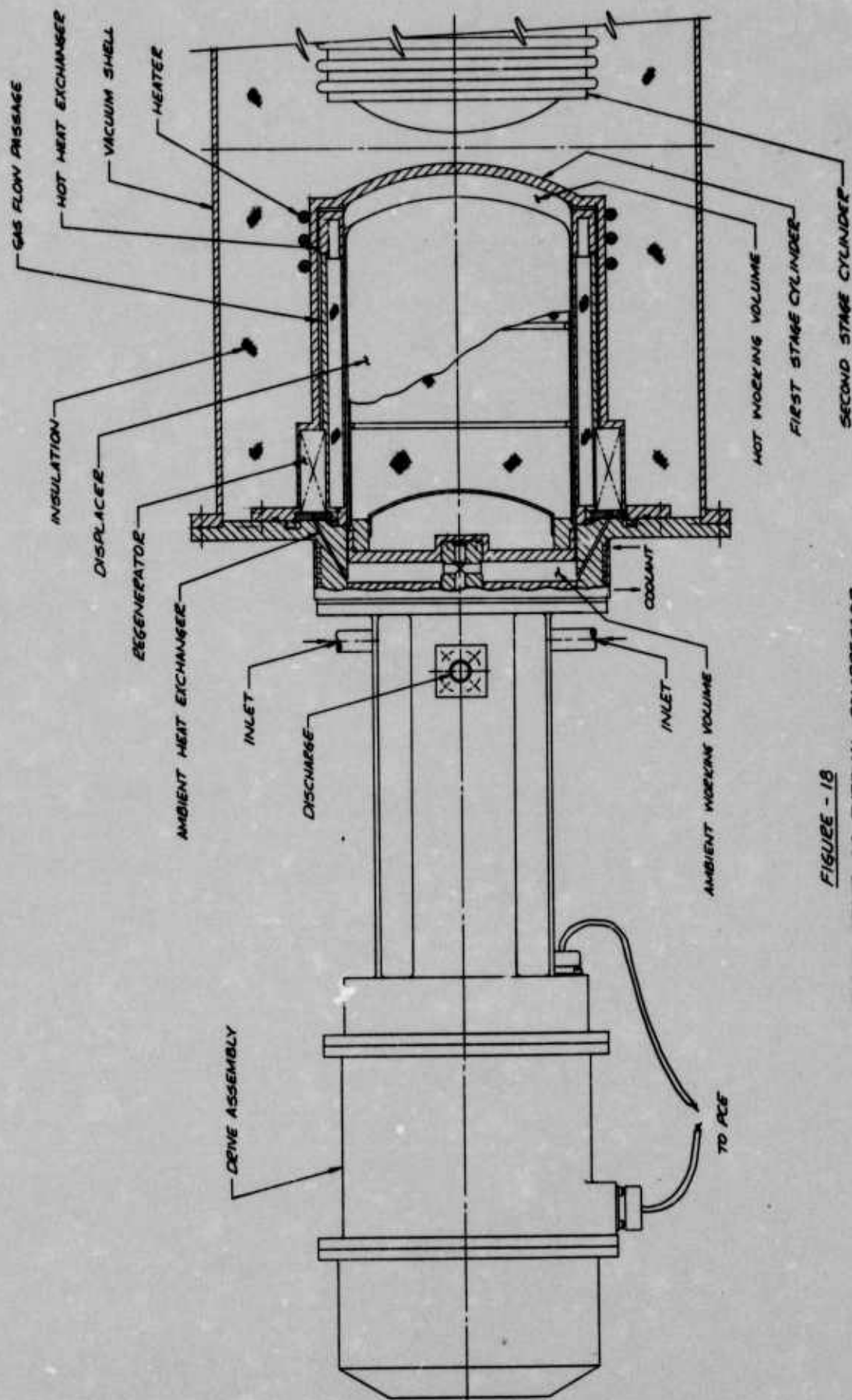


FIGURE - 18
 FIRST STAGE OF THERMAL COMPRESSOR

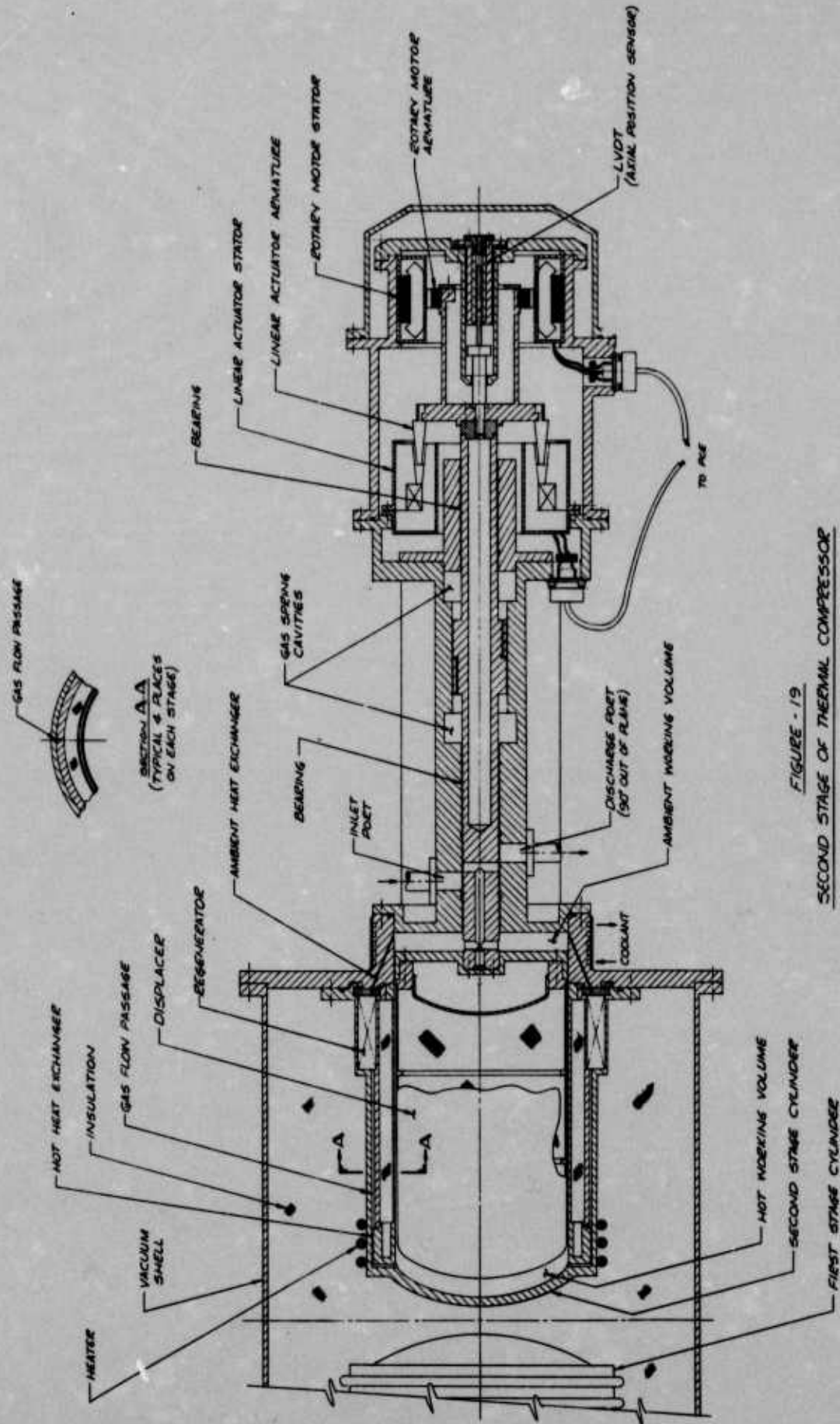


FIGURE - 19
SECOND STAGE OF THERMAL COMPRESSOR

of the regenerator, gas flow passages and the hot heat exchanger. This insert contains a 6 inch long, .010 inch thick section adjacent to the displacer, over which the entire hot end temperature gradient appears. It contains a shorter, .010 inch thick section in the vicinity of the regenerator. The hollow annulus in the insert is evacuated and filled with insulation to reduce heat transfer from the cylinder wall to the hot heat exchanger and regenerator. This is necessary since the temperature gradient in the cylinder wall is different than the temperature gradient in the hot heat exchanger and the regenerator. The outer cylinder and the insert are both made of Inconel 718.

The displacer consists of two pieces, an aluminum disc at the ambient end and an Inconel 718 hat section which is mounted to the aluminum disc. The displacer is 5.6 inches in diameter. It is hollow, and is evacuated and filled with insulation. The wall of the displacer is reduced to the extent possible considering that it is a vacuum vessel. It is .030 inches thick and contains several internal stiffening rings. There is a .020 inch radial gap between the displacer and the cylinder in the zone over which the temperature gradient occurs to reduce the shuttle heat transfer losses. This gap is also sufficient to eliminate any mechanical problem associated with distortion of the hot ends of the displacer or the cylinder. Bypass flow through the annular gap between the displacer and the cylinder is limited by a clearance seal at the ambient end of the displacer. The radial gap in this seal area is .001 inches. The displacer is aligned in the cylinder by the two gas bearings in the drive assembly. The clearance in these bearings is less than the clearance in the displacer seal, and concentricity tolerances are such that there is no contact between displacer and the cylinder.

The regenerator is annular in shape. It is two inches long, and has an inside diameter of 6.6 inches and an outside diameter of 7.9 inches. It is packed with 0.40 inch diameter stainless steel spheres which are spring loaded in the axial direction to prevent the packing from rattling. The effectiveness of the regenerator is calculated to be 97%.

The hot heat exchanger is an annulus defined by the inside of the outer cylinder wall and the outside of the tubular insert. It is 1.3 inches long and has an annular gap of .055 inches. Its effectiveness is specified to be 90%.

The ambient heat exchanger also has an annular configuration. It is fabricated by joining (brazing or welding) a tapered insert into the housing prior to final machining of the housing. The gap between the insert and the main housing serves as the ambient heat exchanger. This heat exchanger is 1.8 inches long and has a radial gap of .035 inches. Its effectiveness is specified to be 90%.

The porting is contained in the displacer drive shaft. It consists of two transverse holes which are connected by an axial hole on the shaft center line. The transverse hole adjacent to the displacer is always in communication with the ambient working volume, while the other transverse hole communicates with the inlet and discharge ports in the housing at appropriate axial positions for correct valving action. Figure 20 indicates the port opening and port closing points. It shows the pressure in the first and second stage ambient working volumes as a function of displacer position for the condition of no pressure drop in the porting. For this condition, the first stage inlet ports start to open .51 inches from top dead center and are completely closed at bottom dead center, while the first stage discharge ports start to open at .43 inches from top dead center and are completely closed at top dead center. The actual location of the two port opening points must take into account the pressure drop through the ports as they start to open. When this pressure drop is taken into account, the opening point of the suction port will be shifted slightly toward top dead center, and the opening point of the discharge port will be shifted slightly toward bottom dead center. There will be little or no change in the location of the port closing points, however, since the piston velocity, and hence porting pressure drop, is very low at the two extremes of stroke.

The porting zone is bounded by two circumferential grooves in the housing; the one adjacent to the inlet port is communicated to inlet pressure, and the one adjacent to the discharge port is communicated to discharge pressure. These grooves confine the axial and circumferential pressure gradients in the porting zone, and provide a constant pressure boundary for the clearance seal on one side and the gas bearing on the other.

The thermal input power to the hot end of the cylinder must be sufficient to provide the ideal P-V energy to the hot working volume and also to make up for thermal losses. For the first stage, the ideal input power is 172 watts and the losses are 380 watts (approximately 2.2 times the ideal input power) so the total heat input to the hot end is 552 watts. A breakdown of this power is shown in Table VIII. Note that the major losses are due to shuttle heat transfer and regenerator ineffectiveness.

In Figure 18 the heat source at the hot end of the cylinder has been shown as an electric heater. This form of heat input has been shown for illustrative purposes only. Other heat sources could also be used--for instance, focused sunlight or heat from a radioisotope. The type of heat source which is most appropriate to a specific application and the means of transferring this heat into the hot cylinder (for instance, via a heat pipe or via radiation) would depend upon system considerations. Of course, the thermal interface at the hot end would have to be tailored to the heat source and the heat transfer means. The fact that both hot cylinders are adjacent to each other will simplify integration of the heat source.

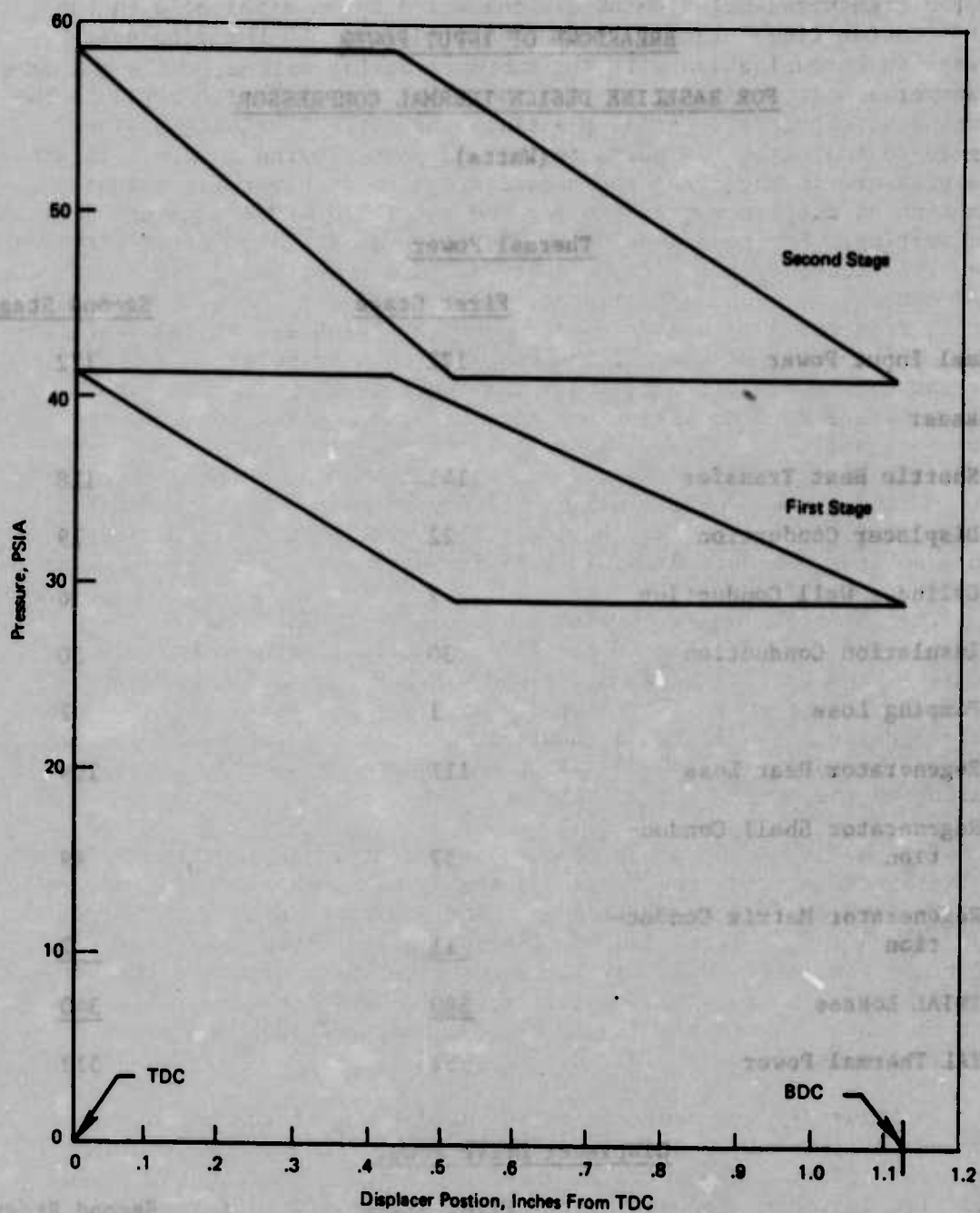


FIGURE 20 PRESSURE IN AMBIENT WORKING VOLUME AS A FUNCTION OF DISPLACER POSITION

TABLE VIII

BREAKDOWN OF INPUT POWER
FOR BASELINE DESIGN THERMAL COMPRESSOR

(Watts)

	<u>Thermal Power</u>	
	<u>First Stage</u>	<u>Second Stage</u>
Ideal Input Power	172	172
Losses:		
Shuttle Heat Transfer	141	118
Displacer Conduction	22	19
Cylinder Wall Conduction	7	6
Insulation Conduction	30	30
Pumping Loss	1	2
Regenerator Heat Loss	111	109
Regenerator Shell Conduction	57	49
Regenerator Matrix Conduction	<u>11</u>	<u>7</u>
TOTAL Losses	<u>380</u>	<u>340</u>
TOTAL Thermal Power	552	512

Displacer Drive Power

	<u>First Stage</u>	<u>Second Stage</u>
Pressure Drop Loss	26	25
Input from Hot End	<u>11</u>	<u>10</u>
Net Drive Power	15	15

Table VIII also gives a breakdown of the displacer drive power, and indicates that the 26 watt pressure drop loss is partially supplied by 11 watts of power from the hot working volume (due to the difference in area between the hot working volume and the cold working volume). Thus, 15 watts of power must be supplied to the displacer from the drive assembly.

Heat rejection at the ambient end of the cylinder is accomplished by circulating a coolant through machined passages in the cylinder housing. An estimate of the power consumption of the pump in the heat rejection system has been included in Section VII, in which a refrigeration system incorporating a thermal compressor and a refrigeration system incorporating an electrical compressor are compared.

C. SECOND STAGE CYLINDER ASSEMBLY

In its overall configuration, the second stage cylinder assembly (Figure 19) is the same as the first stage assembly; the only differences being that some of the dimensions are different. The stroke and speed of the second stage are the same as the first stage (1.12 inches and 600 CPM, respectively) to permit dynamic balance of the compressor as a whole. A displacer diameter of 4.7 inches is required to give the proper throughput at this speed and stroke. The annular regenerator is 2 inches long and has an inside diameter of 5.7 inches and an outside diameter of 6.8 inches. It is packed with .034 inch diameter stainless steel spheres and its effectiveness is calculated to be 97%. The hot and ambient heat exchangers are of an annular configuration. The hot heat exchanger is 1.0 inches long with a radial gap of .038 inches and has an effectiveness of 90%, while the ambient heat exchanger is 1.7 inches long, with a radial gap of .029 inches and has an effectiveness of 90%. A pressure versus displacement diagram and the porting dimensions were shown in Figure 20. It can be seen from this figure, for the condition of no pressure drop in the porting, the inlet port starts to open .51 inches from top dead center and the discharge port starts to open .43 inches from top dead center. The thermal input power to the second stage is 512 watts. The breakdown of this power was shown in Table VIII. As with the first stage, the major losses are due to shuttle heat transfer and regenerator ineffectiveness. The displacer drive power for the second stage is 15 watts. A breakdown of this power was also shown in Table VIII.

D. DRIVE ASSEMBLIES

The two drive assemblies are identical. They each contain two gas bearings to support the displacer, a gas spring to resonate the displacer mass, a linear actuator to drive the displacer, a rotary motor to rotate the displacer, and an LVDT to provide an axial position signal to the amplitude control circuitry. The material of construction is aluminum

throughout, with the exception that the linear actuator and rotary motor use Vanadium Permendur in the magnetic circuits.

The gas bearings are 360° journal bearings which are one inch in diameter by two inches long. They operate at the first stage discharge pressure. Each bearing has a radial clearance of 75 microinches and has a load carrying capacity of 12 pounds at an operating eccentricity ratio of 0.3. This load capacity is sufficient to support weight loads, the pneumatic load in the porting area, plus magnetic forces from the linear actuator and rotary motor. All surfaces on the bearing diameters (that is, bearings, seals, and porting) are coated with plasma-sprayed chromium oxide to provide wear resistance at startup and shutdown.

The clearance seals between the bearings and the gas spring cavities limit the leakage flows from the gas spring cavities. The clearance seal between the outboard bearing and the motor cavity limits the leakage from the bearing (which operates at first stage discharge pressure) and the motor cavity (which operates at the inlet pressure to the stage). All seals have the same clearance as their adjacent bearings.

The gas spring must have an equivalent spring constant such that the resonant frequency of the 6.8 pounds displacer is 600 CPM--that is, an equivalent spring constant of 69 pounds per inch. For the case in which the gas spring pressure is referenced to the first stage inlet pressure at the neutral position, this equivalent spring constant will result from a gas spring which has an outside diameter of 1.7 inches and an inside diameter of 1.0 inches (the bearing diameter), and a dead volume at neutral position which is four times one half of the displacement volume of the gas spring. For this design, the pressure in the gas spring, cavity will fluctuate between 20.2 psia and 47.3 psia. The power loss in the gas spring due to heat transfer effects is estimated to be in the range of 5-10 watts for this design. To be conservative, the larger figure has been used in determining power requirements. Each gas spring cavity is referenced to the first stage inlet pressure each time the displacer passes through the midstroke position. This is accomplished by a porting system located on the large diameter of the gas spring. There are also clearance seals on this diameter to limit leakage flow between the gas spring porting system and the spring cavities.

The linear actuator provides the driving power to reciprocate the displacer. It drives the displacer toward the hot end during half of the stroke, and gas pressure forces drive the displacer toward the ambient end during the other half of the stroke. The power which the linear actuator must supply to the displacer is the sum of all the losses minus the power delivered by the hot working volume. This power is calculated to be 25 watts for each compressor stage (see Table IX).

TABLE IX

ACTUATOR DRIVE POWER REQUIREMENTS

(Watts)

	<u>First Stage</u>	<u>Second Stage</u>
Losses:		
Pressure Drop across Displacer	26	25
Gas Spring Losses	10	10
Viscous Shear in Bearings and Seals	<u>Negligible</u>	<u>Negligible</u>
TOTAL Losses	36	35
Gain Due to Area Difference	<u>11</u>	<u>10</u>
Net Actuator Shaft Power Requirement	25	25

Since all displacer losses are viscous in nature, the peak actuator force will be required at the point in the reciprocating cycle where the velocity is the greatest--that is, at midstroke. This peak force is 14.1 pounds. Iron and copper losses in the actuators are estimated to be 5 watts, so the electrical input power to each actuator is 30 watts (the shaft power plus the actuator losses). The actuator design is similar to actuators which have been built in the past. They will consist of a large number of tapered laminations bonded into the ring. The magnetic material in the actuators is Vanadium Permendur.

The rotary motor must have sufficient starting torque to overcome static friction and sufficient running torque to overcome viscous shear losses in the bearings and seals. It must be able to develop 1.6 pound-inches of starting torque and .018 pound-inches of running torque. At 300 rpm, the rotational speed of the displacers, the running torque is equivalent to .01 watts of input power. A value of 1 watt of input power to each rotary motor has been used in determining input power requirements. The mechanical design of the rotary motor is similar to previous devices. It will incorporate a permanent magnet motor and a two-pole-pair stator of conventional construction. The magnetic material will be Vanadium Permendur.

E. SUMMARY OF THE DESIGN

The salient features of the design of the baseline thermal compressor were given in Table VII. The breakdown of the electrical input power and the weight are given in Tables X and XI.

TABLE X
BREAKDOWN OF ELECTRICAL INPUT POWER FOR BASELINE

<u>THERMAL COMPRESSOR</u>	
(Watts)	
First Stage Linear Actuator	30
First Stage Rotary Motor	1
Second Stage Linear Actuator	30
Second Stage Rotary Motor	1
Power Conditioning Equipment Losses	<u>10</u>
TOTAL	72

2
TABLE XI

WEIGHT BREAKDOWN OF BASELINE THERMAL COMPRESSOR

(Pounds)

Two Moving Masses	13.6
Vacuum Shell and Insulation	22.4
Two Cylinder Assemblies	32.2
Two Housing Assemblies ⁽¹⁾	41.0
Two Linear Actuator Stators	19.8
Two LVDT's	2.0
Two Rotary Motor Stators	7.6
Auxiliaries ⁽²⁾	<u>16.4</u>
TOTAL	155

(1) Includes Porting, Gas Spring, and Motor Housings

(2) Piping, Valves, Surge Chambers, Electrical Fittings

VI. SYSTEM COMPARISONS

In the preceding section, we discussed the baseline thermal compressor as a system component. In this section, we compare the overall characteristics of a complete refrigeration system which incorporates a thermal compressor against a system which incorporates an electric compressor. Both systems are sized to meet the refrigeration specifications which were listed in Table I.

In Table XII, the major features of the two refrigeration systems are compared. In this comparison, the refrigerator is considered to consist of the compressor and expander assemblies, their power conditioning equipment, and the interconnecting piping between the two assemblies. It does not consider either the weight or power consumption of the heat rejection system, or the weight of the electrical or thermal power supplies.

It is seen that the system with a thermal compressor requires considerably more power than the system with an electric compressor; 1,156 watts compared to 587 watts, or twice as much power for the thermal compressor system. However only 92 watts, or 8%, of the power for the thermal compressor system is in the form of electrical energy. This is 15% of the electrical power required by the electric compressor system. From these power figures, and from the power consumption of other systems compared during the course of this study, we can make the following generalizations:

1. The total power requirement of a thermal compressor refrigerator is 2-3 times that of an equivalent electric compressor refrigerator.
2. The electrical power requirement of a thermal compressor refrigerator is 15-25% of that of an equivalent electric compressor refrigerator.
3. The thermal power requirement of a thermal compressor refrigerator is 2-2 1/2 times the electrical power requirement of an equivalent electric compressor refrigerator.

The size of the two refrigerators are virtually the same, while the weight of the thermal compressor refrigerator is somewhat greater (approximately 40%) than the electric compressor refrigerator.

The thermal compressor refrigerator contains a thermal compressor, an expander assembly, a power conditioning equipment module for each assembly, and interconnecting piping. The thermal compressor is as described in the preceding section. The expander assembly is similar to the one being built in a current program (see Reference 3). It consists of a central, cylindrical vacuum shell which contains the expansion engines, heat exchangers, cold piping, and auxiliaries. A rotary reciprocating drive assembly, which controls the motions of the pistons, is mounted on each end of the vacuum shell.

TABLE XII
SYSTEM COMPARISONS

	<u>Refrigerator with Thermal Compressor</u>	<u>Refrigerator with Electric Compressor</u>
Input Power, Watts		
Electric Power		
Compressor	72	567
Expander	<u>20</u>	<u>20</u>
TOTAL Electric	92	587
Thermal Power	1,064	---
Size, Inches⁽¹⁾		
Compressor Assembly	12 DIA x 60	6 DIA x 49
Expander Assembly	14 DIA x 51	14 DIA x 51
Compressor PCE	9 x 4 x 19	9 x 4 x 19
Expander PCE	9 x 4 x 19	9 x 4 x 19
Weight, Pounds		
Compressor Assembly	155	70
Expander Assembly	70	70
Compressor PCE	15	20
Expander PCE	<u>15</u>	<u>15</u>
TOTAL	255	175

(1) The sizes given are overall envelope dimensions.

Each drive assembly contains a rotary motor, a gas spring, a linear actuator, and electrical sensors for the control system. From the thermodynamic flowsheet (Figure 5), it can be seen that the power extracted by the engines is 17.5 watts for the first stage, 4.93 watts for the second stage, and .790 watts for the third stage. It will probably be desirable to split the first stage load between two, identical 8.75 watt engines in order to make the engine capacities for the three stages more nearly the same. This will ease the problem of selecting a speed and stroke length which will result in reasonable dimensions for all three stages. For this design, one first stage engine and the second stage engine are driven by one drive assembly, and the other first stage engine and the third stage engine is driven by the other drive assembly. The two engines on the same drive shaft are mounted in-line. The first stage engine is driven by a shaft from the drive assembly, while the colder engine is driven by a drive shaft which penetrates the head of the first stage engine. The heat exchangers and piping surround the engines within the vacuum shell. Cold gas from the discharge of each engine is piped in a vacuum insulated line from the expander assembly to the item to be cooled.

The power conditioning equipment for each assembly is identical in concept to the equipment presently being developed (see Reference 3). It consists of solid state power and logic components mounted on a number of printed circuit cards and contained within an aluminum enclosure. Since the thermal compressor contains two less linear actuators than the electric compressor, there are two less linear actuator inverters, with a corresponding reduction in components. Additionally, since the electrical power levels in the thermal compressor are less than the electric compressor, the power handling portions of the system (power supplies and inverters) contain fewer, more lightly stressed components. Both of these factors result in a somewhat higher reliability for the thermal compressor electronics. The power conditioning equipment for the expander assembly is nearly identical to that presently under development, except that it handles less power than this equipment.

The electric compressor refrigerator also contains a compressor assembly, an expander assembly, a power conditioning equipment module for each assembly, and interconnecting piping. The expander assembly and its power conditioning equipment are identical to their counterparts in the thermal compressor refrigerator. The compressor assembly and its power conditioning equipment are similar to, but smaller than, equipment presently under development (see Reference 3).

The system comparisons in Table XII did not include an allowance for the weight or power of the heat rejection system (liquid pumps, radiator, and piping). Our experience with similar spaceborne systems has been that the pumping power is in the range of 5-10% of the heat rejected (i.e., the total input power to the refrigerator), and that the weight of the heat rejection system is 50 lb per kilowatt of heat rejected, if the heat is rejected at 300 K.

VII. CONCLUSIONS

Based on the analysis described in this report, it is concluded that the thermal compressor is a viable alternative to an electric compressor in spaceborne, rotary reciprocating, cryogenic refrigeration systems. A thermal compressor is a precision machine, but no extraordinary technical problems are foreseen, either in analyzing machine performance or in designing and fabricating it. A thermal compressor employs existing technology throughout, and the machine evaluated in this study is of a general size which is comparable to existing devices.

The thermal compressor has a number of characteristics which are unique. The most evident is the fact that it uses heat as the driving source. For an ideal thermal compressor, i.e., one with no losses, the thermal input power is the isothermal work of compression multiplied by the efficiency of a reversible heat engine operating between the heat source temperature and the heat sink temperature. In a practical device, the thermal input power is in the vicinity of 3-4 times this power.

The volumetric efficiency of a compression stage is a function of the compression ratio--with high volumetric efficiency resulting from low compression ratios and vice-versa. For a single stage, the maximum volumetric efficiency is approximately 60%, and the maximum pressure ratio is approximately 2. In a practical compression stage, the volumetric efficiency will be in the range of 25-35%, and the pressure ratio will lie in the range of 1.4 to 1.6. Thus, the thermal compressor is a low pressure ratio, low volumetric efficiency machine compared to a positive displacement compressor. Consequently, several stages of compression must be used to achieve the pressure ratios required by cryogenic refrigerators utilizing the reversed Brayton cycle.

Some electric power must be supplied to the thermal compressor to reciprocate the displacer, and there is a trade-off between electrical power and thermal power. The electrical power may be reduced to very low values if one is willing to provide a relatively high amount of thermal power. The electrical drive power is greater for high speed machines than for low speed machines. For spaceborne systems, in which one desires to minimize electric drive power, reasonable designs will result from reciprocating speeds in the range of 300-900 CPM.

In comparing a refrigeration system employing a thermal compressor with one employing an electric compressor, one finds that the weight and size of the two systems are comparable, and that the major differences are in the input power. Using the electrical power requirement of the system with an electric compressor as a baseline, the system with a thermal compressor will require 15-25% as much electrical power and 2-2 1/2 times as much thermal power. The reliability of the system with the thermal compressor appears to be somewhat higher than that of a system with the electrical compressor, due to a reduction in the component count and electrical stress levels in the power conditioning equipment.

Since the thermal compressor utilizes state-of-the-art components, and since it offers the opportunity for substantial reductions in electrical input power, it is an attractive, viable alternative to an electric compressor in spaceborne, rotary reciprocating refrigeration systems. It is recommended that thermal compressor refrigerators be considered along with electric compressor refrigerators in spacecraft system studies in order to determine the relative merits, from the total spacecraft system point of view, of the two refrigeration systems. It is further recommended that an engineering test model of at least one stage of a thermal compressor be designed, built, and tested if system studies indicate that the thermal compressor has system advantages.

REFERENCES

1. Development of a Miniature Reciprocating Cryogenic Refrigerator for Space Applications, R. W. Breckenridge, Jr., Technical Report AFFDL-TR-67-78, May, 1967.
2. Exploratory Development of a 1 Watt, 3.6°K Refrigerator for Space Applications, R. W. Breckenridge, Jr., Technical Report AFFDL-TR-68-59, October, 1968.
3. Development of a Rotary-Reciprocating Cryogenic Refrigerator for Space Applications, R. W. Breckenridge, Jr., et.al., Technical Report AFFDL-TR-72-88, July, 1972.
4. V. Bush, "Apparatus for Compressing Gases," U.S. Patent No. 2,157,229 May 9, 1939.
5. K. E. Buck, "Development of a Stirling Cycle Power System for Artificial Hearts," IECEC 1969 Record/Paper 699016, pp. 115.
6. W. R. Martini, "The Thermocompressor and Its Application to Artificial Heart Power," IECEC 1969 Record/Paper 699015, pp. 107.
7. W. T. Beale, "Free Piston Stirling Engines--Some Model Tests and Simulations," Society of Automotive Engineers, Paper No. 690230, Detroit, Michigan, 1969.
8. Rotary-Reciprocating Cryogenic Refrigeration System Studies, Part II-Computer Program, J. L. Coggins, et.al., Technical Report AFFDL-TR-71-115, Part II, October, 1971.
9. Development of Long-Life, High-Capacity Vuilleumier Refrigeration System for Space Applications, Part IV, F. J. Riha, et.al., Technical Report AFFDL-TR-71-92, Part IV, June, 1974.
10. R. D. McCarty, "Thermo-Physical Properties of Helium-4 from 2 to 1500 K with Pressures to 1000 Atmospheres," NBS Technical Note 631, November, 1972.
11. Compact Heat Exchangers, Kays and London, McGraw-Hill, 1964.
12. G. Walker and V. Vasishta, "Heat-Transfer and Flow-Friction Characteristics of Dense-Mesh Wire Screen Stirling-Cycle Regenerator," Advances in Cryogenic Engineering, Vol. 16, 1970, pp. 324-341.

APPENDIX I

EQUATIONS DESCRIBING THERMODYNAMIC PROCESSES

A. CYLINDER PROCESSES

The mass flow throughput for a cylinder per cycle, MCY is given by

$$MCY = MC - MA \quad (A1)$$

We define the reduced void fraction by

$$RVF \equiv \frac{V2V}{V3D} + \frac{TC}{TH} \cdot \frac{V3V}{V3D} + \frac{TC}{T4} \cdot \frac{V4V}{V3D} \quad (A2)$$

the volumetric efficiency by

$$NV \equiv \frac{MCY \cdot R \cdot TC}{PS \cdot V3D} \quad (A3)$$

and note that

$$\frac{V2D}{V3D} = \frac{A2}{A3} \quad (A4)$$

Then, by expressing MC and MA in terms of the pressures, volumes and temperatures of each element in the system, (A1) through (A4) can be combined to yield

$$NV = \left(\frac{A2}{A3} + RVF \right) - \frac{PD}{PS} \left(\frac{TC}{TH} + RVF \right) \quad (A5)$$

which relates the mass flow throughput per cycle to the pressure ratio. MCY is related to the total mass flow rate by

$$MCY = \frac{W}{N \cdot NC} \quad (A6)$$

Thus, if W, N, NC, PD, PS, TC, TH, RVF and $\frac{A2}{A3}$ are specified, (A3) and (A5) can be used to determine V3D.

Now

$$D = \sqrt[3]{\frac{4}{\pi} \cdot \frac{V3D}{SDR}} \quad (A7)$$

$$A3 = \frac{\pi}{4} D^2 \quad (A8)$$

$$S = SDR \cdot D \quad (A9)$$

and

$$A2 = \left(\frac{A2}{A3} \right) A3 \quad (A10)$$

Thus, if SDR is specified, the basic dimensions of the cylinder can be determined from V3D and (A7) through (A10).

The displacer positions at point b, where the suction valve opens, and at point d, where the discharge valve opens, are obtained from mass balances between points a and b and c and d, respectively, with the result

$$XB = \frac{\left(\frac{PD}{PS} - 1 \right) \left(\frac{TC}{TH} + RVF \right)}{\frac{A3}{V3D} \left(\frac{A2}{A3} - \frac{TC}{TH} \right)} \quad (A11)$$

and

$$XD = \frac{\frac{PS}{PD} \left(\frac{A2}{A3} + RVF \right) - \left(\frac{TC}{TH} + RVF \right)}{\frac{A3}{V3D} \left(\frac{A2}{A3} - \frac{TC}{TH} \right)} \quad (A12)$$

The relationships between displacer motion, regenerator flow rate, inlet and outlet flow rates and pressure depend on the portion of the cycle that is occurring, as noted below.

Re-expansion, a-b:

Cylinder suction and discharge flows are zero. Regenerator flow is obtained from

$$WR = \dot{M2}$$

where the dot indicates a time derivative. By substitution we have:

$$WR = \frac{1}{R \cdot TC} (P \cdot \dot{V2} + V2 \cdot \dot{P}) \quad (A13)$$

P can be related to displacer position by a mass balance on the system between point a, and a point between a and b where the displacer is at position X, to yield

$$P = \frac{\frac{PD \cdot V3D}{TC} \left(\frac{TC}{TH} + RVF \right)}{X \left(\frac{A2}{TC} - \frac{A3}{TH} \right) + \frac{V3D}{TC} \left(\frac{TC}{TH} + RVF \right)} \quad (A14)$$

\dot{P} can be obtained from (A14), while $V2$ and $\dot{V}2$ can be directly related to the displacer position and velocity, so that (A13) can be written as

$$WR = \frac{PD \cdot A2 \cdot XDOT \left(1 - \frac{V2V}{A2} \cdot \beta \right)}{R \cdot TC \cdot (\beta X + 1)^2} \quad (A15)$$

where

$$\beta = \frac{A3}{V3D} \cdot \frac{\left(\frac{A2}{A3} - \frac{TC}{TH} \right)}{\left(\frac{TC}{TH} + RVF \right)} \quad (A16)$$

$$X = \frac{S}{2} \left[1 + \sin \left(2\pi N \cdot \theta - \frac{\pi}{2} \right) \right] \quad (A17)$$

$$XDOT = \pi N \cdot S \cdot \cos \left(2\pi N \cdot \theta - \frac{\pi}{2} \right) \quad (A18)$$

θ is a time parameter chosen so that $X = 0$ at $\theta = 0$.

Suction, b-c:

The pressure is constant at PS . Regenerator flow rate is obtained from

$$WR = -\dot{M}3$$

which can be written as

$$WR = \frac{PS \cdot A3 \cdot XDOT}{R \cdot TH} \quad (A19)$$

The suction flow rate is obtained from

$$WS = \dot{M}2 + \dot{M}3$$

which can be expressed as

$$WS = \frac{PS \cdot A3 \cdot XDOT}{R \cdot TC} \left(\frac{A2}{A3} - \frac{TC}{TH} \right) \quad (A20)$$

Compression, c-d:

Cylinder suction and discharge flow rates are zero. P can be related to displacer position via a mass balance on the system between point c and a point between c and d where the displacer is at position X to yield

$$P = \frac{\frac{PS \cdot V3D}{TC} \left(\frac{A2}{A3} + RVF \right)}{X \left(\frac{A2}{TC} - \frac{A3}{TH} \right) + \frac{V3D}{TC} \left(\frac{TC}{TH} + RVF \right)} \quad (A21)$$

Regenerator flow rate is derived from Equation (A13), as in the re-expansion process, and Equation (A21), with the result

$$WR = \frac{PS \cdot A2 \cdot XDOT \left(1 - \frac{V2V}{A2} \cdot \beta \right)}{(\beta X + 1)^2 R \cdot TC} \cdot \frac{\left(\frac{A2}{A3} + RVF \right)}{\left(\frac{TC}{TH} + RVF \right)} \quad (A22)$$

Discharge, d-a:

The pressure is constant at PD. Expressions for the regenerator and discharge flow rates are derived from the same basic equations used for the suction process yielding

$$WR = \frac{PD \cdot A3 \cdot XDOT}{R \cdot TH} \quad (A23)$$

and

$$WD = \frac{PD \cdot A3 \cdot XDOT}{R \cdot TC} \left(\frac{A2}{A3} - \frac{TC}{TH} \right) \quad (A24)$$

B. REGENERATOR

LR, VFR and DH will be specified. Pressure drop is determined from

$$AC = \frac{VVREG}{LR} \quad (B1)$$

$$AFR = \frac{AC}{VFR} \quad (B2)$$

$$G = \frac{WR}{AC} \quad (B3)$$

$$A = \frac{4 \cdot VVREG}{DH} \quad (B4)$$

$$NR = \frac{DH \cdot |G|}{U^4} \quad (B5)$$

$$F = \text{Function of NR (a curve fit of the friction factor vs. Reynolds number data for the matrix selected)} \quad (B6)$$

$$V = \frac{R \cdot T^4}{P} \quad (B7)$$

and

$$DPREG = F \cdot \frac{A}{AC} \cdot \frac{V \cdot |G|}{2g} \cdot G \quad (B8)$$

Note that WR, G, NR, F, P and DPREG are all functions of X.

Thermal performance is obtained from

$$M3A = \frac{PD \cdot V3D}{R \cdot TC} \left(\frac{TC}{TH} + RVF \right) \quad (B9)$$

$$WRBAR = 2N \cdot M3A \quad (B10)$$

$$GBAR = \frac{WRBAR}{AC} \quad (B11)$$

$$NRBAR = \frac{DH \cdot GBAR}{U^4} \quad (B12)$$

$$JBAR = \text{Function of NRBAR (a curve fit of the Colburn factor vs. Reynolds number data for the matrix selected)} \quad (B13)$$

$$HBAR = JBAR \cdot NPR^{-\frac{2}{3}} \cdot (CP \cdot GBAR) \quad (B14)$$

$$NTUBAR = \frac{1}{2} \cdot \frac{HBAR \cdot A}{WRBAR \cdot CP} \quad (B15)$$

$$(1 - E) = \frac{1}{1 + NTUBAR} \quad (B16)$$

and

$$QREG = \frac{1}{2} \cdot WRBAR \cdot CP (TH - TC) (1 - E) \quad (B17)$$

Thus, thermal performance is based on mean flow rate through the regenerator.

C. HEAT EXCHANGERS

The approach is to specify a configuration, the effectiveness, E, allot to the exchanger a certain void volume, then determine its pressure drop as a function of stroke.

The approach ΔT in the exchanger, TWGO, is given by

$$TWGO = \frac{2 \cdot QINBAR}{WRBAR \cdot CP} \left(\frac{1 - E}{E} \right) \quad (C1)$$

and

$$NTU = \ln \left(\frac{1}{1 - E} \right) \quad (C2)$$

For an annular design (Figure 11), we specify BAN, then

$$NRBAR = \frac{2 \cdot WRBAR}{BAN \cdot U} \quad (C3)$$

$$NST = \frac{7.54}{NRBAR \cdot NPR} \quad (C4)$$

based on fully developed laminar flow.

Now, by definition

$$NTU = NST \cdot \frac{4L}{DH} \quad (C5)$$

where

$$DH = 2C \quad (C6)$$

for an annulus. Also

$$VHX = BAN \cdot C \cdot L \quad (C7)$$

(C5) through (C7) determine C, L and DH.

Now

$$G = \frac{WR \cdot L}{VHX} \quad (C8)$$

$$V = \frac{R \cdot T}{P} \quad (C9)$$

$$F = \frac{24}{NR} \quad (C10)$$

so that

$$DPHX = \frac{96 L \cdot U \cdot V \cdot G}{DH^2 \cdot 2g} \quad (C11)$$

in which V and G are functions of the displacer position.

For a multipassage design (Figure 11), we specify LP. TWGO and NTU are determined by (C1) and (C2). Then

$$NTU = NST \cdot \frac{4 LP}{DH} \quad (C12)$$

$$DH = BP \quad (C13)$$

$$NST = \frac{2.89}{NRBAR \cdot NPR} \quad (C14)$$

$$NRBAR = \frac{WRBAR}{NP \cdot BP \cdot U} \quad (C15)$$

$$VHX = NP \cdot BP^2 \cdot LP \quad (C16)$$

$$G = \frac{WR}{NP \cdot BP^2} \quad (C17)$$

$$F = \frac{14.2}{NR} \quad (C18)$$

so that

$$DPHX = \frac{56.8 L \cdot U \cdot V \cdot G}{DH^2 \cdot 2g} \quad (C19)$$

Again, V and G are functions of displacer position.

The viscosity, U, in the above equations is based on TC for the ambient end heat exchanger and TH for the hot end heat exchanger.

D. VOID VOLUMES

Void volume relationships include

$$V2V = VCL2 + VCHX + VCFP \quad (D1)$$

$$V3V = VCL3 + VHHX + VHFP \quad (D2)$$

$$V4V = VVREG + VPDC \quad (D3)$$

where

$$VCL2 = XCL2 \cdot A2 \quad (D4)$$

$$VCL3 = XCL3 \cdot A3 \quad (D5)$$

$$VPDC = \pi D \cdot C (LHC + S) \quad (D6)$$

$$VCFP = ACFP \cdot LCFP \quad (D7)$$

$$VHFP = AHFP \cdot LHFP \quad (D8)$$

ACFP and AHFP are determined from the same equation, i.e.,

$$ACFP \text{ or } AHFP = \frac{WRBAR}{\sqrt{2g \cdot RHO \cdot DYNH}} \quad (D9)$$

where

$$RHO = \frac{PS}{R \cdot T} \quad (D10)$$

and T is TC in determining ACFP, and TH in determining AHFP. DYNH, the dynamic head in the fluid passage, is specified as an input parameter.

E. HOT END POWER INPUT

p-V Input

The p-V, or ideal heat input, Q3, is obtained from

$$Q3 = -N \int P3 \cdot A3 \cdot dX$$

which can be shown to be

$$Q3 = \frac{N \cdot NV \cdot PS \cdot V3D}{\left(\frac{A2}{A3} - \frac{TC}{TH}\right)} \cdot \ln \left(\frac{PD}{PS}\right) \quad (E1)$$

It is interesting to determine the ratio $\frac{Q_3}{W}$, which is

$$\frac{Q_3}{W} = \frac{TH}{\left(\frac{A_2}{A_3} \cdot TH - TC\right)} \left[R \cdot TC \cdot \ln \left(\frac{PD}{PS} \right) \right] \quad (E2)$$

The term in the brackets is the isothermal work of compression between PS and PD. When $\frac{A_2}{A_3} = 1$, the other term is the reciprocal of the Carnot efficiency of an engine operating between TH and TC.

Thus, the ideal heat input to a thermal compressor is the same as that to a reversible engine driving an isothermal compressor. In principle, then, the thermal compressor is a reversible device. In practice, a number of thermal loss mechanisms prevent a close approach to ideal performance. These losses are evaluated by the relations that follow.

Shuttle Heat Transfer

$$Q_{SH} = \frac{\pi \cdot KG \cdot D \cdot S^2}{5.4 C \cdot LHC} (TH - TC) \quad (E3)$$

Displacer Conduction

$$Q_{DIS} = \frac{\pi \cdot K_{DIS} \cdot D \cdot TD}{LHC} (TH - TC) \quad (E4)$$

Cylinder Wall Conduction

$$Q_{CW} = \frac{\pi \cdot K_{CW} \cdot D \cdot TCW}{LHC} (TH - TC) \quad (E5)$$

Regenerator Shell and Matrix Conduction

$$Q_{RS} = \frac{\pi \cdot K_{RS} \cdot D_{RS} \cdot TRS}{LR} (TH - TC) \quad (E6)$$

$$Q_{RM} = \frac{K_{RM} \cdot A_{FR}}{LR} (TH - TC) \quad (E7)$$

Insulation Conduction

$$Q_{INS} = \frac{K_{INS} \cdot A_{INS}}{T_{INS}} (TH - TC) \quad (E8)$$

Pumping Losses

The average mass flow rate into (and out of) the radial clearance between displacer and cylinder each half cycle is given by

$$\text{MPDOT} = \frac{4\pi \cdot N \cdot D \cdot C (PD - PS)(LHC + S)}{R(TH + TC)} \quad (\text{E9})$$

The heat transfer between this gas flow and the walls is characterized by the NTU's, given by

$$\text{NTU} = \frac{1.89 \pi \cdot D \cdot KG (LHC + S)}{C \cdot \text{MPDOT} \cdot CP} \quad (\text{E10})$$

in which fully developed laminar flow is assumed.

The pumping heat loss is then given by

$$\text{QPL} = \frac{\text{MPDOT} \cdot CP (TH - TC)}{2 (\text{NTU} + 1)} \quad (\text{E11})$$

Total Hot End Power Input

The total heat input is the summation of the ideal input and the losses, viz.,

$$\begin{aligned} \text{QINBAR} = & \text{Q3} + \text{QREG} + \text{QSH} + \text{QDIS} + \text{QCW} \\ & + \text{QRS} + \text{QRM} + \text{QINS} + \text{QPL} \end{aligned} \quad (\text{E12})$$

F. DISPLACER POWER INPUT

The work done on the displacer by the gas (and vice versa) each cycle is comprised of two parts, that due to the pressure difference between hot and ambient end, WDP, and that due to the area difference, WDA, given by

$$\text{WDP} = \oint A_2 (P_2 - P_3) DX \quad (\text{F1})$$

and

$$\text{WDA} = - \oint P_3 (A_3 - A_2) DX \quad (\text{F2})$$

The associated powers are

$$\text{PDP} = N \cdot \text{WDP} \quad (\text{F3})$$

$$\text{PDA} = N \cdot \text{WDA} \quad (\text{F4})$$

and the total displacer power is given by

$$PDISP = PDP + PDA \quad (F5)$$

In (F1) the pressure drop is obtained from

$$(P2 - P3) = - (DPREG + DPHHX + DPCHX + DPHFP + DPCFP) \quad (F6)$$

in which all the quantities are evaluated as functions of the displacer position, X.

We also note that (F2) is equivalent to

$$WDA = - \left(1 - \frac{A2}{A3}\right) \int P3 \cdot A3 \cdot DX$$

so that

$$PDA = - \left(1 - \frac{A2}{A3}\right) \cdot N \int P3 \cdot A3 \cdot DX$$

or

$$PDA = \left(1 - \frac{A2}{A3}\right) Q3 \quad (F7)$$

Thus, as one would expect, the work done on the area $(A3 - A2)$ is the fraction $\left(\frac{A3 - A2}{A3}\right)$ of the p-V work done on A3.

APPENDIX II

DESCRIPTION OF THERMAL COMPRESSOR COMPUTER PROGRAM

A. GENERAL

Our analysis of the behavior of a thermal compressor necessitates the specification of a large number of parameters prior to making any calculations. The calculations themselves are straightforward; however, they are tedious and would be time-consuming to perform by hand. We have opted for a simple computer program to do these calculations: optimization of the machine is then a matter of judgment, requiring the exploration of several of the more critical input parameters over their appropriate ranges.

The program is a simple, single-stream computational sequence as shown in Figure 21. It consists of a main program and two subroutines: one for the regenerator and one for the heat exchanger designs. Execution proceeds as follows: the forty-one input parameters are read in from card input and printed with their respective descriptions on a title page. This page serves to completely define the problem, and it eliminates the need for a title card. Next, the program calculates the geometric aspects of the thermal compressor (cylinder diameter, void volumes, port locations) and also calculates the displacer position and velocity at one hundred increments of the cycle. At the same time, the ambient end pressure and the regenerator flow rate are evaluated at each of these 100 displacer positions.

Once the regenerator flow rates are defined, the regenerator design subroutine is called and a thermal design is obtained using mean flow properties. After this step, the pressure drop (based on instantaneous flow) across the regenerator is computed at each of the 100 cycle increments. In a similar fashion, the heat exchanger subroutine is called to design the hot and ambient end heat exchangers.

Returning to the main program, we proceed to evaluate thermal losses for the machine using the calculated geometry and the input values of thermal conductivities, wall thicknesses, etc. The last event in the computational sequence is a stepwise trapezoidal integration of the pressure drops in the regenerator and the two heat exchangers. The total loss through these three elements must be offset by a shaft power input to the machine. This power input is simply a product of the speed and the integral of the total pressure drop over a single cycle.

The nomenclature used in the program is defined in the list of abbreviations and symbols.

B. INPUT DATA

Input data for the program consist of 41 parameters on 6 cards. Definition of these variables and the required format on the input computer cards

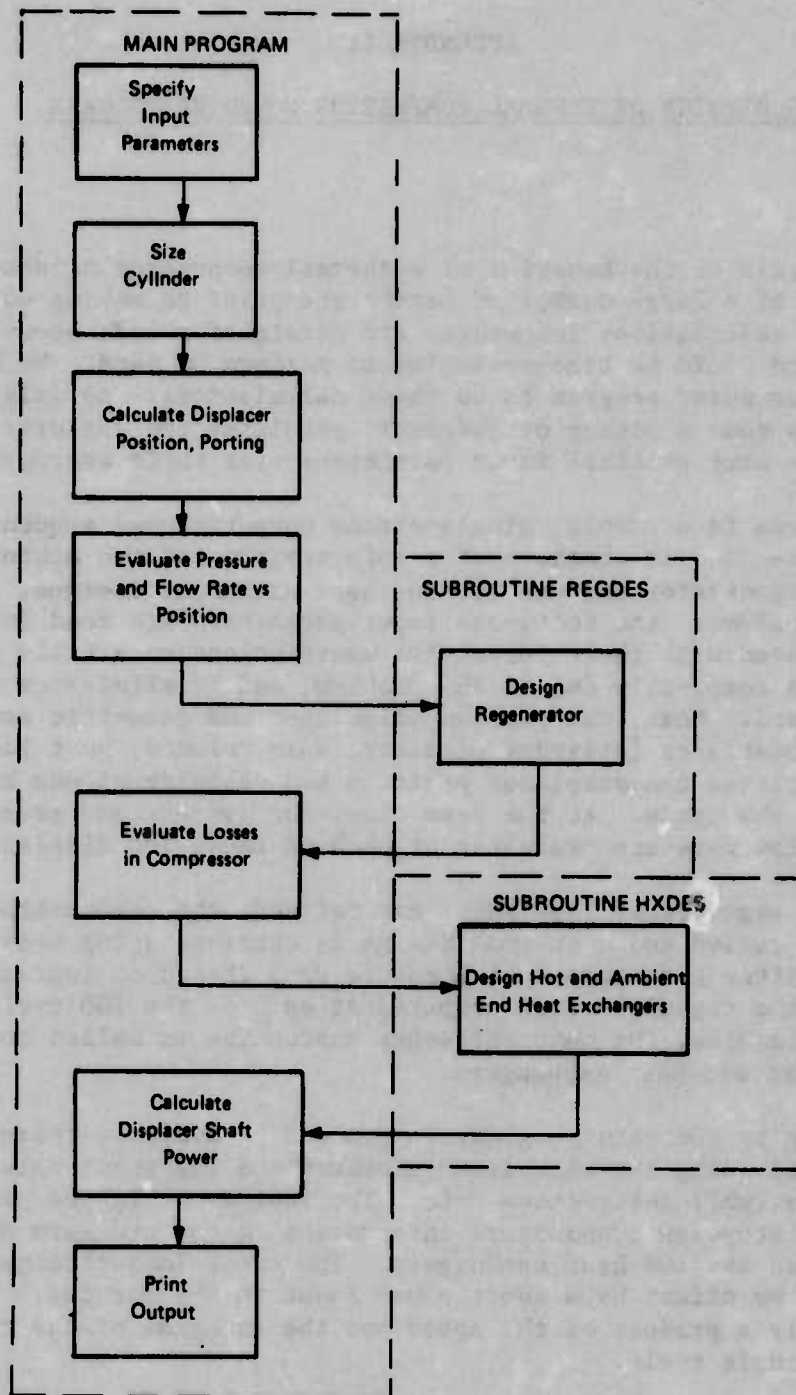


FIGURE 21 FLOWSHEET OF THERMAL COMPRESSOR COMPUTER PROGRAM

are shown in Table XIII in the order in which the cards are read. Units for all variables are listed, along with the proper location of each parameter on the data cards. There is no title card included in the input since virtually all of the input parameters are listed in the output, thereby completely defining the problem. Some of the input parameters are discussed in the following paragraphs.

1. Void Fractions

All void fractions are defined as the respective void volume relative to the hot end swept volume.

The hot and ambient end void fractions account for the clearance volume at cylinder's end, for the heat exchangers, and for the gas flow passages. Porting void fraction is the dead volume of the ambient end ports. It is also included in the ambient end void fraction, but it must also be listed as a separate entry.

Intermediate void fraction includes the regenerator void volume and the annular clearance between the displacer and the cylinder.

2. Displacer Area Ratio

On Card 2 the ratio of ambient displacer area to hot displacer area must be specified. The deviation of this value from unity is in recognition of the presence of a shaft on the ambient end of the displacer. Hence, this area ratio is always less than one.

3. Cylinder Length

The cylinder length is the length of the cylinder over which the hot end-to-ambient temperature difference occurs.

4. Regenerator Configuration

Column 4 of the third input card sets a flag which determines the regenerator configuration. The two choices available are (1) an annular regenerator which is integral with the cylinder, and (2) a cylindrical regenerator which is separate from the cylinder. In the latter case, the volume of flow passages to the regenerator must be included as part of the hot end and ambient void volumes. Neither of the regenerator configurations has a unique matrix material; rather, one of three matrices (spheres, screens, and round tubes) may be selected by the appropriate flag in Column 8 of the same card.

TABLE XIII

INPUT DATA TO PROGRAM

		<u>Representative Values</u>
<u>CARD 1: FORMAT (10F8.0)</u>		
TH	High temperature source (K)	800 - 1,000
TC	Low temperature sink (K)	300 - 350
PD	Absolute discharge pressure (atm)	$\left\{ 1.25 < \frac{PD}{PS} < 2.0; .5 < PS < 4 \right.$
PS	Absolute suction pressure (atm)	
N	Speed (Hz)	5 - 20
NC	Number of cylinders	1 - 2
W	Total mass flow rate, all cylinders (g/sec)	0.2 - 1.0
VFH	Hot end void fraction	.05 - .25
VFC	Ambient end void fraction	.05 - .25
VFI	Intermediate void fraction	.3 - 1.0
<u>CARD 2: FORMAT (10F8.0)</u>		
TCW	Cylinder wall thickness (cm)	.025 - .050
TD	Displacer wall thickness (cm)	.05 - .10
TINS	Insulation thickness, hot end (cm)	3 - 10
XCL3	End clearance, hot end (cm)	.05 - .10
XCL2	End clearance, ambient end (cm)	.05 - .10
SDR	Stroke-to-diameter ratio	.1 - .5
A2A3	Ratio of ambient displacer area to hot displacer area; this ratio is less than one	.9 - .95
C	Radial clearance between displacer and cylinder wall (cm)	.03 - .10
LHC	Cylinder length between hot and ambient ends (cm)	5 - 20
VFPORT	Porting void fraction	.01 - .05
<u>CARD 3: FORMAT (2I4, 9F8.0)</u>		
IREG	In Column 4: 1 = regenerator is integral with cylinder 2 = regenerator is separate from cylinder	
IMTX	In Column 8: 1 = spheres 2 = screens 3 = tubes	
DH	Hydraulic diameter of regenerator matrix (cm)	.01 - .10
LR	Regenerator length (cm)	1 - 10
VFR	Regenerator void fraction	.02 - .10
TRS	Regenerator shell thickness (cm)	.025 - .050

TABLE XIII

(Concluded)

		<u>Representative Values</u>
<u>CARD 4:</u>	FORMAT (I4, 9F8.0) HOT END HEAT EXCHANGER	
IHHX	In Column 4: 1 = annular heat exchanger 2 = multipassage heat exchanger	
LPH	Passage length in multipassage design (cm); leave blank in annular design	1 - 10
EHHX	Effectiveness	.8 - .9
LHFP	Length of fluid passage between hot end and heat exchanger (cm)	0 - 15
DYNNH	Dynamic head in fluid passage (atm)	.01 - .1
<u>CARD 5:</u>	FORMAT (I4, 9F8.0) AMBIENT END HEAT EXCHANGER	
ICHX	In Column 4: 1 = annular heat exchanger 2 = multipassage heat exchanger	
LPC	Passage length in multipassage design (cm); leave blank in annular design	1 - 5
ECMX	Effectiveness	.8 - .9
LCFP	Length of fluid passage between ambient end and heat exchanger (cm)	0 - 5
DYNHC	Dynamic head in fluid passage (atm)	.01 - .1
<u>CARD 6:</u>	FORMAT (10F8.0)	
KCW	Thermal conductivity of cylinder wall (watt/cm-K)	.1 - .2
KDIS	Thermal conductivity of displacer wall (watt/cm-K)	.1 - .2
KRS	Thermal conductivity of regenerator wall (watt/cm-K)	.1 - .2
KINS	Thermal conductivity of insulation on hot end (watt cm-K)	.0001 - .001
KRMM	Thermal conductivity of regenerator matrix material (watt/cm-K)	.1 - .2

5. Regenerator Void Fraction

Porosity of the regenerator matrix material must be taken into account by specifying the matrix void fraction in Columns 33-40 of Card 4.

6. Choice of Heat Exchanger

If a multipassage heat exchanger is selected, the length of a single passage must be specified in Columns 5-12 of Card 4 or 5. If an annular configuration is selected, there need not be an entry for length. The program will set the perimeter of the annulus equal to that of the cylinder for the annular heat exchanger.

7. Fluid Passages

The fourth and fifth data entries on Cards 4 and 5 specify the length of the fluid passages to the heat exchangers and the dynamic head in those passages. Together with the calculated regenerator flow, these parameters will determine the cross-sectional area of the fluid passages. The volumes of the passages are then subtracted from the total void volume to yield the volume available for the heat exchangers.

C. HELIUM PROPERTIES

We have modeled the working fluid as an ideal gas since, in the range considered (2-4 atmospheres, 300-900 K), the gas is indeed ideal, and furthermore, has a constant specific heat and Prandl number. Fitting the thermal conductivity exponentially in temperature then, we obtained close agreement with published NBS data (Reference 10). The viscosity also has a functional dependence on temperature. The constant of proportionality was derived from the specific heat and Prandl number.

D. REGENERATOR DESIGN

1. Heat Transfer and Friction Data

Three matrix configurations are incorporated in regenerator subroutine REGDES: spheres, screens, and round tubes. Wherever possible, the analytical correlations provided by Kays and London (Reference 11) are used. In cases where correlations were not available, the graphical or tabular data in Kays and London were curve-fitted in Chebyshev polynomials.

In the case of tubes, virtually any porosity may be specified, making the algorithm quite general in that respect. On the other hand, the correlation for spheres is valid only for porosities in the 0.37-0.39 range

(the maximum theoretical packing density yields a porosity of 0.37); and the correlation for screens is valid only for the minimum porosity (0.65) for which Kays and London provide data.

2. Shell Conduction

Conduction through the regenerator shell is straightforward. Two regenerator configurations are allowed: (1) an annular regenerator which is integral with the cylinder wall, and (2) a separate external regenerator connected to the heat exchangers via piping. For the annular regenerator, two shells are required since we allow for insulation between the inside of the regenerator and the cylinder wall. This arrangement permits us to choose a regenerator length which is shorter than the cylinder length and still maintain separate temperature profiles in each. The diameter of this inside shell is set to be 1.0 inch larger than the cylinder diameter. Thermal paths through both shells are accounted for in the conduction loss. Should the regenerator and cylinder lengths be chosen equal, the insulation is not required and a single regenerator shell would suffice.

3. Regenerator Matrix Conduction

We have invoked a rigorous analysis of matrix conduction effects only in the case of round tubes. Given a hydraulic diameter and regenerator void fraction, the tube diameter and wall thickness may be calculated if the tubes are arranged in a hexagonal packing. The actual conduction loss may be calculated from this result given the frontal area and length of the regenerator.

In the case of spheres, we based the loss formulation on a cubic packing, i.e., a packing with the spheres centered at the corners of a cubic lattice. Inspection of a single stack of spheres reveals that the thermal path is simply a series of contact resistances, assuming that the thermal resistance through the sphere itself is negligible. We have assumed a mechanical loading of 0.068 atm (1.0 psi) on the spheres as a deterrent to matrix movement. For the total matrix, then, multiple conductive paths are present, the number being a function of sphere diameter and regenerator frontal area. There is an inconsistency in this conduction model since our heat transfer and friction data is based on a matrix porosity of 0.37-0.39, which would require a "hexagonal close packed" lattice. The cubic packing yields a porosity of 0.48. Our principal justification for this approach to calculating matrix conduction is its simplicity. In spite of the inconsistency, it is at least a tacit recognition of the existence of matrix conduction.

Screens are no easier to analyze than spheres. Hence, our rationale in evaluating solid conduction through a matrix of screens follows very closely the rationale applied to spheres, viz., in the interests of simplicity, try a formulation which will be cognizant of the phenomenon and which will yield some useful results. Accordingly, we have modeled the

screen as a "crossed-rod" lattice with the rods in each layer oriented at 90° to those in the adjacent layer. The mesh size and wire diameter of this configuration may be derived solely from a matrix hydraulic diameter if one assumes that: (1) each layer is two wire diameters thick, and (2) the wire spacing is the same for all layers (Reference 12). Correlations of wire diameter and wire density as functions of hydraulic diameter are used for this calculation. A series of contact resistances at the intersection of two wires then form the thermal path through the matrix. Given the regenerator length, we can determine the number of resistances in series; the frontal area will then yield the number in parallel.

E. HEAT EXCHANGER DESIGN

In subroutine HXDES, a heat exchanger for either the hot or ambient end is designed. Two configurations are permitted: (1) annular, in which the heat exchanger consists of an uninterrupted annular space in the cylinder wall; and (2) multipassage, in which the annular space is broken up into a number of square passages around the perimeter of the cylinder. In each of these cases, there is a provision for a "fluid passage" to and from the heat exchanger. The actual volume available for the heat exchanger is the void volume for the particular end (hot or ambient) being examined, minus the volume of the end clearance in the cylinder and the volume of fluid passage(s).

For an annular design, the program sets the annulus diameter equal to the cylinder diameter plus 1.0 inch, and calculates a perimeter from that. As in the regenerator, thermal design is based on mean flow properties, and the pressure drop is based on instantaneous flow. In the printout, the perimeter, length, and width of the annulus are given along with the thermal design parameters.

The procedure for a multipassage design is similar to that for the annular design, viz., thermal design is based on mean flow properties, pressure drop on instantaneous. The printout lists the passage length (input parameter), passage width, number of passages, and the thermal design parameters.

F. DISPLACER POWER

At the end of the main program, a trapezoidal integration technique is used to evaluate the shaft power required to overcome the pressure drop losses in the regenerator, heat exchangers, and fluid passages. It should be remembered that we have evaluated the instantaneous flow through the regenerator at 100 points in the cycle. These 100 points are distributed in four regimes (25 points to each): (1) reexpansion, (2) suction, (3) compression, and (4) discharge. The pressure drops in the regenerator and in each heat exchanger and fluid passage are calculated at each instantaneous flow rate and then stored in arrays. From these values, the pressure drop--displacer area--stroke increment product is summed around one cycle

to obtain the displacer shaft work required for a single cycle. Displacer power is simply the product of this work per cycle and the speed of the machine.

Work output may be derived from the thermal compressor as a result of the difference in hot and ambient displacer areas due to the presence of a shaft on the cold end. This work output may be calculated in a straightforward manner from the ratio of displacer areas and the ideal hot end power input. Subtracting this value from the pressure drop losses yields the net displacer shaft power which will have to be furnished to the machine by the linear actuators. The printout lists all of the contributions to the net displacer shaft power requirement, as well as the flow rate and pressure drops through the regenerator, heat exchangers, and fluid passages at each of the 100 stroke positions in a single cycle.

G. LISTING AND SAMPLE PROBLEMS

A listing of the program is shown in Figure 22, and two sample problems are shown in Figures 23 and 24. The sample problems correspond to the final design point which was described in Section V.


```

C
C *****
C THIS PROGRAM DESIGNS A ROTARY-RECIPROCATING THERMAL COMPRESSOR,
C THE PROGRAM OUTPUT WILL LIST ALL OF THE INPUT DATA AS WELL AS THE
C GEOMETRIC ASPECTS OF THE MACHINE, ITS THERMAL AND SHAFT POWER
C REQUIREMENTS, AND THE LOSSES ASSOCIATED WITH THE DESIGN,
C *** CASE NO, 77056 (WPAFB-AFFDL) ***
C *** P,M, O'FARRELL, 15 JULY 74 ***
C *****
C
0001 REAL KCW,KDIS,KG,KINS,KRS,LHC,LCFP,LHFP,LR,LPH,LPC,KRMM
0002 REAL N,NC,NPR
0003 REAL NV,MCY,MPDOT,NTU
0004 DIMENSION DPHHX(100),DPCHX(100),X1(100),TYP(16),WCHX(12)
0005 DIMENSION DPHFP(100),DPCFP(100)
0006 COMMON/INPUT/TH,TC,TCR,PS,PD,N
0007 COMMON/REG/VVREG,VFR,V3D,LR,DH,DPREG(100),QREG,QRS,QRM,KRS,TRS,
1 IREG,IMTX,D,LHC,KRMM
0008 COMMON/SAVE/WR(100),P(100)
0009 DATA R,CP,NPR,PI/2,0.79,5,193,667,3,1415926536/
0010 DATA TYP/4HANNU,4HLAR,4HSEPA,4HRATE,4HSPHE,4HRES,4HSCRE,4HENS,
14HTUBE,4HS,4HANNU,4HLAR,4H,4HMULT,4HIPAS,4HSAGF/
0011 DATA WCHX/4HPERI,4HMETF,4HRCM,4H,4H,4HLENG,4HTH 0,
14HFP,4HSSAG,4HECM,4H /
C
C READ THE INPUT DATA
C
0012 2 READ(2,500) TH,TC,PD,PS,N,NC,W,VFH,VFC,VFI
0013 READ(2,500) TCW,TD,TINS,XCL3,XCL2,SDR,A2A3,C,LHC,VFPORT
0014 READ(2,501) IREG,IMTX,DH,LR,VFR,TRS
0015 READ(2,502) IHXX,LPH,EHXX,LHFP,DYNHH
0016 READ(2,502) ICHX,LPC,ECHX,LCFP,DYNHC
0017 READ(2,500) KCW,KDIS,KRS,KINS,KRMM
C
C PRINT THE INPUT DATA
C
0018 WRITE(5,700)
0019 WRITE(5,701)
0020 WRITE(5,702) TH,TYP(2*IREG+1),TYP(2*IREG)
0021 WRITE(5,703) TC,TCW,TYP(2*IMTX+3),TYP(2*IMTX+4)
0022 WRITE(5,704) PD,TD,DH
0023 WRITE(5,705) PS,TINS,LR
0024 WRITE(5,706) N,VFR
0025 WRITE(5,707) NC,XCL3,TRS
0026 WRITE(5,708) W,XCL2
0027 WRITE(5,709) SDR
0028 WRITE(5,710) VFH,A2A3
0029 WRITE(5,711) VFC,C
0030 WRITE(5,712) VFI,LHC,VFPORT
0031 WRITE(5,713)
0032 IHX=IHXX
0033 WRITE(5,714) KCLW,TYP(3*IHX+8),TYP(3*IHX+9),TYP(3*IHX+10),
1 TYP(3*ICHX+8),TYP(3*ICHX+9),TYP(3*ICHX+10)
0034 GO TO (10,11),IHX
0035 10 WRITE(5,715) KDIS

```

Figure 22. LISTING OF COMPUTER PROGRAM


```

0036      GO TO 12
0037      11 WRITE(5,716) KDIS,LPH,(MCHX(6+ICHX=6+IW),IW=1,6),LPC
0038      12 WRITE(5,717) KRS,EHHX,ECHX
0039      WRITE(5,718) KINS
0040      WRITE(5,719) KRMM,LHFP,LCFP
0041      WRITE(5,723) DYNHH,DYNHC

      C
      C      SIZE THE CYLINDER
      C

0042      RVF=VFC+VFH*TC/TH+VFI*TC/TH
0043      TCR=TC/TH+RVF
0044      AT=A2A3-TC/TH
0045      AR=A2A3+RVF
0046      NV=A2A3+RVF+TCR+PD/PS
0047      KG=2.861F=5+(.5*(TH+TC))*+.700
0048      MCY=W/N/NC
0049      V3D=MCY+R*TC/(PS+NV)/.101325
0050      V2V=VFC+V3D
0051      V3V=VFH+V3D
0052      V4V=VFI+V3D
0053      D=(4.+V3D/PI/SDR)*+.333J
0054      S=D+SDR
0055      A3=PI*D*D/4.
0056      A2=A3+A2A3
0057      VCL2=A2+XCL2
0058      VCL3=A3+XCL3
0059      VPDC=PI*D*C*(LHC+S)
0060      VVREG=V4V-VPDC

      C
      C      DISPLACER POSITIONS AT OPENING OF SUCTION AND DISCHARGE PORTS
      C

0061      XB=(PD/PS-1.)*TCR/(A3+AT/V3D)
0062      XD=((PS/PD)+AR+TCR)/(A3+AT/V3D)

      C
      C      EVALUATE FLOW RATE AND PRESSURE VERSUS POSITION
      C
      C      REEXPANSION A=B
      C

0063      DO 50 I=1,25
0064      X=I*XB/25.
0065      X1(I)=X
0066      XDOT=S*PI*N*SQRT(1.-(2.+X/S-1.))*2)
0067      Z=V3D+TCR/TC
0068      P(I)=PD+Z/(X+(A2/TC+A3/TH)+Z)
0069      Z=(PD/R/TC)+TCR+(TCR=A2A3+VFC+AT)+A2+XDOT
0070      Z1=(A3+X+AT/V3D+TCR)*2
0071      WR(I)=.101325*Z/Z1
0072      50 CONTINUE

      C
      C      SUCTION, B-C
      C

0073      DO 00 I=26,50
0074      X=XB+(I-25)*(S-XB)/25.
0075      X1(I)=X
0076      IF(X,GT,S) X=S
0077      XDOT=S*PI*N*SQRT(1.-(2.+X/S-1.))*2)

```

Figure 22 (Continued)

```

0078      WR(I)=PS+A3*XDOT*,101325/(R*TH)
0079      P(I)=PS
0080      60 CONTINUE
      C
      C      COMPRESSION, C=D
      C
0081      DO 70 I=51,75
0082      X=S-(I-50)*(S-XD)/25,
0083      X1(I)=X
0084      IF(X,GT,S) X=S
0085      XDOT=S*PI*N*SQR(1,+(2,*(X/S-1,)+2)*(-1,))
0086      P(I)=PS*AR/(X+A3*AT/V3D+TCR)
0087      Z=(PS/R/TC)*AR*(TCR-VFC+A2A3*AT)+A2*XDOT
0088      Z1=X+A3*AT/V3D+TCR
0089      WR(I)=,101325*Z/Z1
0090      70 CONTINUE
      C
      C      DISCHARGE, D=A
      C
0091      DO 80 I=76,100
0092      X=XD*(1,-(I-75)/25,)
0093      X1(I)=X
0094      XDOT=S*PI*N*SQR(1,+(2,*(X/S-1,)+2)*(-1,))
0095      WR(I)=PD+A3*XDOT*,101325/(R*TH)
0096      P(I)=PD
0097      80 CONTINUE
      C
      C      DESIGN THE REGENERATOR
      C
0098      WRITE(5,724)
0099      WRITE(5,720) TYP(2+IREG-1),TYP(2+IREG)
0100      CALL REGDES
      C
      C      CALCULATE THE IDEAL HEAT INPUT PER CYCLE
0101      Q3=,101325*N*V*PS*V3D*ALOG(PD/PS)/AT
0102      Q3=N*Q3
      C
      C      SHUTTLE LOSS
      C
0103      QSH=KG*PI*D*S*(TH-TC)/(5,4+C*LHC)
      C
      C      CONDUCTION THROUGH DISPLACER
0104      QDIS=KDIS*PI*D*TD*(TH-TC)/LHC
      C
      C      CONDUCTION THROUGH CYLINDER WALLS
0105      QCW=KCW*PI*D*TCW*(TH-TC)/LHC
      C
      C      CONDUCTION THROUGH INSULATION
0106      AINS=PI*(D+TINS)*((D+TINS)/4,+(S+LR+TINS))
0107      QINS=KINS*AINS*(TH-TC)/TINS
      C

```

Figure 22 (Continued)

```

C      PUMPING LOSSES
C
0108      MPDOT=4.0*PI*D*C*(PD-PS)*(LHC+S)/R/(TH-TC)
0109      MPDOT=MPDOT+.101325
0110      NTU=1.89*PI*D*(LHC+S)*KG/(C*MPDOT*CP)
0111      QPL=MPDOT*CP*(TH-TC)/(2.0*(NTU+1.))

C
C      TOTAL HOT END POWER INPUT
C
0112      QINBAR=Q3+QREG+QSH+QDIS+QCH+QRS+QRM+QINS+QPL

C
C      DESIGN THE HEAT EXCHANGERS
C
C      HOT END HX
C
0113      WRITE(5,721) TYP(3+IH*8),TYP(3+IH*9),TYP(3+IH*10)
0114      CALL HXDES(TH,QINBAR,EHHX,V3V,VCL3,IHHX,DPHHX,LPH,LHFP,DYNHH,D,DPH
1FP)

C
C      AMBIENT END HX
C
0115      IHX=ICHX
0116      WRITE(5,722) TYP(3+IH*8),TYP(3+IH*9),TYP(3+IH*10)
C      SUBTRACT THE PORTING VOLUME FROM THE TOTAL COLD VOID VOLUME
0117      V2VP=V2V-VFPORT*V3D
0118      CALL HXDES(TC,QINBAR,ECHX,V2VP,VCL2,ICHX,DPCHX,LPC,LCFP,DYNHC,D,DP
1CFP)

C
C      EVALUATE DISPLACER POWER
C
0119      ADIF=A3-A2
0120      P2P3=(DPREG(1)+DPHHX(1)+DPCHX(1))
0121      WDP=.5*A2*(P2P3+.0)*(XB/25.)*.101325
0122      Z=P2P3
0123      P3=P(1)-P2P3
0124      WDA=.5*ADIF*(PD+P3)*DX*.101325
0125      Z1=P3

C
0126      DO 150 I=2,100
0127      P2P3=(DPREG(I)+DPHHX(I)+DPCHX(I)+DPHFP(I)+DPCFP(I))
0128      DX=XB/25.
0129      IF(I,GT,25) DX=(S-XB)/25.
0130      IF(I,GT,50) DX=(S-XD)/25.
0131      IF(I,GT,75) DX=(S-XD)/25.
0132      WDP=WDP+.5*A2*(P2P3+Z)*DX*.101325
0133      P3=P(I)-P2P3
0134      WDA=WDA+.5*ADIF*(P3+Z1)*DX*.101325
0135      Z=P2P3
0136      Z1=P3
0137      150 CONTINUE
0138      PDP=N+WDP
0139      PDA=N+WDA
0140      PDA=(1.0-A2A3)*Q3
0141      PDISP=PDP-PDA

```

Figure 22 (Continued)


```

C      PRINT THE COMPRESSOR GEOMETRY AND POWER REQUIREMENTS
C
0142      WRITE(5,730) RVF,Q3,NV,QSH,MCY,QDIS,V3D,QCW
0143      WRITE(5,731) V2V,QINS,V3V,QPL,V4V,D,QREG
0144      WRITE(5,732) S,QRS,A3,QRM,A2,QINBAR,VCL2
0145      WRITE(5,733) VCL3,VPDC,VVREG,PDP,XB,PDA
0146      WRITE(5,734) XD,PDISP

C
C      PRINT THE PRESSURE DROPS AT EACH CYCLE INCREMENT
C
0147      WRITE(5,510)
0148      DO 200 IW=1,100
0149      200 WRITE(5,601) IW,X1(IW),P(IW),WR(IW),DPREG(IW),DPHMX(IW),DPCMX(IW),
        1DPHFP(IW),DPCFP(IW)

C
0150      GO TO 2
0151      500 FORMAT(10F8.0)
0152      501 FORMAT(2I4,9F8.0)
0153      502 FORMAT(14,9F8.0)
0154      510 FORMAT(/T10,'X',T22,'P2',T34,'WR',T45,'DPREG',T57,'DPHMX',T69,'DPC
        1HMX',T82,'DPHFP',T94,'DPCFP'/)
0155      550 FORMAT(/2X,'INPUT DATA'/)
0156      600 FORMAT(/8(1PE12.4))
0157      601 FORMAT(2X,I3,8(1PE12.4))
0158      700 FORMAT(1H1,T45,'THERMAL COMPRESSOR: INPUT DATA'/)
0159      701 FORMAT(T16,'** CYCLE **',T50,'** GEOMETRY **',T92,'** REGENERATOR
        1**'/)
0160      702 FORMAT(T2,'HOT END TEMP(K)',T25,1PE12.4,T39,'THICKNESS(CM)',T84,A4
        1,A4,T93,'CONFIGURATION')
0161      703 FORMAT(T2,'AMBIENT END TEMP(K)',
        1T25,1PE12.4,T41,'CYLINDER WALL',T65,1
        1PE12.4,T84,A4,A4,T93,'MATRIX')
0162      704 FORMAT(T2,'DISCHARGE PRESSURE(ATM)',T25,1PE12.4,T41,'DISPLACER WAL
        1L',
        1T65,1PE12.4,T84,'HYDRAULIC DIA(CM)',T105,1PE12.4)
0163      705 FORMAT(T2,'SUCTION PRESSURE(ATM)',T25,1PE12.4,T41,'INSULATION ',
        1T65,1PE12.4,T84,'LENGTH(CM)',T105,1PE12.4)
0164      706 FORMAT(T2,'SPEED(HZ)',T25,1PE12.4,T39,'AXIAL CLEARANCE(CM)',T84,1V
        1OID FRACTION',T105,1PE12.4)
0165      707 FORMAT(T2,'NUMBER OF CYLINDERS',T25,1PE12.4,T41,'HOT END',T65,1PE1
        12.4,T84,'SHELL THICKNESS(CM)',T105,1PE12.4)
0166      708 FORMAT(T2,'TOTAL FLOW RATE(G/SEC)',T25,1PE12.4,T41,'AMBIENT END',
        1T65,1PE12.4)
0167      709 FORMAT(T2,'VOID FRACTIONS',T39,'STROKE/DIAMETER RATIO',T65,1PE12.4
        1)
0168      710 FORMAT(T6,'HOT',T25,1PE12.4,T39,'AREA RATIO: AMBIENT/HOT',T65,
        11PE12.4)
0169      711 FORMAT(T6,'AMBIENT(INCL. PORT)',T25,1PE12.4,T39,'RADIAL CLEARAN
        1CE(CM)',T65,1PE12.4)
0170      712 FORMAT(T6,'INTERMEDIATE',T25,1PE12.4,T39,'CYLINDER LENGTH(CM)',T65
        1,1PE12.4/T6,'PORTING',T25,1PE12.4)
0171      713 FORMAT(/T8,'** THERMAL CONDUCTIVITY **',T46,'** HOT HEAT EXCHANGE
        1R **',T88,'** AMBIENT HEAT EXCHANGER **'/)
0172      714 FORMAT(/T2,'CYLINDER WALL(W/CM-K)',T25,1PE12.4,T39,JA4,T52,'TYPE',
        1T84,JA4,T98,'TYPE')
0173      715 FORMAT(T2,'DISPLACER WALL',T25,1PE12.4)

```

Figure 22 (Continued)

```

0174      716 FORMAT(T2,'DISPLACER WALL',T25,1PE12,4,T39,'LENGTH OF PASSAGE(CM)'
          1,T65,1PE12,4,T84,6A4,T105,1PE12,4)
0175      717 FORMAT(T2,'REGENERATOR SHELL',T25,1PE12,4,T39,      'EFFECTIVENESS'
          1,T65,1PE12,4,T84,'EFFECTIVENESS',T105,1PE12,4)
0176      718 FORMAT(T2,'INSULATION      ',T25,1PE12,4)
0177      719 FORMAT(T2,'REGENERATOR MATRIX',T25,1PE12,4,
          1      T39,'LENGTH OF FLUID',T84,'LENGTH OF FLUID'/T44,'PASSAGE(CM'
          1)1,T65,1PE12,4,T89,'PASSAGE(CM)',T105,1PE12,4)
0178      720 FORMAT(//T21,'REGENERATOR DESIGN(1,2A4,1)1//)
0179      721 FORMAT(//T16,'HOT HEAT EXCHANGER DESIGN(1,3A4,1)1//)
0180      722 FORMAT(//T15,'AMBIENT HEAT EXCHANGER DESIGN(1,3A4,1)1//)
0181      723 FORMAT(T39,'DYNAMIC HEAD(ATM)',T65,1PE12,4,T84,'DYNAMIC HEAD(ATM)'
          1,T105,1PE12,4)
0182      724 FORMAT(///T40,'THERMAL COMPRESSOR: RESULTS OF THE ANALYSIS')
0183      730 FORMAT(///T44,'THERMAL COMPRESSOR DESIGN'//T30,'GEOMETRY',T78,
          1'LOSSES(WATTS)'/T10,'REDUCED VOID FRACTION',T45,1PE12,4,T65,
          2'IDEAL HEAT INPUT',T95,1PE12,4/T10,'VOLUMETRIC EFFICIENCY',T45,1PE
          3'12,4,T65,'SHUTTLE',T95,1PE12,4/T10,'MASS FLOW PER CYCLE(G)',T45,1P
          4'12,4,T65,'DISPLACER CONDUCTION',T95,1PE12,4/T10,'HOT END VOLUME(C
          5C)1,      T45,1PE12,4,T65,'CYLINDER WALL CONDUCTION',T95,1PE12,4/)
0184      731 FORMAT(T10,'AMBIENT VOID VOLUME(CC)1,
          6      T45,1PE12,4,T65,'INSULATION CONDUCT
          7'ION',T95,1PE12,4/T10,'HOT VOID VOLUME(CC)1,      T45,1PE12,4,T65,'P
          8'UMPING',T95,1PE12,4/T10,'INTERMEDIATE VOID VOLUME(CC)1,      T45,1PE
          9'12,4,T65,'REGENERATOR'//T10,'CYLINDER DIAMETER(CM)',T45,1PE12,4,
          1T67,'HEAT LOSS',T95,1PE12,4/)
0185      732 FORMAT(
          T10,'STROKE(CM)',T45,1PE12,4,T67,
          2'ISHELL CONDUCTION',T95,1PE12,4/T10,'DISPLACER AREA=HOT END(30 CM)'
          3,T45,1PE12,4,T67,'MATRIX CONDUCTION',T95,1PE12,4/T10,'DISPLACER AR
          4'EA=AMBIENT END(30 CM)1,
          4      T45,1PE12,4,T65,'TOTAL HOT END POWER INPUT',
          5T95,1PE12,4/T10,'CLEARANCE VOLUME=AMBIENT(CC)1, T45,1PE12,4/)
0186      733 FORMAT(T10,
          6'CLEARANCE VOLUME=HOT(CC)1,      T45,1PE12,4,T76,'DISPLACER POWER(WA
          7'TTS)'/T10,'PERIPHERAL CLEARANCE VOLUME(CC)1,      T45,1PE12,4/
          1T10,'REGENERATOR VOID VOLUME(CC)1,      T45,1PE12,4,T65,
          8'DELTA P LOSS',T95,1PE12,4/T10,'SUCTION PORT OPENS(CM)',T45,1PE12,
          9'4,T65,'DELTA A GAIN',      T95,1PE12,4/)
0187      734 FORMAT(
          T10,'DISCHARGE PORT OPEN
          13(CM)1,T45,1PE12,4,T65,'NET POWER REQUIREMENT',T95,1PE12,4)
0188      END

```

ROUTINES CALLED:

SQRT , REGDES, ALOG , HXDES

OPTIONS =/OP:3

BLOCK	LENGTH
MAIN	5261 (024432)*
INPUT	12 (000030)
REG	230 (000714)
SAVE	400 (001440)

```

**COMPILER ---- CORE**
  PHASE      USED FREE
DECLARATIVES 01151 08886
EXECUTABLES  01023 06214
ASSEMBLY     02407 12190

```

Figure 22 (Continued)

```

0001      SUBROUTINE REGDES
0002      REAL K4,LR,N,MJA,NRBAR,JBAR,NNU,NTUBAR,NR,KRS,NPR,KRM,KRMM
0003      COMMON/INPUT/TH,TC,TCR,PS,PD,N
0004      COMMON/HX/WRBAR,NRBAR
0005      COMMON/REG/VVREG,VFR,VJD,LR,DH,DPREG(100),QREG,QRS,QRM,KRS,TRS,
0006      1INEG,IMTX,D,LHC,KRMM
0007      COMMON/SAVE/WR(100),P(100)
0007      DATA R,CP,NPR,PI/2,079,5,193,,667,3,1415925636/

      C
      C
      C      REGENERATOR THERMAL DESIGN IS BASED ON MEAN FLOW PARAMETERS--
      C      J FACTOR IS FROM CURVE FIT OF KAYS AND LONDON DATA
      C

0008      T4=(TH-TC)/ALOG(TH/TC)
0009      U4=3.674F-6+T4**,.700
0010      K4=2.861E-5+T4**,.700
0011      AC=VVREG/LR
0012      AFR=AC/VFR
0013      A=4, +VVREG/DH
0014      MJA=.101325+PD+VJD+TCH/(R+TC)
0015      WRBAR=2, +N+MJA
0016      GBAR=WRBAR/AC
0017      NRBAR=DH+GBAR/U4

      C
0018      GO TO (10,20,30),IMTX

      C
      C      SPHERES
      C

0019      10  JBAR=.221+NRBAR**(-.297)
0020      HBAR=JBAR+.1,30993+CP+GBAR
0021      GO TO 40

      C
      C      SCREENS
      C

0022      20  JBAR=.495+NRBAR**(-.394)
0023      HBAR=JBAR+.1,30993+CP+GBAR
0024      GO TO 40

      C
      C      ROUND TUBES
      C

0025      30  Z=2, +LR/(NRBAR+NPR+DH)
0026      IF(Z,LT,.020) GO TO 35
0027      Z=.43429+ALOG(Z)
0028      Z=1.4307+Z+1,0
0029      Z=.7509572+,1211183+Z+,02800129+(2, +Z+Z=1,)
0030      NNU=10, **Z
0031      HBAR=NNU+K4/DH
0032      GO TO 40
0033      35  NNU=2,230+Z**(-.391)
0034      HBAR=NNU+K4/DH
0035      40  NTUBAR=.5+HBAR+A/(WRBAR+CP)
0036      IF(NRBAR,GT,2000,) WRITE(5,750)
0037      E=NTUBAR/(1, +NTUBAR)

      C
0038      QREG=.5+WRBAR+CP*(TH-TC)*(1,-E)

```

Figure 22 (Continued)


```

0039      WRITE(5,700) AC,AFR,A,NRBAR,NRBAR
0040      WRITE(5,701) NTUBAR,E
      C
      C      REGENERATOR PRESSURE DROP IS BASED ON INSTANTANEOUS FLOW--
      C      F FACTOR IS FROM CURVE FIT OF KAYS AND LONDON DATA
      C
0041      GO TO (50,50,60),IMTX
      C
      C      SPHERES OR SCREENS
      C
0042      50 DO 55 I=1,100
0043          G=NR(I)/AC
0044          NR=DM*ABS(G)/U4
0045          IF(NR,GT,0.) GO TO 52
0046          DPREG(I)=0.
0047          GO TO 55
0048      52 Z=(2.,+.43429*ALOG(NR)-5.6990)/(-3.6990)
0049          Z=-.055028770+.58128345*Z+.15975869*(2.,+Z+Z+1.)+.036087174*(4.,+Z+Z
      1 +Z-3.,+Z)
0050          F=10.,**Z
0051          V=R*T4/(P(I)+.101325)
0052          DPREG(I)=.5*F*A*V*ABS(G)*G+.9,96939E-7/AC
0053      55 CONTINUE
0054      GO TO 65
      C
      C      ROUND TUBES
      C
0055      60 DO 61 I=1,100
0056          G=NR(I)/AC
0057          NR=DM*ABS(G)/U4
0058          IF(NR,GT,0.) GO TO 62
0059          DPREG(I)=0.
0060          GO TO 63
0061      62 Z=.43429*ALOG(NR*DM/LR)
0062          Z=(2.,+Z-3.4772)/1.9208
0063          Z=1.529678+.322540*Z+.04956261*(2.,+Z+Z+1.)
0064          F=10.,**Z/NR
0065          V=R*T4/P(I)/.101325
0066      63 DPREG(I)=.5*F*A*V*ABS(G)*G+.9,96939E-7/AC
      C
      C      CONDUCTION THROUGH SHELL
      C
0067      65 CONTINUE
0068      GO TO (60,70),IREG
      C
      C      REGENERATOR SEPARATE FROM CYLINDER
      C
0069      70 DRS=SQRT(4.,+AFR/PI)
0070      WRITE(5,702) DRS
0071      GRS=KRS*PI*DRS*TRS*(TH-TC)/LR
0072      GO TO 110
      C
      C      REGENERATOR INTEGRAL WITH CYLINDER
      C
0073      80 DRSI=D+2.54
0074      DRS=SQRT(4.,+AFR/PI+DRSI*DRSI)

```

Figure 22 (Continued)


```

0075      IF(LR=LHC) 100,90,100
0076      90 QRS=KRS*PI*(DRS+TRS*(TH=TC))/LR
0077      WRITE(5,705) DRS,D
0078      GO TO 110
0079      100 QRS=KRS*PI*(DRS+DRSI)+TRS*(TH=TC)/LR
0080      WRITE(5,705) DRS,DRSI
0081      110 GO TO (120,130,140),IMTX

C
C      MATRIX CONDUCTION
C
C      SPHERES
C
0082      120 KRM=4,*KRM/(241,*PI)
0083      QRM=KRM*AFR*(TH=TC)/LR
0084      RETURN

C
C      SCREENS
C
0085      130 RH=.25*DH
0086      DW=10,*(.4676*(=ALOG10(RH))+1.271)
0087      RHOW=10,*(.1477*(=ALOG10(RH))+1.974)
0088      KRM=KRM*RHOW*RHOW*DW*DW*3.568E-3
0089      QRM=KRM*AFR*(TH=TC)/LR
0090      RETURN

C
C      ROUND TUBES
C
0091      140 KRM=.9069*KRM*(VFR=.0931)
0092      QRM=KRM*AFR*(TH=TC)/LR
0093      600 FORMAT(/BE12,4)
0094      700 FORMAT(T10,'FLOW AREA(SQ CM)',T45,1PE12,4/T10,'FRONTAL AREA(SQ CM)
1',T45,1PE12,4/T10,'HEAT TRANSFER AREA(SQ CM)',T45,1PE12,4/T10,'MEA
IN FLOW RATE(G/SEC)',T45,1PE12,4/T10,'MEAN REYNOLDS NUMBER',
1T45,1PE12,4)
0095      701 FORMAT(T10,'MEAN HEAT TRANSFER UNITS',T45,1PE12,4/T10,'MEAN EFFECT
IVENESS',T45,1PE12,4)
0096      702 FORMAT(T10,'DIAMETER(CM)',T45,1PE12,4)
0097      705 FORMAT(T10,'OUTSIDE SHELL DIAMETER(CM)',T45,1PE12,4/T10,'INSIDE SH
ELL DIAMETER(CM)',T45,1PE12,4)
0098      750 FORMAT(/T10,'***** FLOW IS TURBULENT *****1//)
0099      RETURN
0100      END

```

SFORTN BI:HXDES

ROUTINES CALLED:

ALOG , ABS , SQRT , ALOG10

OPTIONS =/OP:3

BLOCK	LENGTH
REGDES	1444 (005510)*
INPUT	12 (000030)
HX	4 (000010)
REG	230 (000714)
SAVE	400 (001440)

Figure 22 (Continued)

```

0001      SUBROUTINE HXDES(T,QINBAR,E,VV,VCL,IXH,DPHX,LP,LFP,DYNH,D,DPFP)
0002      REAL N,NTU,NRBAR,NST,L,NP,NPR,LP,LFP,NR
0003      DIMENSION DPHX(100),DPFP(100)
0004      COMMON/HX/WRBAR,NRBAR
0005      COMMON/INPUT/TH,TC,TCR,PS,PD,N
0006      COMMON/SAVE/WR(100),P(100)
0007      DATA R,CP,NPR,PI/2,079,5,193,.667,3,1415926536/

      C
      C      THERMAL DESIGN OF THE HEAT EXCHANGER IS BASED ON MEAN FLOW PROPERTY
      C

0008      U=3.674E-6*T+.700
0009      TWGO=2,+.QINBAR*(1,=E)/E/(NRBAR*CP)
0010      RHO=.101325*PS/R/T
0011      AFP=NRBAR/SQRT(DYNH*RHO/9.86939E-7)
0012      VFP=AFP*LFP
0013      VHX=VV-VCL-VFP
0014      NTU=ALOG(1,/(1,=E))
0015      WRITE(5,700) TWGO,RHO,AFP,VFP,VHX,NTU

      C

0016      IF(VHX.GT.0,.) GO TO 20
0017      WRITE(5,501)
0018      RETURN
0019      20 BAN=(D+2,54)*PI

      C
      C      CALCULATE THE PRESSURE DROP IN THE FLUID PASSAGE
      C

0020      SQA=SQRT(AFP)
0021      DO 25 I=1,100
0022      AWR=ABS(WR(I))
0023      IF(AWR.NE.0,.) GO TO 22
0024      DPFP(I)=0,
0025      GO TO 25
0026      22 NR=AWR/(2,+.U+SQA)
0027      F=1,0253*NR+.0,9422)
0028      DPFP(I)=4,+.9,86939E-7*F*(LFP/SQA/RHO)*WR(I)*AWR/AFP/AFP
0029      25 CONTINUE

      C
      C      PRESSURE DROP IN THE HEAT EXCHANGER IS BASED ON INSTANTANEOUS FLOW
      C

0030      GO TO (30,40),IXH

      C
      C      ANNULAR
      C

0031      30 NRBAR=2,+.NRBAR/BAN/U
0032      IF(NRBAR.GT.2000,.) WRITE(5,750)
0033      NST=7,54/NRBAR/NPR
0034      L=SQRT(.5*NTU*VHX/NST/BAN)
0035      C=SQRT(2,+.VHX*NST/BAN/NTU)
0036      DH=2,+.C
0037      WRITE(5,701) NRBAR,NST,BAN,C,L,E
0038      DO 35 I=1,100
0039      G=WR(I)*L/VHX
0040      V=R*T/P(I)/.101325
0041      35 DPHX(I)=40,0*L*U*V*G+.9,86939E-7/DH/DH

```

Figure 22 (Continued)

```

0042      RETURN
C
C      MULTIPASSAGE
C
0043      40  HP=SQRT(4.02.89*U*VHX/(NTU*NPR*WKBAR))
0044      NP=VHX/(HP*BP*LP)
0045      NRBAR=WRBAR/(NP*BP*U)
0046      IF (NRBAR.GT.2000.) WRITE(5,750)
0047      DH=BP
0048      WRITE(5,702) HP,NP,LP
0049      DO 45 I=1,100
0050      G=WR(I)/(NP*BP*BP)
0051      V=R*T/P(I)/.101325
0052      45  DPHX(I)=28.4*L*U*V*G+9.86939E-7/DH/DH
0053      RETURN
0054      500 FORMAT(/2X,'HX',8(1PE12,4))
0055      501 FORMAT(/' *** HEAT EXCHANGER VOLUME IS ZERO OR NEGATIVE ***!//)
0056      700 FORMAT(T10,'EXIT DELTA T (K)',T45,1PE12,4/T10,'GAS DENSITY(G/C
      1C)',T45,1PE12,4/T10,'FLUID PASSAGE AREA(SQ CM)',T45,1PE12,4/
      1T10,'FLUID PASSAGE VOLUME(CC)',T45,1PE12,4/T10,'HEAT EXCHANGE
      1R VOLUME(CC)',T45,1PE12,4/T10,'HEAT TRANSFER UNITS',T45,1PE12,4)
0057      701 FORMAT(T10,'MEAN REYNOLDS NUMBER',T45,1PE12,4/T10,'FAN STANTON NU
      1MHEI',T45,1PE12,4/T10,'PERIMETER OF ANNULUS(CM)',T45,1PE12,4/
      1T10,'ENTRANCE WIDTH(CM)',T45,1PE12,4/T10,'LENGTH(CM)',T45,1PE12,4/
      1T10,'EFFECTIVENESS',T45,1PE12,4)
0058      702 FORMAT(T10,'PASSAGE WIDTH(CM)',T45,1PE12,4/T10,'NUMBER OF PASSAGES
      1',T45,1PE12,4/T10,'LENGTH OF PASSAGE(CM)',T45,1PE12,4)
0059      750 FORMAT(/T10,'***** FLOW IS TURBULENT *****!//)
0060      END

```

ROUTINES CALLED:
SQRT , ALOG , ABS

OPTIONS =/OP13

BLOCK	LENGTH
HXDES	1112 (004260)*
HX	4 (000010)
INPUT	12 (000030)
SAVE	400 (001440)

••COMPILER ••••• CORE••
 PHASE USED FREE
 DECLARATIVES 00622 00415
 EXECUTABLES 01297 00740
 ASSEMBLY 01659 13018

Figure 22 (Continued)

THERMAL COMPRESSOR: INPUT DATA

```

** CYCLE **
HOT END TEMP(K) 9.2200E-02
AMBIENT END TEMP(K) 3.1100E-02
DISCHARGE PRESSURE(ATM) 2.0200E-01
SUCTION PRESSURE(ATM) 2.0000E-01
SPEED(M2) 1.0000E-01
NUMBER OF CYLINDERS 1.0000E-01
TOTAL FLOW RATE(G/SEC) 4.0200E-01
VOID FRACTIONS
HOT 1.7500E-01
AMBIENT(INCL. PORT) 1.0000E-01
INTERMEDIATE 5.0000E-01
PORTING 2.5000E-02

** GEOMETRY **
THICKNESS(CM) 2.5000E-02
CYLINDER WALL 7.0200E-02
DISPLACER WALL 5.0000E-00
INSULATION 6.3500E-02
AXIAL CLEARANCE(CM) 6.3500E-02
HOT END 6.3500E-02
AMBIENT END 6.3500E-02
STROKE/DIAMETER RATIO 2.0000E-01
AREA RATIO AMBIENT/HOT 9.3750E-01
RADIAL CLEARANCE(CM) 5.0000E-02
CYLINDER LENGTH(CM) 1.5000E-01

** REGENERATOR **
ANNULAR CONFIGURATION
SPHERES MATRIX 4.0000E-02
HYDRAULIC DIA(CM) 5.0000E-01
LENGTH(CM) 3.0000E-01
VOID FRACTION 2.5000E-02
SHELL THICKNESS(CM) 2.5000E-02

```

** THERMAL CONDUCTIVITY **

```

CYLINDER WALL(W/CM-K) 1.0100E-01
DISPLACER WALL 1.0100E-01
REGENERATOR SHELL 1.0100E-01
INSULATION 1.0100E-01
REGENERATOR MATRIX 1.0100E-01

** HOT HEAT EXCHANGER **
ANNULAR TYPE
EFFECTIVENESS 9.0000E-01
LENGTH OF FLUID PASSAGE(CM) 1.0000E-01
DYNAMIC HEAD(ATM) 3.4000E-03

** AMBIENT HEAT EXCHANGER **
ANNULAR TYPE
EFFECTIVENESS 9.0000E-01
LENGTH OF FLUID PASSAGE(CM) 1.3000E-00
DYNAMIC HEAD(ATM) 3.4000E-03

```

THERMAL COMPRESSOR: RESULTS OF THE ANALYSIS

REGENERATOR DESIGN(ANNULAR)

```

FLOW AREA(SQ CM) 3.7300E-01
FRONTAL AREA(SQ CM) 9.0391E-01
HEAT TRANSFER AREA(SQ CM) 1.0694E-04
MEAN FLOW RATE(G/SEC) 2.6743E-00
MEAN REYNOLDS NUMBER 9.2507E-00
MEAN HEAT TRANSFER UNITS 3.7372E-01
MEAN EFFECTIVENESS 9.7394E-01
OUTSIDE SHELL DIAMETER(CM) 2.0100E-01
INSIDE SHELL DIAMETER(CM) 1.6770E-01

```

HOT HEAT EXCHANGER DESIGN(ANNULAR)

```

EXIT DELTA T (K) 8.0200E-00
GAS DENSITY(G/CC) 1.0572E-04
FLUID PASSAGE AREA(SQ CM) 4.4314E-01
FLUID PASSAGE VOLUME(CC) 4.4314E-01
HEAT EXCHANGER VOLUME(CC) 2.4977E-01
HEAT TRANSFER UNITS 2.3223E-02
MEAN REYNOLDS NUMBER 4.0670E-02
MEAN STANTON NUMBER 5.2700E-01
PERIMETER OF ANNULUS(CM) 1.4159E-01
ENTRANCE WIDTH(CM) 3.3477E-00
LENGTH(CM) 9.0000E-01
EFFECTIVENESS

```

Figure 23

SAMPLE PROBLEM - FIRST STAGE DESIGN

AMH1E1 HEAT EXCHANGER DESIGN (ANNULIUM)

EXIT DELTA T (K) 4.0200E-04
 GAS DENSITY(G/CC) 3.1142E-04
 FLUID PASSAGE AREA(SQ CM) 2.5717E-04
 FLUID PASSAGE VOLUME(CC) 3.1450E-04
 HEAT EXCHANGER VOLUME(CC) 2.1200E-01
 HEAT TRANSFER UNITS 2.1020E-04
 MEAN REYNOLDS NUMBER 4.0602E-02
 MEAN STATION NUMBER 2.2749E-02
 PERIMETER OF ANNULUS(CM) 5.2749E-01
 ENTRANCE WIDTH(CM) 8.0159E-02
 LENGTH(CM) 4.5123E-04
 EFFECTIVENESS 9.0000E-01

THERMAL COMPRESSOR DESIGN

GEOMETRY
 REDUCED VOID FRACTION 3.2760E-01
 VOLUMETRIC EFFICIENCY 3.2488E-01
 MASS FLOW PER CYCLE(G) 4.6200E-02
 MOT END VOLUME(CC) 4.5372E-02
 AMBIENT VOID VOLUME(CC) 4.5372E-01
 MOT VOID VOLUME(CC) 7.9400E-01
 INTERMEDIATE VOID VOLUME(CC) 2.2406E-02
 CV INDEX DIAMETER(CM) 1.4210E-01
 STROKE(CM) 2.8475E-02
 DISPLACER AREA-MOT END(SQ CM) 1.5021E-02
 DISPLACER AREA-AMBIENT END(SQ CM) 1.4926E-02
 CLEARANCE VOLUME-AMBIENT(CC) 9.4779E-04
 CLEARANCE VOLUME-MOT(CC) 1.0110E-01
 PERIPHERAL CLEARANCE VOLUME(CC) 3.9915E-01
 REGENERATOR VOID VOLUME(CC) 1.0694E-02
 SUCTION PORT OPENS(CM) 1.3072E-02
 DISCHARGE PORT OPENS(CM) 1.0000E-02

LOSSES(WATTS)

IDEAL HEAT INPUT 1.7241E-02
 SHUTTLE 1.4047E-02
 DISPLACER CONDUCTION 2.2352E-01
 CYLINDER WALL CONDUCTION 7.3334E-04
 INSULATION CONDUCTION 3.0000E-01
 PUMPING 1.1742E-04
 REGENERATOR 1.1057E-02
 HEAT LOSS 5.7000E-01
 SHELL CONDUCTION 1.0227E-01
 MATRIX CONDUCTION 5.5163E-02
 TOTAL MOT END POWER INPUT

DISPLACER POWER(WATTS)

DELTA P LOSS 2.5041E-01
 DELTA A GAIN 1.0770E-01
 NET POWER REQUIREMENT 1.5005E-01

	X	P2	WR	DPHFG	DPHFX	DPCHX	DPHFP	DPCHP
1	5.2200E-02	2.7019E-04	1.4075E-04	1.4073E-02	1.1403E-03	9.4313E-04	3.5202E-05	2.2701E-06
2	1.0450E-01	2.7373E-04	1.0001E-04	2.0550E-02	1.5292E-03	1.3001E-03	4.0500E-05	3.1339E-06
3	1.5607E-01	2.6942E-04	2.2433E-04	2.4931E-02	1.0257E-03	1.5521E-03	5.7638E-05	3.7170E-06
4	2.0915E-01	2.6523E-04	2.4060E-04	2.8428E-02	2.0551E-03	1.7472E-03	6.4254E-05	4.1430E-06
5	2.6114E-01	2.6117E-04	2.6082E-04	3.1299E-02	2.2400E-03	1.9044E-03	6.9246E-05	4.4655E-06
6	3.1373E-01	2.5724E-04	2.8007E-04	3.3600E-02	2.3923E-03	2.0338E-03	7.3453E-05	4.7110E-06
7	3.6602E-01	2.5342E-04	2.9117E-04	3.5600E-02	2.5192E-03	2.1417E-03	7.5940E-05	4.8970E-06
8	4.1831E-01	2.4972E-04	2.9904E-04	3.7364E-02	2.6250E-03	2.2322E-03	7.8120E-05	5.0370E-06
9	4.7060E-01	2.4612E-04	3.0477E-04	3.8764E-02	2.7151E-03	2.3003E-03	7.9704E-05	5.1400E-06
10	5.2200E-01	2.4262E-04	3.0874E-04	3.9920E-02	2.7901E-03	2.3720E-03	8.0803E-05	5.2100E-06
11	5.7517E-01	2.3922E-04	3.1124E-04	4.0870E-02	2.8522E-03	2.4252E-03	8.1495E-05	5.2555E-06
12	6.2740E-01	2.3592E-04	3.1250E-04	4.1650E-02	2.9043E-03	2.4692E-03	8.1845E-05	5.2780E-06
13	6.7975E-01	2.3270E-04	3.1271E-04	4.2240E-02	2.9464E-03	2.5049E-03	8.1902E-05	5.2817E-06
14	7.3204E-01	2.2950E-04	3.1201E-04	4.2722E-02	2.9790E-03	2.5334E-03	8.1710E-05	5.2693E-06
15	7.8433E-01	2.2633E-04	3.1054E-04	4.3056E-02	3.0057E-03	2.5554E-03	8.1302E-05	5.2430E-06
16	8.3661E-01	2.2350E-04	3.0840E-04	4.3273E-02	3.0240E-03	2.5714E-03	8.0700E-05	5.2040E-06
17	8.8890E-01	2.2060E-04	3.0567E-04	4.3385E-02	3.0371E-03	2.5821E-03	7.9955E-05	5.1562E-06
18	9.4119E-01	2.1700E-04	3.0244E-04	4.3400E-02	3.0430E-03	2.5878E-03	7.9061E-05	5.0985E-06
19	9.9348E-01	2.1512E-04	2.9877E-04	4.3320E-02	3.0452E-03	2.5890E-03	7.8045E-05	5.0330E-06
20	1.0450E-01	2.1244E-04	2.9470E-04	4.3177E-02	3.0410E-03	2.5859E-03	7.6923E-05	4.9600E-06
21	1.0901E-01	2.0983E-04	2.9030E-04	4.2953E-02	3.0333E-03	2.5790E-03	7.5700E-05	4.8823E-06

Figure 23 (Continued)

22	1.1503F	MM	2.0728F	MM	2.0560F	MM	4.2062F	-02	3.0214F	-03	2.5083F	-03	7.4411F	-05	4.7006F	-06
23	1.2026F	MM	2.0480F	MM	2.0663F	MM	4.2309F	-02	3.0444F	-03	2.5543F	-03	7.3542F	-05	4.7103F	-06
24	1.2549F	MM	2.0237F	MM	2.0754F	MM	4.1090F	-02	2.0841F	-03	2.5378F	-03	7.1014F	-05	4.6100F	-06
25	1.3072F	MM	2.0000F	MM	2.0700F	MM	4.1436F	-02	2.0601F	-03	2.5106F	-03	7.0123F	-05	4.5221F	-06
26	1.3688F	MM	2.0000F	MM	1.5040F	MM	4.1054F	-02	1.6405F	-03	1.4024F	-03	3.7776F	-05	2.4301F	-06
27	1.4304F	MM	2.0000F	MM	1.5057F	MM	4.1075F	-02	1.6507F	-03	1.4034F	-03	3.7006F	-05	2.4300F	-06
28	1.4929F	MM	2.0000F	MM	1.5040F	MM	4.1040F	-02	1.6480F	-03	1.4018F	-03	3.7764F	-05	2.4351F	-06
29	1.5537F	MM	2.0000F	MM	1.4995F	MM	4.1095F	-02	1.6480F	-03	1.3970F	-03	3.7640F	-05	2.4273F	-06
30	1.6153F	MM	2.0000F	MM	1.4921F	MM	4.1069F	-02	1.6357F	-03	1.3907F	-03	3.7443F	-05	2.4146F	-06
31	1.6769F	MM	2.0000F	MM	1.4818F	MM	4.1015F	-02	1.6244F	-03	1.3810F	-03	3.7109F	-05	2.3974F	-06
32	1.7386F	MM	2.0000F	MM	1.4685F	MM	4.1017F	-02	1.6099F	-03	1.3687F	-03	3.6818F	-05	2.3743F	-06
33	1.8001F	MM	2.0000F	MM	1.4522F	MM	4.1022F	-02	1.5920F	-03	1.3535F	-03	3.6305F	-05	2.3464F	-06
34	1.8617F	MM	2.0000F	MM	1.4327F	MM	4.0744F	-02	1.5707F	-03	1.3354F	-03	3.5870F	-05	2.3132F	-06
35	1.9233F	MM	2.0000F	MM	1.4100F	MM	4.0447F	-02	1.5458F	-03	1.3142F	-03	3.5268F	-05	2.2744F	-06
36	1.9850F	MM	2.0000F	MM	1.3830F	MM	4.0060F	-02	1.5171F	-03	1.2890F	-03	3.4576F	-05	2.2298F	-06
37	2.0466F	MM	2.0000F	MM	1.3540F	MM	4.0222F	-02	1.4844F	-03	1.2620F	-03	3.3780F	-05	2.1790F	-06
38	2.1082F	MM	2.0000F	MM	1.3294F	MM	4.0229F	-02	1.4475F	-03	1.2305F	-03	3.2901F	-05	2.1217F	-06
39	2.1698F	MM	2.0000F	MM	1.2825F	MM	4.0578F	-02	1.4060F	-03	1.1953F	-03	3.1903F	-05	2.0574F	-06
40	2.2314F	MM	2.0000F	MM	1.2400F	MM	4.0955F	-02	1.3594F	-03	1.1550F	-03	3.0788F	-05	1.9854F	-06
41	2.2930F	MM	2.0000F	MM	1.1925F	MM	4.1204F	-02	1.3074F	-03	1.1155F	-03	2.9541F	-05	1.9051F	-06
42	2.3546F	MM	2.0000F	MM	1.1393F	MM	4.1520F	-02	1.2491F	-03	1.0662F	-03	2.8149F	-05	1.8153F	-06
43	2.4162F	MM	2.0000F	MM	1.0796F	MM	4.1627F	-02	1.1836F	-03	1.0062F	-03	2.6591F	-05	1.7140F	-06
44	2.4779F	MM	2.0000F	MM	1.0122F	MM	4.1488F	-02	1.1097F	-03	9.4340F	-04	2.4837F	-05	1.6017F	-06
45	2.5395F	MM	2.0000F	MM	9.3541F	-01	4.1625F	-02	1.0255F	-03	8.7184F	-04	2.2849F	-05	1.4735F	-06
46	2.6011F	MM	2.0000F	MM	8.4675F	-01	4.2032F	-02	9.2020F	-04	7.8920F	-04	2.0565F	-05	1.3262F	-06
47	2.6627F	MM	2.0000F	MM	7.4194F	-01	4.1072F	-02	8.3308F	-04	6.9152F	-04	1.7802F	-05	1.1532F	-06
48	2.7243F	MM	2.0000F	MM	6.1276F	-01	4.1535F	-03	6.7176F	-04	5.7112F	-04	1.4666F	-05	9.4192F	-07
49	2.7859F	MM	2.0000F	MM	4.3816F	-01	4.0435F	-04	4.0435F	-04	4.0830F	-04	1.0244F	-05	6.0808F	-07
50	2.8475F	MM	2.0000F	MM	3.0000F	-01	3.0000F	-01	3.0000F	-01	3.0000F	-01	0.0000F	-01	0.0000F	-01
51	2.9091F	MM	2.0000F	MM	2.0000F	-01	2.0000F	-01	2.0000F	-01	2.0000F	-01	2.0000F	-01	2.0000F	-01
52	2.9707F	MM	2.0000F	MM	1.0000F	-01	1.0000F	-01	1.0000F	-01	1.0000F	-01	1.0000F	-01	1.0000F	-01
53	3.0323F	MM	2.0000F	MM	0.0000F	-01	0.0000F	-01	0.0000F	-01	0.0000F	-01	0.0000F	-01	0.0000F	-01
54	3.0939F	MM	2.0000F	MM	0.0000F	-01	0.0000F	-01	0.0000F	-01	0.0000F	-01	0.0000F	-01	0.0000F	-01
55	3.1555F	MM	2.0000F	MM	0.0000F	-01	0.0000F	-01	0.0000F	-01	0.0000F	-01	0.0000F	-01	0.0000F	-01
56	3.2171F	MM	2.0000F	MM	0.0000F	-01	0.0000F	-01	0.0000F	-01	0.0000F	-01	0.0000F	-01	0.0000F	-01
57	3.2787F	MM	2.0000F	MM	0.0000F	-01	0.0000F	-01	0.0000F	-01	0.0000F	-01	0.0000F	-01	0.0000F	-01
58	3.3403F	MM	2.0000F	MM	0.0000F	-01	0.0000F	-01	0.0000F	-01	0.0000F	-01	0.0000F	-01	0.0000F	-01
59	3.4019F	MM	2.0000F	MM	0.0000F	-01	0.0000F	-01	0.0000F	-01	0.0000F	-01	0.0000F	-01	0.0000F	-01
60	3.4635F	MM	2.0000F	MM	0.0000F	-01	0.0000F	-01	0.0000F	-01	0.0000F	-01	0.0000F	-01	0.0000F	-01
61	3.5251F	MM	2.0000F	MM	0.0000F	-01	0.0000F	-01	0.0000F	-01	0.0000F	-01	0.0000F	-01	0.0000F	-01
62	3.5867F	MM	2.0000F	MM	0.0000F	-01	0.0000F	-01	0.0000F	-01	0.0000F	-01	0.0000F	-01	0.0000F	-01
63	3.6483F	MM	2.0000F	MM	0.0000F	-01	0.0000F	-01	0.0000F	-01	0.0000F	-01	0.0000F	-01	0.0000F	-01
64	3.7099F	MM	2.0000F	MM	0.0000F	-01	0.0000F	-01	0.0000F	-01	0.0000F	-01	0.0000F	-01	0.0000F	-01
65	3.7715F	MM	2.0000F	MM	0.0000F	-01	0.0000F	-01	0.0000F	-01	0.0000F	-01	0.0000F	-01	0.0000F	-01
66	3.8331F	MM	2.0000F	MM	0.0000F	-01	0.0000F	-01	0.0000F	-01	0.0000F	-01	0.0000F	-01	0.0000F	-01
67	3.8947F	MM	2.0000F	MM	0.0000F	-01	0.0000F	-01	0.0000F	-01	0.0000F	-01	0.0000F	-01	0.0000F	-01
68	3.9563F	MM	2.0000F	MM	0.0000F	-01	0.0000F	-01	0.0000F	-01	0.0000F	-01	0.0000F	-01	0.0000F	-01
69	4.0179F	MM	2.0000F	MM	0.0000F	-01	0.0000F	-01	0.0000F	-01	0.0000F	-01	0.0000F	-01	0.0000F	-01
70	4.0795F	MM	2.0000F	MM	0.0000F	-01	0.0000F	-01	0.0000F	-01	0.0000F	-01	0.0000F	-01	0.0000F	-01
71	4.1411F	MM	2.0000F	MM	0.0000F	-01	0.0000F	-01	0.0000F	-01	0.0000F	-01	0.0000F	-01	0.0000F	-01
72	4.2027F	MM	2.0000F	MM	0.0000F	-01	0.0000F	-01	0.0000F	-01	0.0000F	-01	0.0000F	-01	0.0000F	-01
73	4.2643F	MM	2.0000F	MM	0.0000F	-01	0.0000F	-01	0.0000F	-01	0.0000F	-01	0.0000F	-01	0.0000F	-01
74	4.3259F	MM	2.0000F	MM	0.0000F	-01	0.0000F	-01	0.0000F	-01	0.0000F	-01	0.0000F	-01	0.0000F	-01
75	4.3875F	MM	2.0000F	MM	0.0000F	-01	0.0000F	-01	0.0000F	-01	0.0000F	-01	0.0000F	-01	0.0000F	-01
76	4.4491F	MM	2.0000F	MM	0.0000F	-01	0.0000F	-01	0.0000F	-01	0.0000F	-01	0.0000F	-01	0.0000F	-01
77	4.5107F	MM	2.0000F	MM	0.0000F	-01	0.0000F	-01	0.0000F	-01	0.0000F	-01	0.0000F	-01	0.0000F	-01
78	4.5723F	MM	2.0000F	MM	0.0000F	-01	0.0000F	-01	0.0000F	-01	0.0000F	-01	0.0000F	-01	0.0000F	-01
79	4.6339F	MM	2.0000F	MM	0.0000F	-01	0.0000F	-01	0.0000F	-01	0.0000F	-01	0.0000F	-01	0.0000F	-01
80	4.6955F	MM	2.0000F	MM	0.0000F	-01	0.0000F	-01	0.0000F	-01	0.0000F	-01	0.0000F	-01	0.0000F	-01
81	4.7571F	MM	2.0000F	MM	0.0000F	-01	0.0000F	-01	0.0000F	-01	0.0000F	-01	0.0000F	-01	0.0000F	-01
82	4.8187F	MM	2.0000F	MM	0.0000F	-01	0.0000F	-01	0.0000F	-01	0.0000F	-01	0.0000F	-01	0.0000F	-01
83	4.8803F	MM	2.0000F	MM	0.0000F	-01	0.0000F	-01	0.0000F	-01	0.0000F	-01	0.0000F	-01	0.0000F	-01
84	4.9419F	MM	2.0000F	MM	0.0000F	-01	0.0000F	-01	0.0000F	-01	0.0000F	-01	0.0000F	-01	0.0000F	-01
85	5.0035F	MM	2.0000F	MM	0.0000F	-01	0.0000F	-01	0.0000F	-01	0.0000F	-01	0.0000F	-01	0.0000F	-01
86	5.0651F	MM	2.0000F	MM	0.0000F	-01	0.0000F	-01	0.0000F	-01	0.0000F	-01	0.0000F	-01	0.0000F	-01
87	5.1267F	MM	2.0000F	MM	0.0000F	-01	0.0000F	-01	0.0000F	-01	0.0000F	-01	0.0000F	-01	0.0000F	-01

Figure 23 (Continued)

88	5.2365F-W1	2.828NF-W1	-1.6806E-W1	-1.7417E-W2	-1.2794E-W3	-1.8074E-W3	-4.1614E-W5	-2.6852E-W6
89	4.8442E-W1	2.828NF-W1	-1.5942E-W1	-1.6417E-W2	-1.2364E-W3	-1.8584E-W3	-4.4159E-W5	-2.5898E-W6
90	4.3634E-W1	2.828NF-W1	-1.5339E-W1	-1.5774E-W2	-1.1893E-W3	-1.6111E-W3	-3.8555E-W5	-2.4844E-W6
91	3.9274E-W1	2.828NF-W1	-1.4883E-W1	-1.5274E-W2	-1.1384E-W3	-9.6784E-W4	3.8813E-W5	-2.3748E-W6
92	3.4914E-W1	2.828NF-W1	-1.3966E-W1	-1.4324E-W2	-1.0824E-W3	-9.2456E-W4	-3.4914E-W5	-2.2515E-W6
93	3.0544E-W1	2.828NF-W1	-1.3124E-W1	-1.3524E-W2	-1.0217E-W3	-8.6884E-W4	-3.2832E-W5	-2.1123E-W6
94	2.6183E-W1	2.828NF-W1	-1.2344E-W1	-1.2687E-W2	-9.5397E-W4	-8.1194E-W4	-3.0515E-W5	-1.9692E-W6
95	2.1819E-W1	2.828NF-W1	-1.1327E-W1	-1.1622E-W2	-8.7817E-W4	-7.4859E-W4	-2.7875E-W5	-1.8048E-W6
96	1.7455E-W1	2.828NF-W1	-1.0215E-W1	-1.0521E-W2	-7.9195E-W4	-6.7329E-W4	-2.5174E-W5	-1.6172E-W6
97	1.3091E-W1	2.828NF-W1	-8.9184E-W1	-9.2644E-W3	-6.9142E-W4	-5.8783E-W4	-2.1724E-W5	-1.4009E-W6
98	8.7276E-W2	2.828NF-W1	-7.3397E-W1	-7.7739E-W3	-5.9986E-W4	-4.8398E-W4	-1.7679E-W5	-1.1801E-W6
99	4.3634E-W2	2.828NF-W1	-5.2365E-W1	-5.6495E-W3	-4.8556E-W4	-3.4479E-W4	-1.2355E-W5	-7.9676E-W7
100	0.0000E-W1	2.828NF-W1	0.0000E-W1	0.0000E-W1	0.0000E-W1	0.0000E-W1	0.0000E-W1	0.0000E-W1

Figure 23 (Continued)

THERMAL COMPRESSOR: INPUT DATA
 .. CYCLE ..
 HOT END TEMP(K) 9.2200E-02
 AMBIENT END TEMP(K) 3.1100E-02
 DISCHARGE PRESSURE(ATM) 4.0000E-02
 SUCTION PRESSURE(ATM) 2.0000E-02
 SPEED(M2) 1.0000E-01
 NUMBER OF CYLINDERS 1.0000E-01
 TOTAL FLOW RATE(G/SEC) 4.0000E-01
 VOID FRACTIONS
 HOT 1.7500E-01
 AMBIENT(INCL. PORT) 1.0000E-01
 INTERMEDIATE 5.0000E-01
 PORTING 2.5000E-02
 .. GEOMETRY ..
 THICKNESS(CM)
 CYLINDER WALL 2.5000E-02
 DISPLACER WALL 7.0000E-02
 INSULATION 5.0000E-00
 AXIAL CLEARANCE(CM)
 HOT END 0.3500E-02
 AMBIENT END 0.3500E-02
 STROKE/DIAMETER RATIO 2.3750E-01
 AREA RATIO: AMBIENT/HOT 9.3750E-01
 RADIAL CLEARANCE(CM) 5.0000E-02
 CYLINDER LENGTH(CM) 1.5000E-01
 .. REGENERATOR ..
 ANNULAR CONFIGURATION
 SPHERES 3.0000E-02
 HYDRAULIC DIA(CM) 5.0000E-00
 LENGTH(CM) 3.0000E-01
 VOID FRACTION 2.5000E-02
 SHELL THICKNESS(CM) 2.5000E-02

.. THERMAL CONDUCTIVITY ..
 CYLINDER WALL(W/CM-K) 1.0100E-01
 DISPLACER WALL 1.0100E-01
 REGENERATOR SHELL 1.0100E-01
 INSULATION 1.0000E-04
 REGENERATOR MATRIX 1.0100E-01
 .. HOT HEAT EXCHANGER ..
 ANNULAR TYPE
 EFFECTIVENESS 9.0000E-01
 LENGTH OF FLUID PASSAGE(CM) 1.0000E-01
 DYNAMIC HEAD(ATM) 3.4000E-03
 .. AMBIENT HEAT EXCHANGER ..
 ANNULAR TYPE
 EFFECTIVENESS 9.0000E-01
 LENGTH OF FLUID PASSAGE(CM) 1.3000E-00
 DYNAMIC HEAD(ATM) 3.4000E-03

THERMAL COMPRESSOR: RESULTS OF THE ANALYSIS

REGENERATOR DESIGN(ANNULAR)

FLOW AREA(SQ CM) 2.5300E-01
 FRONTAL AREA(SQ CM) 6.0000E-01
 HEAT TRANSFER AREA(SQ CM) 1.4110E-04
 MEAN FLOW RATE(G/SEC) 2.0000E-00
 MEAN REYNOLDS NUMBER 1.2279E-01
 MEAN HEAT TRANSFER UNITS 3.0100E-01
 MEAN EFFECTIVENESS 9.7400E-01
 OUTSIDE SHELL DIAMETER(CM) 1.7200E-01
 INSIDE SHELL DIAMETER(CM) 1.4522E-01

HOT HEAT EXCHANGER DESIGN(ANNULAR)

EXIT DFLTA T (K) 0.1020E-00
 GAS DENSITY(G/CC) 1.4040E-04
 FLUID PASSAGE AREA(SQ CM) 3.7310E-00
 FLUID PASSAGE VOLUME(CC) 3.7310E-01
 HEAT EXCHANGER VOLUME(CC) 1.1731E-01
 HEAT TRANSFER UNITS 2.3020E-00
 MEAN REYNOLDS NUMBER 2.0000E-02
 MEAN STANTON NUMBER 4.2000E-02
 PERIMETER OF ANNULUS(CM) 4.5024E-01
 ENTRANCE -10TH(CM) 9.0000E-02
 LENGTH(CM) 2.0522E-00
 EFFECTIVENESS 9.0000E-01

Figure 24

SAMPLE PROBLEM - SECOND STAGE DESIGN

22	1.150MF	MM	2.0311F	MM	2.0044F	MM	5.7445E-02	6.0903E-03	3.5420F-03	7.4672E-05	4.0154F-06
23	1.2031F	MM	2.0455F	MM	2.0044F	MM	5.7354E-02	6.0508E-03	3.5233F-03	7.4294E-05	4.7246F-06
24	1.2554F	MM	2.0615F	MM	2.0754F	MM	5.6736E-02	6.0155F-03	3.4993F-03	7.3855E-05	4.6338E-06
25	1.3077F	MM	2.0784F	MM	2.1020F	MM	5.6047F-02	5.9670F-03	3.4711E-03	7.3391E-05	4.5373E-06
26	1.3692E	MM	2.0954F	MM	1.5061E	MM	2.0630E-02	3.3259F-03	1.9347F-03	3.7914E-05	2.4450F-06
27	1.4307F	MM	2.1124F	MM	1.5071E	MM	2.0651E-02	3.3202F-03	1.9311F-03	3.7942E-05	2.4468F-06
28	1.4923E	MM	2.1294F	MM	1.5087F	MM	2.0615E-02	3.3243F-03	1.9338F-03	3.7895E-05	2.4438F-06
29	1.5538E	MM	2.1464F	MM	1.5097F	MM	2.0519E-02	3.3144F-03	1.9270F-03	3.7722E-05	2.4359E-06
30	1.6153E	MM	2.1634F	MM	1.4933E	MM	2.0365E-02	3.2977F-03	1.9183F-03	3.7574E-05	2.4231F-06
31	1.6769E	MM	2.1804F	MM	1.4829F	MM	2.0151E-02	3.2740E-03	1.9059E-03	3.7290E-05	2.4053E-06
32	1.7384F	MM	2.1974F	MM	1.4696F	MM	2.0787E-02	3.2455F-03	1.8979E-03	3.6945E-05	2.3825E-06
33	1.7999F	MM	2.2144F	MM	1.4533F	MM	2.0530E-02	3.2093F-03	1.8869E-03	3.6510E-05	2.3544E-06
34	1.8614E	MM	2.2314F	MM	1.4330F	MM	2.0713E-02	3.1663F-03	1.8418F-03	3.5992E-05	2.3210E-06
35	1.9230E	MM	2.2484F	MM	1.4114F	MM	2.0673E-02	3.1166F-03	1.8126F-03	3.5307E-05	2.2821E-06
36	1.9845F	MM	2.2654F	MM	1.3848E	MM	2.0140E-02	3.0581F-03	1.7789E-03	3.4603E-05	2.2373E-06
37	2.0460E	MM	2.2824F	MM	1.3550F	MM	2.0553E-02	2.9922E-03	1.7406E-03	3.3902E-05	2.1863E-06
38	2.1075E	MM	2.2994F	MM	1.3212F	MM	2.0480E-02	2.9177F-03	1.6973F-03	3.3011E-05	2.1208E-06
39	2.1691E	MM	2.3164F	MM	1.2833F	MM	2.0180E-02	2.8340F-03	1.6486E-03	3.2009E-05	2.0425E-06
40	2.2306E	MM	2.3334F	MM	1.2400E	MM	2.0255E-02	2.7402E-03	1.5940E-03	3.0895E-05	1.9920E-06
41	2.2921F	MM	2.3504F	MM	1.1933F	MM	2.0325E-02	2.6351E-03	1.5329F-03	2.9638E-05	1.9113E-06
42	2.3536E	MM	2.3674F	MM	1.1400F	MM	2.0129E-02	2.5170F-03	1.4645E-03	2.8241F-05	1.8212E-06
43	2.4152E	MM	2.3844F	MM	1.0802E	MM	2.0141E-02	2.3855E-03	1.3877E-03	2.6677E-05	1.7203E-06
44	2.4767E	MM	2.4014F	MM	1.0120E	MM	1.9862E-02	2.2365F-03	1.3010E-03	2.4910E-05	1.6009E-06
45	2.5382F	MM	2.4184F	MM	0.9354F	MM	1.7428E-02	2.0660E-03	1.2023E-03	2.2923E-05	1.4702E-06
46	2.5997F	MM	2.4354F	MM	0.8471F	MM	1.5803E-02	1.8700E-03	1.0883E-03	2.0633E-05	1.3304E-06
47	2.6613E	MM	2.4524F	MM	0.7423E	MM	1.3923E-02	1.6393F-03	9.5362E-04	1.7939E-05	1.1509E-06
48	2.7228F	MM	2.4694F	MM	0.6100F	MM	1.1671E-02	1.3539E-03	7.0750E-04	1.4653E-05	9.4492E-07
49	2.7843F	MM	2.4864F	MM	0.4309E	MM	0.7366E-03	9.6011E-04	5.6316E-04	1.0276E-05	6.6270E-07
50	2.8458E	MM	2.5034F	MM	0.0000E	MM	0.0000E-01	0.0000E-01	0.0000E-01	0.0000E-01	0.0000E-01
51	2.9073E	MM	2.5204F	MM	0.0109E	MM	-1.4790E-02	-1.7470E-03	-1.0167E-03	-1.9444E-05	-1.2539E-06
52	2.9688E	MM	2.5374F	MM	-1.1319E	MM	-2.0630E-02	-2.4402E-03	-1.4195E-03	-2.0028E-05	-1.0075E-06
53	3.0303E	MM	2.5544F	MM	-1.3040E	MM	-2.5212E-02	-2.9466E-03	-1.7150E-03	-3.4692E-05	-2.2372E-06
54	3.0918E	MM	2.5714F	MM	-1.5069E	MM	-2.9091E-02	-3.3681E-03	-2.0546E-03	-4.8337E-05	-2.6013E-06
55	3.1533E	MM	2.5884F	MM	-1.7027E	MM	-3.2483E-02	-3.7049E-03	-2.1552E-03	-6.3317E-05	-2.9224E-06
56	3.2148E	MM	2.6054F	MM	-1.9025E	MM	-3.5802E-02	-4.0410E-03	-2.3274E-03	-8.9011E-05	-3.2122E-06
57	3.2763E	MM	2.6224F	MM	-2.1013E	MM	-3.9151E-02	-4.3704E-03	-2.4770E-03	-1.1939E-05	-3.4770E-06
58	3.3378E	MM	2.6394F	MM	-2.2111E	MM	-4.2466E-02	-4.6940E-03	-2.6804E-03	-1.6734E-05	-3.7229E-06
59	3.3993E	MM	2.6564F	MM	-2.3709E	MM	-4.5805E-02	-5.0222E-03	-2.7372E-03	-2.1271E-05	-3.9512E-06
60	3.4608E	MM	2.6734F	MM	-2.5417E	MM	-4.9092E-02	-5.3505E-03	-2.8251E-03	-2.6457E-05	-4.1646E-06
61	3.5223E	MM	2.6904F	MM	-2.7144E	MM	-5.2385E-02	-5.6794E-03	-2.9140E-03	-3.1600E-05	-4.3646E-06
62	3.5838E	MM	2.7074F	MM	-2.8871E	MM	-5.5679E-02	-6.0084E-03	-2.9915E-03	-3.7600E-05	-4.5522E-06
63	3.6453E	MM	2.7244F	MM	-3.0600E	MM	-5.8974E-02	-6.3374E-03	-3.0585E-03	-4.4200E-05	-4.7203E-06
64	3.7068E	MM	2.7414F	MM	-3.2327E	MM	-6.2269E-02	-6.6664E-03	-3.1157E-03	-5.1000E-05	-4.8934E-06
65	3.7683E	MM	2.7584F	MM	-3.4054E	MM	-6.5564E-02	-6.9954E-03	-3.1637E-03	-5.8274E-05	-5.0477E-06
66	3.8298E	MM	2.7754F	MM	-3.5781E	MM	-6.8859E-02	-7.3244E-03	-3.2027E-03	-6.6505E-05	-5.1916E-06
67	3.8913E	MM	2.7924F	MM	-3.7508E	MM	-7.2154E-02	-7.6534E-03	-3.2332E-03	-7.5745E-05	-5.3200E-06
68	3.9528E	MM	2.8094F	MM	-3.9235E	MM	-7.5449E-02	-7.9824E-03	-3.2553E-03	-8.4479E-05	-5.4479E-06
69	4.0143E	MM	2.8264F	MM	-4.0962E	MM	-7.8744E-02	-8.3114E-03	-3.2694E-03	-9.4216E-05	-5.5599E-06
70	4.0758E	MM	2.8434F	MM	-4.2689E	MM	-8.2039E-02	-8.6404E-03	-3.2753E-03	-1.0470E-05	-5.6680E-06
71	4.1373E	MM	2.8604F	MM	-4.4416E	MM	-8.5334E-02	-8.9694E-03	-3.2733E-03	-1.1665E-05	-5.7501E-06
72	4.1988E	MM	2.8774F	MM	-4.6143E	MM	-8.8629E-02	-9.2984E-03	-3.2633E-03	-1.3000E-05	-5.8272E-06
73	4.2603E	MM	2.8944F	MM	-4.7870E	MM	-9.1924E-02	-9.6274E-03	-3.2452E-03	-1.4400E-05	-5.8912E-06
74	4.3218E	MM	2.9114F	MM	-4.9597E	MM	-9.5219E-02	-9.9564E-03	-3.2180E-03	-1.5800E-05	-5.9413E-06
75	4.3833E	MM	2.9284F	MM	-5.1324E	MM	-9.8514E-02	-1.0285E-03	-3.1841E-03	-1.7200E-05	-5.9744E-06
76	4.4448E	MM	2.9454F	MM	-5.3051E	MM	-1.0140E-02	-1.0606E-03	-3.1466E-03	-1.8600E-05	-5.9975E-06
77	4.5063E	MM	2.9624F	MM	-5.4778E	MM	-1.0465E-02	-1.0927E-03	-3.1044E-03	-2.0000E-05	-5.9975E-06
78	4.5678E	MM	2.9794F	MM	-5.6505E	MM	-1.0790E-02	-1.1248E-03	-3.0580E-03	-2.1400E-05	-5.9975E-06
79	4.6293E	MM	2.9964F	MM	-5.8232E	MM	-1.1115E-02	-1.1569E-03	-3.0080E-03	-2.2800E-05	-5.9975E-06
80	4.6908E	MM	3.0134F	MM	-6.0000E	MM	-1.1440E-02	-1.1890E-03	-2.9530E-03	-2.4200E-05	-5.9975E-06
81	4.7523E	MM	3.0304F	MM	-6.1727E	MM	-1.1765E-02	-1.2211E-03	-2.8930E-03	-2.5600E-05	-5.9975E-06
82	4.8138E	MM	3.0474F	MM	-6.3454E	MM	-1.2090E-02	-1.2532E-03	-2.8280E-03	-2.7000E-05	-5.9975E-06
83	4.8753E	MM	3.0644F	MM	-6.5181E	MM	-1.2415E-02	-1.2853E-03	-2.7580E-03	-2.8400E-05	-5.9975E-06
84	4.9368E	MM	3.0814F	MM	-6.6908E	MM	-1.2740E-02	-1.3174E-03	-2.6880E-03	-2.9800E-05	-5.9975E-06
85	5.0000E	MM	3.0984F	MM	-6.8635E	MM	-1.3065E-02	-1.3495E-03	-2.6180E-03	-3.1200E-05	-5.9975E-06
86	5.0615E	MM	3.1154F	MM	-7.0362E	MM	-1.3390E-02	-1.3816E-03	-2.5480E-03	-3.2600E-05	-5.9975E-06
87	5.1230E	MM	3.1324F	MM	-7.2089E	MM	-1.3715E-02	-1.4137E-03	-2.4780E-03	-3.4000E-05	-5.9975E-06

Figure 24 (Continued)

88	5.2274E-01	4.0000E-01	-1.6509E-01	-2.2305E-02	-2.5775E-03	-1.4994E-03	-4.1711E-05	-2.6944E-06
89	4.7914E-01	4.0000E-01	-1.5953E-01	-2.1562E-02	-2.4900E-03	-1.4409E-03	-4.1204E-05	-2.5900E-06
90	4.3550E-01	4.0000E-01	-1.5359E-01	-2.0668E-02	-2.3967E-03	-1.3942E-03	-3.8606E-05	-2.5940E-06
91	3.9203E-01	4.0000E-01	-1.4694E-01	-1.9724E-02	-2.2941E-03	-1.3345E-03	-3.6930E-05	-2.3820E-06
92	3.4847E-01	4.0000E-01	-1.4076E-01	-1.8665E-02	-2.1820E-03	-1.2693E-03	-3.5431E-05	-2.2591E-06
93	3.0491E-01	4.0000E-01	-1.3418E-01	-1.7530E-02	-2.0580E-03	-1.1976E-03	-3.3942E-05	-2.1244E-06
94	2.6135E-01	4.0000E-01	-1.2713E-01	-1.6310E-02	-1.9224E-03	-1.1103E-03	-3.2663E-05	-1.9757E-06
95	2.1770E-01	4.0000E-01	-1.1934E-01	-1.4941E-02	-1.7690E-03	-1.0294E-03	-2.8460E-05	-1.8100E-06
96	1.7423E-01	4.0000E-01	-1.1221E-01	-1.3460E-02	-1.5950E-03	-9.2831E-04	-2.5161E-05	-1.6226E-06
97	1.3067E-01	4.0000E-01	-9.9237E-02	-1.1755E-02	-1.3933E-03	-8.1047E-04	-2.1795E-05	-1.4055E-06
98	8.7110E-02	4.0000E-01	-8.3444E-02	-9.7451E-03	-1.1467E-03	-6.6703E-04	-1.7737E-05	-1.1438E-06
99	4.3550E-02	4.0000E-01	-5.2341E-02	-7.1752E-03	-8.1720E-04	-4.7537E-04	-1.2396E-05	-7.9937E-07
100	0.0000E-01	4.0000E-01	0.0000E-01	0.0000E-01	0.0000E-01	0.0000E-01	0.0000E-01	0.0000E-01

PORTENDING END OF FILE OR END OF MEDIUM
 NAME SFO
 MAIN. 00012

Figure 24 (Continued)

UNCLASSIFIED

Security Classification

DOCUMENT CONTROL DATA - R & D

(Security classification of title, body of abstract and indexing annotation must be entered when the overall report is classified)

1. ORIGINATING ACTIVITY (Corporate author) Arthur D. Little, Inc. Acorn Park Cambridge, Massachusetts 02140		2a. REPORT SECURITY CLASSIFICATION Unclassified	
		2b. GROUP N/A	
3. REPORT TITLE DESIGN STUDY OF A ROTARY RECIPROCATING THERMAL COMPRESSOR			
4. DESCRIPTIVE NOTES (Type of report and inclusive dates) Final Technical Report for Period April 1974 - August 1974			
5. AUTHOR(S) (First name, middle initial, last name) R. W. Breckenridge, Jr.; R. W. Moore, Jr.; P. M. O'Farrell			
6. REPORT DATE October, 1974		7a. TOTAL NO. OF PAGES 106	7b. NO. OF REFS 12
8a. CONTRACT OR GRANT NO. F33615-74-C-3082		8b. ORIGINATOR'S REPORT NUMBER(S) N/A	
a. PROJECT NO. 6146			
c. TASK No. 6146 03 19		9b. OTHER REPORT NO(S) (Any other numbers that may be assigned this report) AFFDL-TR-74-127	
4.			
10. DISTRIBUTION STATEMENT Distribution limited to U.S. Government agencies only; test and evaluation; statement applied August, 1974. Other requests for this document must be referred to AFFDL, W-PAFB.			
11. SUPPLEMENTARY NOTES N/A		12. SPONSORING MILITARY ACTIVITY Air Force Flight Dynamics Laboratory Wright-Patterson Air Force Base Ohio 45433	
13. ABSTRACT <p>This report presents the results of a design study program on a rotary reciprocating compressor which uses heat as the source of driving energy. The objective of the study program was to determine the feasibility of using a thermal compressor in a spaceborne, cryogenic refrigeration system. The report explains the principles of operation of a thermal compressor, and presents the equations which describe its behavior. It also describes a computer program constructed to manipulate these equations. The results of a number of runs made with this program are discussed, and the design of a thermal compressor to meet a specific set of performance requirements is described. Finally, a comparison is made between two types of spaceborne, closed-cycle, cryogenic refrigeration systems--one incorporating a thermal compressor and the other incorporating an electrically driven compressor.</p> <p>It is concluded that a thermal compressor is a viable alternative to an electrically driven compressor in refrigeration systems where heat is preferred over electricity as the energy source. For the specific case studied, the refrigeration system incorporating a thermal compressor required 92 watts of electrical power and 1,064 watts of heat at 1,250°F; while the system incorporating an electric compressor required 587 watts of electrical power. The weights and sizes of the two refrigeration systems were comparable. No serious technical problems are foreseen in building a thermal compressor.</p>			

DD FORM 1473

REPLACES DD FORM 1473, 1 JAN 64, WHICH IS OBSOLETE FOR ARMY USE.

UNCLASSIFIED

Security Classification

